The role of Tm5NM1/2 on early neuritogenesis

Yee-Ka Agnes Chan

A thesis submitted in fulfilment of the requirements for the degree of Master of Philosophy (Medicine)

Discipline of Paediatrics and Child Health, Faculty of Medicine, The University of Sydney

Cellular Oncology Group, Oncology Research Unit, The Children's Hospital at Westmead

April 2009

Declaration

I certify that the work described in this thesis describes original research work, the majority of which was undertaken at The Children's Hospital at Westmead, as part of the Faculty of Medicine at the University of Sydney, in conjunction with the Discipline of Paediatrics and Child Health. These results have not been previously submitted for any degree, and will not be submitted for any other degree or qualification. Unless otherwise specified in the text, all studies reported within this thesis were performed by the author. Ethical approval was obtained for the use of mouse tissue from the Animal Ethics Committee at CMRI/Children's Hospital at Westmead (#111/05).

Yee-Ka Agnes Chan

2009

Abstract

The actin cytoskeleton is important in many cellular processes such as motility, and establishing and maintaining cell morphology. Members of the tropomyosin protein family associate with the actin cytoskeleton along the major groove of actin filaments (F-actin), stabilising them and regulating actin-filament dynamics. To date over 40 non-muscle tropomyosin isoforms have been identified, which are encoded by 4 different genes (α, β, γ, δ). Individual tropomyosin isoforms define functionally distinct F-actin populations. Previous studies have shown that tropomyosins sort to distinct subcellular compartments at different stages of development in polarised cells. Neuronal growth cones are highly dynamic polarised structures, dependent on a constant reorganisation of the actin cytoskeleton. By eliminating tropomyosins in a knockout (KO) mouse model, we investigated the role of two tropomyosin isoforms, Tm5NM1 and Tm5NM2 (γTm gene products) in growth cone dynamics and neurite outgrowth. Growth cone protrusion rates were significantly increased in one day old Tm5NM1/2 KO hippocampal neurons compared to WT controls. Neuritogenesis was significantly affected by the elimination of Tm5NM1/2, with a slight decrease in neurite length and an increase in neuronal branching in neurons cultured for four days. At the molecular level, the depletion of Tm5NM1/2 had no impact on the protein levels and activity of ADF/cofilin in hippocampal neurons while in cortical neurons a subtle but significant increase in ADF/cofilin activity was observed. The subtle phenotype in the early stages of neuritogenesis observed from eliminating Tm5NM1/2 may be explained with functional compensation by other

tropomyosin isoforms. Functional compensation for the loss of Tm5NM1/2 may be provided by isoforms Tm5a/5b, TmBr2 and Tm4 as they localise to the growth cones, structures where Tm5NM1/2 are normally found. These results suggest that Tm5NM1/2 may not be required for early stages of neuritogenesis but may still play a fine-tuning role for this process.

Acknowledgements

I would like to begin by thanking my supervisor, Peter Gunning and associate supervisor, Thomas Fath for giving me the opportunity to undertake this Master's degree. Thanks to you both for your wonderful support and encouragement over the last two years. In particular, thank you Peter for your expertise, for your invaluble advice and for keeping me on track by reminding me to see the bigger picture. Thank you Thomas for your patience, guidance, expertise in neuronal cultures and taking time to review my work. I am so privileged to have had the opportunity to work with you both and this worthwhile experience has enriched me as a scientist.

I would also like to thank all the members of the Oncology Research Unit for making it such an interesting and stimulating place to work. Thank you to all the members of the Cellular Oncology Group, in particular Galina Schevzov, Justine Stehn, Jeff Hook, Sarah Creed and Nikki Curthoys for your technical advice and increasing my understanding of tropomyosin, the cytoskeleton and its involvement in cancers. Many thanks to Helen Jankowski for genotyping all the mice used for my experiments and also to Lisa Corcoran and Nikki Curthoys for your assistance in dissecting and culturing neurons. A big thank you to all the administrative staff, in particular Janett Clarkson, Vanita D'souza and Julie Ward for processing all my paper work and making the whole procedure a bit more bearable.

Many people outside of the Oncology Research Unit have also helped me in my research in various ways. Thanks to the animal staff for looking after the

mice, to Laurence Cantrill for help on the SPOT and live cell microscopes, and also to Cornelis Biesheuvel for assistance with statistics. A big thank you to Russell Dale, Jennifer Byrne, Denise Yuille and Sandra Harris for all your fantastic support of postgraduate students at CHW.

Thank you to my lunch buddies Maha Mahmassani, Helen Jankowski as well as Jayne Hardy, Cuc Bach and Andrea Connor for your friendship, light discussions and laughter. My experience would not be the same without your encouragement and support and it has been a pleasure knowing all of you.

A big thank you to Wendy Cornish for proofreading my thesis. I appreciate the enormous amount of time and effort you have put into reviewing my work. Also, I would like to thank my family for their endless love and support. Thank you to my parents, Fred and Candice Chan for believing in me and for encouraging me to pursue my goals to the best of my abilities. Thank you to my sister Michelle Chan for your understanding and to my cousin Alan Hui for your encouragement over these last couple of months. Many thanks for all your hugs and kisses when I needed it most, and for the laughter to brighten up my day. I am grateful for this invaluable experience and it would not have been possible without the encouragement from my patient and supportive family so thank you!

Finally, I would also like to acknowledge the support of a Faculty of Medicine Postgraduate Scholarship from the University of Sydney, a top up scholarship from the Oncology Children's Foundation and financial support from the Oncology Research Unit.

Presented abstracts arising from this thesis

Chan A., Corcoran L., Clarke H., Gunning P. and Fath T. Functional redundancy among tropomyosin isoforms: Consequences for growth cone dynamics and neurite outgrowth. Presented at "From Cell to Society 6" Faculties of Health Research Conference, University of Sydney, 11th-12th November 2008.

Chan A., Corcoran L., Clarke H., Gunning P. and Fath T. Functional redundancy among tropomyosin isoforms: Consequences for growth cone dynamics and neurite outgrowth. Presented at the Westmead Hospital Research Symposium, NSW. 29th August 2008.

Chan A., Corcoran L., Clarke H., Gunning P. and Fath T. Functional redundancy among tropomyosin isoforms: Consequences for growth cone dynamics and neurite outgrowth. Presented at ComBio2008 Combined Conference, 21st-25th September 2008.

Chan A., Corcoran L., Clarke H., Gunning P. And Fath T. Impact of tropomyosin on neuronal growth cone dynamics and neurite outgrowth. Presented at Postgraduate Student Conference conducted by the Discipline of Paediatrics and Child Health, University of Sydney, 15th August 2008 *(Oral Presentation).*

Chan A., Curthoys N., Clarke H., Schevzov G., Gunning P. and Fath T, Functional redundancy among tropomyosin isoforms: Consequences for growth cone dynamics and neurite outgrowth. Presented at the Australian Society for Medical Research (ASMR) NSW Research Day, 2nd June 2008.

Chan A., Clarke H., Schevzov G., Gunning P., and Fath T. Impact of tropomyosin on axon outgrowth and growth cone dynamics. Presented at ComBio2007 Combined Conference, 22nd-26th September 2007.

Chan A., Clarke H., Schevzov G., Gunning P. and Fath T. Impact of tropomyosin on axon outgrowth and growth cone dynamics. Presented at Postgraduate Student Conference conducted by the Discipline of Paediatrics and Child Health, University of Sydney, 17th August 2007 *(Oral Presentation).*

Table of Contents

List of Abbreviations

Abp1	F-actin-binding protein 1
ADF	Actin depolymerising factor
ADP	Adenosine Di-Phosphate
ATP	Adenosine Tri-Phosphate
DAPI	4,6-diamidino-2-phenylindole
ddH_2O	Water for irrigation
DMEM	Dulbecco's Modified Eagle's medium
DNase	Deoxyribonuclease
CALI	Chromophore-assisted laser inactivation
C-terminal	Carboxyl-terminal
F-actin	Filamentous actin
FAK	Focal Adhesion Kinase
FBS	Fetal bovine serum
G-actin	Globular actin
HMW	High molecular weight
KO	Knockout
LIMK	LIM kinase
LMW	Low molecular weight
MLC	Myosin light chain
MRLC	Myosin regulatory light chain
NB	Neurobasal medium
NP40	Nonidet P-40

N-terminal	Amino-terminal
Phosphor-ADF/cofilin	pADF/cofilin
PAK	p21-activated kinase
PBS	Phosphate buffered saline
PFA	Paraformaldehyde
ROCK	RhoA Kinase
Sem3A	Semphorin 3A
Tg	Transgenic
Tm	Tropomyosin
WASP	Wiskott-Aldrich Syndrome Protein
WAVE	WASP (Wiskott-Aldrich Syndrome Protein)-family Verprolin homologous proteins)
WT	Wild-type

List of Figures

Chapter 1

Chapter 2

Chapter 3

Chapter 4

Chapter 5

Chapter 6

List of Tables

Chapter 2

Chapter 5

Chapter 1

Introduction

The cytoskeleton is a complex structure located in the cytoplasm of all eukaryotic cells and is critical for many diverse cellular processes. The various functions that the cytoskeleton is involved in include cell motility, endocytosis, intracellular transport of organelles as well as establishing and maintaining cell morphology. It is crucial in mitosis to pull chromosomes apart and to split the two daughter cells. In muscle cells, it provides the main machinery for contraction (reviewed in Alberts *et al.*, 2002). Determining the regulation of the cytoskeleton will be important to understand these physiological processes.

Changes in the structure and dynamics of the cytoskeleton are observed in malignant cancer cells. Malignant cancer cells are characterised by their altered cell morphology and motility. This causes the abnormal cells to metastasise by migrating away from the local tissue and invade other parts of the body. Hence, a better understanding of the cytoskeleton and molecular mechanisms that regulate the cytoskeleton will provide invaluable information into how cancer progresses.

The actin cytoskeleton is of particular interest because the stability of actin filaments determines the shape and motility of cells.

1.1 The actin cytoskeleton

Actin is a globular 42kDa protein and it is the major component of the microfilament cytoskeleton. There are six different actin genes that give rise to six distinct isoforms. Four isoforms are expressed in muscles. The isoform found in skeletal muscles is α-skeletal actin, the isoforms α- and γ-actin are expressed in smooth muscle while α-cardiac actin is expressed in cardiac muscle. In non-muscle cells two cytoskeletal isoforms, β- and γ-actin are expressed. In muscles, the actin filaments are involved in muscle contraction while in non-muscles they play a role in a number of cellular processes such as determining cell shape and motility.

The actin microfilaments have a diameter of 5-9nm and are formed by head to tail polymerisation of globular actin (G-actin) monomers. The actin polymer is referred to as filamentous actin (F-actin). Each actin microfilament is made up of two helical strands of F-actin. These actin filaments are dynamic and undergo a process of polymerisation and depolymerisation. The rate of assembly and disassembly of actin filaments is regulated by many actin binding proteins. This regulation is important as the rate of polymerisation and depolymerisation controls many important processes such as cell motility.

1.1.1 Polymerisation and Depolymerisation of the actin filament

The actin filament assembly and disassembly process can be divided into three main stages. The first stage is called actin nucleation which involves the assembly of three G-actin monomers to form a stable trimer (Figure 1.1). This trimer acts as a nucleus for further polymerisation. The second stage is known as actin filament elongation. It involves the addition of G-actin monomers to the stable nucleus of G-actin trimer to form a F-actin polymer (Figure 1.1). These G-actin subunits have a nucleotide binding domain which can either bind to ATP (Adenosine Tri-Phosphate) or ADP (Adenosine Di-Phosphate) although these monomers bind to ATP with much higher affinity than ADP (Engel and Neidl, 1979). Also, the ATP-bound G-actin has a higher affinity to the F-actin than ADP-bound G-actin. The addition of ATP bound G-actin monomers to the F-actin in a head to tail manner maintains the polarity of actin filaments. The polarity property of the actin filament is important for the last stage of the polymerisation process known as treadmilling or steady state dynamics. The polar actin filament contains a barbed or plus end which is fast growing while the other end, known as the pointed or minus end is slow growing based on the total available pool of monomeric actin. The treadmilling process of the F-actin polymer involves the addition of ATP-bound G-actin monomers to the barbed or plus end and dissociation of ADP-bound monomers from the pointed or minus end (Figure 1.2). This creates a dynamic F-actin polymer although the net length of the filament is unaltered (reviewed in Dos Remedios *et al.*, 2003; Ishikawa and Kohama, 2007).

The rate of polymerisation and depolymerisation of the F-actin polymer is tightly regulated by many actin binding proteins. One such actin binding protein that is the main focus of this project is tropomyosin and this is discussed below.

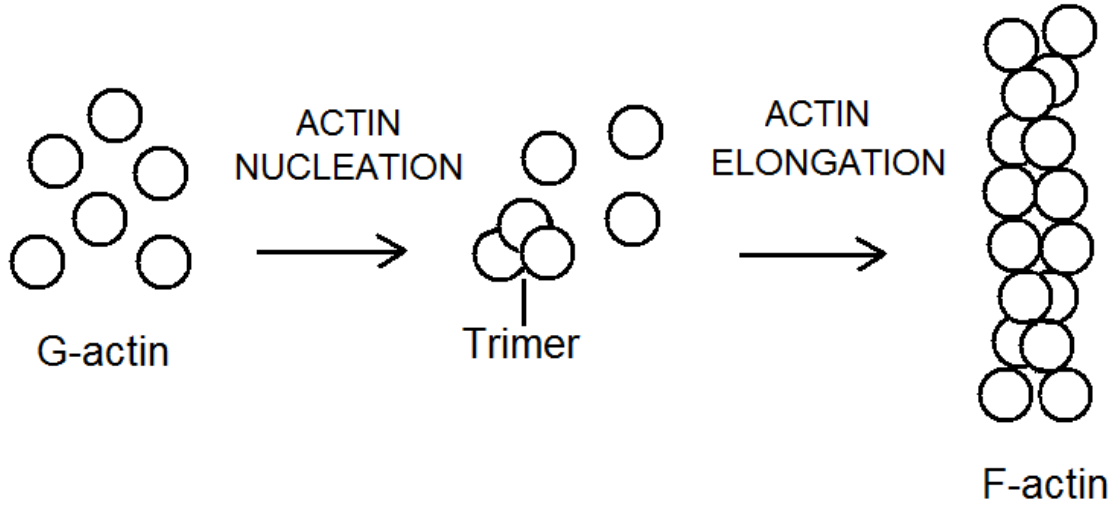

Figure 1.1 Schematic diagram of actin nucleation and elongation. Actin nucleation involves three G-actin monomers joining together to form a trimer. These trimers are sites for further polymerisation. Actin elongation is a process where trimers act as a seed for further addition of G-actin monomers to form F-actin polymers.

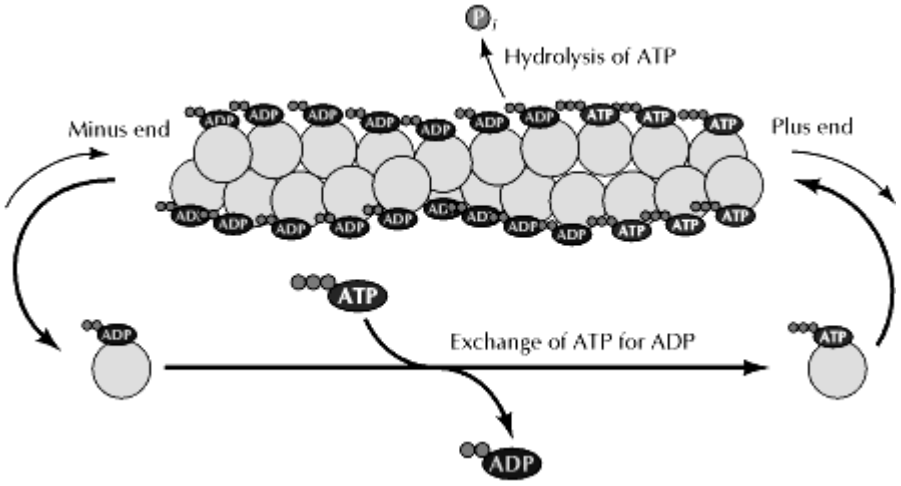

Figure 1.2 Schematic diagram of the treadmilling process of a F-actin polymer. The treadmilling process of F-actin involves the addition of ATP-bound G-actin monomers to the plus or barbed end and dissociation of ADP-bound monomers from the minus or pointed end (from http://kc.njnu.edu.cn/swxbx/shuangyu/6.htm).

1.2 Tropomyosin

Tropomyosin is an actin associated protein that is found in all eukaryotic cells. This protein is known to play a role in muscle contraction but it is also involved in regulating the flexibility and stability of the actin filament system in non-muscles. There are four genes (α, β, γ, δ) within the mammalian tropomyosin protein family. These genes encode over 40 known non-muscle tropomyosin isoforms as a result of alternative splicing (Helfman *et al.*, 1986; Lees-Miller and Helfman, 1991) (Figure 1.3). The different tropomyosin isoforms can be classified as high molecular weight (HMW) (~284 amino acids and 40kDa) and low molecular weight (LMW) isoforms (~248 amino acids and ~28-32kDa). Tropomyosin isoforms can form coiled-coil homodimers with each other or hetero-dimers with other isoforms (Araya *et al.*, 2002). These tropomyosin dimers align along the major groove of the actin filament and can influence the stability of the associated actin filament (Phillips *et al.*, 1979).

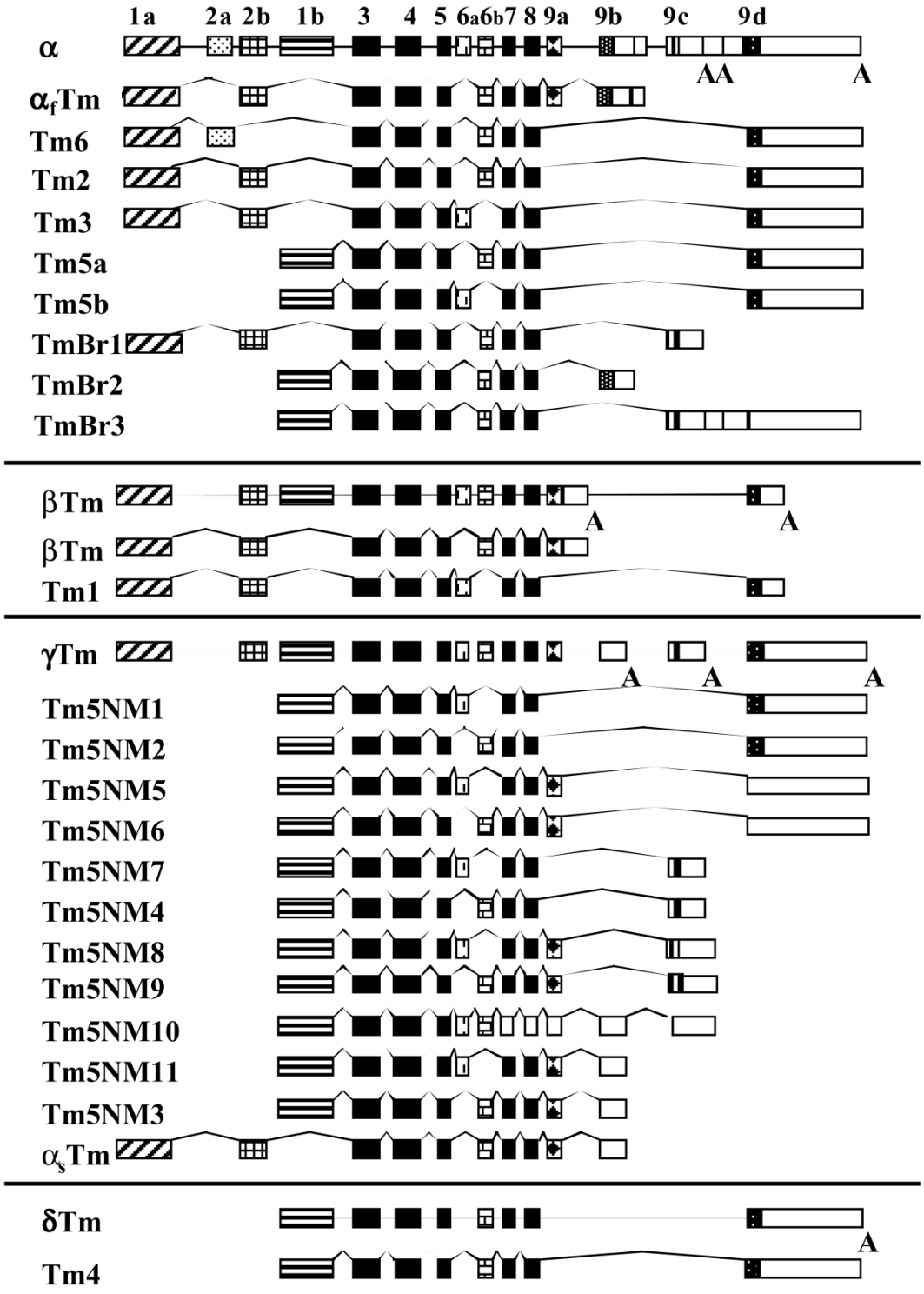

Figure 1.3 Schematic diagram of the four tropomyosin genes (α, β, γ, δ) and their corresponding isoforms generated by alternative splicing. Shaded boxes are exons while unshaded boxes are untranslated sequences. Introns are depicted as lines and A represents poly A tail. Black shaded exons are common to all genes. (from Stehn *et al.*, 2006)

1.2.1 Tropomyosin isoforms are spatially and temporally regulated

The expression and localisation of different tropomyosin isoforms are spatially and temporally regulated during development (reviewed in Gunning *et al.*, 2005; Gunning *et al.*, 2008). The tropomyosin profiles also differ between different cell types such as neurons and fibroblasts.

Neurons have distinct subcellular compartments. These compartments include the cell body, dendrites and the axon with growth cones structures located at their tips. Tropomyosin isoforms localise to different compartments at different stages of development. Immunohistochemistry studies on neurons from cultured embryos have shown that Tm5NM1/2 isoforms are concentrated in the neurite shaft and the growth cone structure of immature axons (Weinberger *et al.*, 1996). Further analyses using more specific antibodies have shown that Tm5NM1 localises to the outer region of the growth cone (Schevzov *et al.*, 2005a) while Tm5NM2 is mainly located in the neurite shaft (Schevzov *et al.,* 1997; Hannan *et al.,* 1998). After neuronal maturation, Tm5NM1/2 relocate to the somatodendritic compartment (Weinberger *et al.*, 1996; Hannan *et al.*, 1998). During this time of Tm5NM1/2 relocation, the brain specific isoform TmBr3 have been revealed by immunofluorescence and immunohistochemistry to localise to the axon compartment, suggesting that the Tm5NM1/2 isoforms are displaced by TmBr3 (Had *et al.*, 1994; Weinberger *et al.*, 1996). Similar to the localisation pattern of Tm5NM1/2, immunofluorescence stainings of cultured neurons have shown that Tm4 is expressed in growth cones of

developing neurites and after maturation was restricted to the postsynaptic compartment (Had *et al.*, 1994). Other tropomyosin isoforms Tm5a/5b were found to also localise to the growth cone of cortical neurons but over time when the growth cones diminish in size, these isoforms are excluded from this structure (Schevzov *et al.*, 1997). Taken together this demonstrates that tropomyosin isoforms such as Tm5NM1/2, Tm5a/5b and Tm4 define distinct actin filament populations within neurite and growth cones and these microfilaments are subject to spatial and temporal regulation.

Tropomyosin isoform localisation in fibroblasts has been shown to be cell cycle dependent. During early G1 phase, the αTm and βTm gene products localise to stress fibres in fibroblasts while the γTm gene products are found in the perinuclear zone. As cells progress through G1 phase, expression of the γTm gene products (LMW tropomyosins) increases with the exception of two isoforms Tm5NM1 and Tm5NM2 (Percival *et al.*, 2000). The γTm gene products that increased in expression translocate from the periphery to stress fibres while Tm5NM1/2 did not show a change in localisation (Percival *et al.*, 2000). Further analysis by transfecting fluorescently tagged tropomyosins in fibroblasts showed that Tm5NM1 predominantly localises to stress fibres while Tm5NM2 targets to the Golgi complex (Percival *et al.*, 2004). Immunogold labelling confirmed this observation showing that Tm5NM2 localises to actin filaments found in the Golgi (Percival *et al.*, 2004). This suggests that Tm5NM1 may regulate stress fibres while Tm5NM2 may be involved in vesicle budding from the Golgi complex. This demonstrates that the actin filament populations defined by different tropomyosin isoforms such as Tm5NM1 and Tm5NM2 are likely to play distinct roles in the fibroblasts.

The differences in the localisation pattern of tropomyosin isoforms during development show that tropomyosins define distinct actin filament populations and perform unique functions in a variety of cell types.

1.2.2 Tropomyosin isoform specific effect on actin filaments

Differentially sorted tropomyosin isoforms define distinct actin filament populations. There is evidence to show that distinct tropomyosin isoforms exert different effects on the actin filaments that they are associated with. For example, when Tm5NM1 associates with actin filaments, they become more stable due to the inhibition of actin depolymerising factor/cofilin (ADF/cofilin). In contrast, the TmBr3 isoform causes more instable actin filaments as ADF/cofilin associates with TmBr3 decorated filaments (Bryce *et al.*, 2003; Schevzov *et al.*, 2005a). This demonstrates that different tropomyosin isoforms can affect the stability of the associated actin filaments.

Tropomyosin isoforms can form homodimers or heterodimers with each other and may define a wide range of actin filament populations. Muscle tropomyosins have a preference for heterodimerisation. Cotransfection studies

on skeletal muscle αTm and smooth muscle αTm isoforms have revealed formation of heterodimers with non-muscle HMW tropomyosins. Also, skeletal muscle βTm can heterodimerise with HMW tropomyosin isoforms, Tm1, Tm2 and Tm3 (Gimona *et al.*, 1995). In contrast, cytoskeletal tropomyosins mainly form homodimers (Matsumura and Yamashiro-Matsumura, 1985) even though heterodimerisation can occur (Temm-Grove *et al.*, 1996). Western blot analysis and cotransfection studies on tagged HMW tropomyosins show that these isoforms prefer homodimerisation (Gimona *et al.*, 1995). Also, cotransfection of tagged LMW tropomyosin isoforms, Tm5NM1/2, Tm4, Tm5a/5b have revealed that these isoforms cannot heterodimerise with muscle tropomyosins as well as HMW tropomyosins, Tm1, Tm2 and Tm3 (Gimona *et al.*, 1995; Temm-Grove *et al.*, 1996). However, further cotransfection studies on LMW tropomyosins have shown that Tm5NM1, Tm4 and Tm5a/5b can form heterdimers with each other even though Tm5a and Tm5b cannot (Temm-Grove *et al.*, 1996; Araya *et al.*, 2002). Heterodimerisation of tropomyosin isoforms is possible and can confer properties to actin filaments that are different from homodimerised tropomyosin isoforms.

In addition to homodimerisation and heterodimerisation, the actin affinity which is different for individual tropomyosin isoforms may also contribute to the isoform specifc effects on actin filaments (Matsumura and Yamashiro-Matsumura, 1985). The overall binding of tropomyosins to actin is very low and instead they appear to “float” in the major groove of the actin polymer, this interaction being held together by ionic forces (Perry, 2001). However, the actin affinity is different for individual tropomyosin isoforms as it depends on

their N-terminal (amino-terminal) and C-terminal (carboxyl-terminal) sequences (Moraczewska *et al.*, 1999). TmBr3 had the lowest affinity to actin out of all tropomyosin isoforms that were studied and this may correlate with associating to less stable filaments that are decorated with ADF/cofilin (Moraczewska *et al.*, 1999; Bryce *et al.*, 2003). The low affinity of TmBr3 to actin may allow ADF/cofilin to bind and depolymerise the actin filament generating less stable filaments. Tm5a/5b on the other hand may stabilise actin filaments as they have the highest affinity to F-actin compared to any other tropomyosin isoforms that have been studied (Moraczewska *et al.,* 1999). Therefore, the degree of affinity by different tropomyosins to actin may explain the isoform specific regulation of the activity of other actin binding proteins on actin filaments.

1.2.3 Tropomyosins protect the actin filament and regulate the activity of other actin binding proteins

Tropomyosins stabilise and protect the actin filament from the action of other actin binding proteins thereby regulating the polymerisation and depolymerisation of actin filaments. Tropomyosin isoforms have been shown to protect the actin filament from the activity of actin depolymerising factor /cofilin (ADF/cofilin), Arp2/3, gelsolin and formin (Bernstein and Bamburg, 1982; DesMarais *et al.*, 2002). These protective effects on actin filaments by tropomyosins are isoform specific (Bryce *et al.*, 2003).

ADF/cofilin is an actin depolymerising protein that competes with tropomyosin isoforms for actin filament binding (Bernstein and Bamburg, 1982; Cooper, 2002; reviewed in Ono and Ono, 2002). Cofilin and its closely related protein, actin depolymerising factor (ADF) function by enhancing the depolymerisation of F-actin at the pointed end of the polymer as it has a higher affinity to ADP-bound actin. ADF functions by severing the actin filament and providing new barbed ends for further polymerisation. By carrying out cryo-electron microscopy and image reconstruction experiments, cofilin has been shown to bind between two actin subunits and alter the F-actin twist (McGough *et al.*, 1997), thereby greatly destabilising the actin filament. The competition of tropomyosin with ADF/cofilin has been shown using saturation studies. The saturation of F-actin with tropomyosins displayed no active ADF/cofilin activity on those filaments, suggesting that ADF/cofilin binds specifically to actin

filaments that are not decorated with tropomyosins (Bernstein and Bamburg, 1982). However, previous studies have shown that different tropomyosins confer different protective properties to the actin filaments. The overexpression of a LMW tropomyosin, Tm5NM1 significantly increased the phosphorylated or inactive form of ADF/cofilin while the overexpression of a HMW tropomyosin Tm3 displayed no difference in ADF/cofilin levels as compared to WT controls (Bryce *et al.*, 2003). This indicates that some tropomyosin isoforms such as Tm5NM1 are strong inhibitors of ADF/cofilin activity.

Tropomyosin isoforms also regulate the action of actin related protein 2 and 3 (Arp2/3) on actin filaments (Blanchoin *et al.*, 2001). Arp2/3 is a protein that contains 2 actin-homologous subunits and actin-related proteins 2 and 3. This protein functions as a seed for actin polymerisation by binding to G-actin and increasing the number of barbed ends (reviewed in Ishikawa and Kohama, 2007). The Arp2/3 complex can also enhance actin polymerisation by generating new branch points in existing actin filaments (reviewed in Amann and Pollard, 2001). Fluorescence studies have shown that Arp2/3 is partially inhibited to varying degrees by different tropomyosin isoforms. Tm5a is a better inhibitor of Arp2/3 than Tm2 shown by the percentage of filament branches formed (Blanchoin *et al.*, 2001).

Apart from ADF/cofilin and Arp2/3, tropomyosins are also shown to regulate the activity of gelsolin. Gelsolin is a severing and capping protein that functions by first binding and severing F-actin in a calcium dependent manner and then capping the barbed end of the filament thereby preventing further actin polymerisation (Sun *et al.*, 1999). Tropomyosin is able to dissociate the

severing and capping protein, gelsolin and promote the annealing of short actin filaments (Ishikawa *et al.*, 1989a; Maciver *et al.*, 2000; Nyakern-Meazza *et al.*, 2002). SDS-polyacrylamide gel analysis has revealed that HMW but not LMW tropomyosin isoforms can directly inhibit and protect the actin filament from the severing activity of gelsolin (Ishikawa *et al.*, 1989b). However, HMW and LMW tropomyosins can both indirectly inhibit the severing action of gelsolin by collaborating with non-muscle caldesmon. LMW tropomyosins and caldesmon alone cannot inhibit the action of gelsolin to actin filaments and this may be explained by the fact that LMW tropomyosins have lower affinity to actin than HMW isoforms (Matsumura and Yamashiro-Matsumura, 1985). When caldesmon works with LMW tropomyosin, caldesmon can enhance the binding of LMW tropomyosin to actin filaments therefore increasing the inhibition of the severing effects of gelsolin on actin filaments (Ishikawa *et al.*, 1989b).

Tropomyosin isoforms have been shown to regulate the barbed ends of actin filaments by working with formin. Formin is a barbed end binding protein with weak capping activity. This means that when formin caps actin, the polymer can still elongate at the barbed end but at a controlled rate. Tropomyosin isoforms can uncouple the capping function of formin in an isoform specific manner thereby promoting and regulating the formation of unbranched actin filaments at the barbed end (Wawro *et al.*, 2007).

Tropomyosins have also been shown to recruit or inhibit myosin, an actin motor protein to the actin filament in an isoform specific manner. In B35 neuro-epithelial cells the overexpression of the exogenous Tm5NM1 was able to

recruit myosin II to stress fibres (Bryce *et al.*, 2003). Also observed in primary cortical neurons, the enhanced expression of Tm5NM1 recruited myosin IIB to the cell periphery (Schevzov *et al.*, 2005a). In contrast, colocalisation studies on cortical neurons overexpressing HMW Tm3 have shown that myosin IIB was not enriched in the growth cone or periphery areas where exogenous Tm3 was found (Schevzov *et al.*, 2005a).

These studies demonstrate that tropomyosins regulate and inhibit a range of actin binding proteins in an isoform specific manner which results in the stabilisation and stiffening of the F-actin polymer. Furthermore, certain tropomyosin isoforms can recruit myosin II to actin filaments to regulate actin based cell motility.

1.2.4 Understanding the role the γTm gene products using an isoform specific knockout mouse model

Tropomyosins have been implicated in many cancers (reviewed in Stehn *et al.*, 2006). Generally, the expression of HMW tropomyosin isoforms, Tm1, Tm2 and Tm3 in primary human cancers such as breast, prostate and gastric cancers is mainly decreased. Hence, there appears to be a reliance on LMW tropomyosins in malignant cells. In a recent study using B35 neuro-epithelial cells, it has been shown that the degree of susceptibility of the actin filament population to actin targeting drugs is determined by the tropomyosin composition (Creed *et al.*, 2008). Therefore, tropomyosins are the ideal candidate target to develop drugs in order to treat cancers (reviewed in Stehn *et al.*, 2006). Generally, HMW isoforms contribute to the stability of actin filaments and function in regulating the cell morphology and division while LMW tropomyosins have been shown to localise to the leading edge of fibroblasts which indicates that they may play a specific role in membrane organisation, motility and cell growth (reviewed in Gunning *et al.*, 2005). Therefore, the predominance of LMW tropomyosin isoforms in cancers indicates that these malignant cells rely on LMW tropomyosins for motility and migration and eventual invasion into other parts of the body. Hence, targeting a subset of these LMW isoforms may slow motility and migration and make the malignant cells more vulnerable. In addition, tropomyosins found in actin filaments of cardiac and skeletal muscle are distinct from those found in the cytoskeleton of non-muscle cells. This strongly suggests that drugs targeting non-muscle

tropomyosins would not impact on critical cellular processes such as the contraction of the heart or the skeletal muscles in the diaphragm required for breathing. Furthermore, another aspect to consider in drug development is the possibility that the drug can pass the blood brain barrier. As the brain is the centre of the nervous system and involved in many processes such as controlling movement, speech, memory and thought, understanding the effect of the drug in neuronal development and function is important.

In an initial step to develop chemotherapy drugs targeting certain LMW tropomyosin isoforms, one must consider the effect the drug has on neuronal development and function if it passes through the blood brain barrier. Therefore the aim of this project is to analyse the role of a subset of LMW tropomyosins in neuronal cells.

To understand the role of LMW tropomyosins in cells, isoforms from the γTm gene were analysed. The γTm gene expresses at least 11 non-muscle isoforms that are all classified as LMW tropomyosins. Complete knockout (KO) of the γTm gene showed that the non-muscle products from this gene were required for embryonic development and cell survival (Hook *et al.*, 2004). However, knockout of a subset of isoforms from this gene containing exon 9c (Tm5NM4/7) are not lethal (Vrhovski *et al.*, 2004). Tm5NM4/7 are specifically expressed in the brain (Vrhovski *et al.*, 2003). Analysis of brains from Tm5NM4/7 KO mice showed that they were structurally normal as the loss of Tm5NM4/7 is compensated by exon 9a containing isoforms from the γTm gene (Tm5NM3/5/6/8/9/11) (Vrhovski *et al.*, 2004). The exon 9d (Tm5NM1/2) and 9a

containing isoforms from the γTm gene are also expressed in the brain although these isoforms are found in other tissue with Tm5NM1/2 being the most widespread (Vrhovski *et al.*, 2003; Schevzov *et al.*, 2005b). Nevertheless, the level of Tm5NM1/2 expression in the brain is higher than exon 9a and exon 9c containing isoforms from the γTm gene (Vrhovski *et al.*, 2004). The upregulation of exon 9a containing isoforms and the high level of Tm5NM1/2 may explain why there were no abnormalities in the brain (Vrhovski *et al.*, 2004) and this suggests that Tm5NM1/2 may play a role in brain development.

As Tm5NM1/2 mRNA and protein are found in axons of embryonic mice, these isoforms may be involved in axon formation as well as the establishment of neuronal polarity (Hannan *et al.*, 1995). Further analysis of Tm5NM1/2 protein using immunohistochemical analysis of brain slices revealed that these isoforms are localised to developing axons but relocate to somatodendritic compartments after maturation (Weinberger *et al.*, 1996; Vrhovski *et al.*, 2003). As Tm5NM1/2 levels are high in embryonic brains and downregulated after birth, Tm5NM1/2 may be involved in the initial stages of neuronal development (Vrhovski *et al.*, 2003). In contrast, exon 9a and 9c containing products from the γTm gene, Tm5NM3/5/6/8/9/11 and Tm5NM4/7 respectively are upregulated after birth (Vrhovski *et al.*, 2003), suggesting a more critical role later in brain development.

To investigate the role of Tm5NM1/2 in early neuronal development, transgenic mice which overexpress Tm5NM1 (Schevzov *et al.*, 2005a) and mice deficient in Tm5NM1/2 expression (Tm5NM1/2 KO mice) have been analysed (Fath *et al.,* manuscript in preparation). Tm5NM1/2 KO mice do not express the exon 9d

containing isoforms from the γTm gene but still express the other γTm gene products (Fath *et al.,* manuscript in preparation). In addition, western blot analysis of cell lysates of cultured KO cortical neurons from these mice has shown a partial compensation of Tm5NM1/2 by Tm5NM4/7 isoforms (Fath *et al.,* manuscript in preparation).

Studies on cortical neurons from embryonal day 16.5 mouse embryos revealed the formation of bigger growth cones upon increased Tm5NM1 and smaller growth cones when Tm5NM1/2 are eliminated. In terms of neurite outgrowth, there was an increase in the number and total length of dendrites. Furthermore, the number of axonal branches and total axon length is significantly increased in cortical neurons from Tm5NM1 transgenic mice (Schevzov *et al.*, 2005a). Significant differences in growth cones and neurite outgrowth observed in Tm5NM1 transgenic mice suggest that Tm5NM1 may play a role in neurite formation and development, a process known as neuritogenesis. Therefore, the aim of this project is to use the Tm5NM1/2 KO mouse model to further characterise the role of Tm5NM1/2 in the early stages of neuritogenesis. As this research is on the analysis of neuronal cells with a focus on growth cone function and neuritogenesis, the structure and process of neuronal development will be discussed in the next sections.

1.3 The Neuronal Cytoskeleton

Neurons are the primary functional unit of the nervous system. They form processes (neurites) via which they establish synaptic connections with other neurons in a controlled manner. Both neurite outgrowth and synapse formation rely heavily on the organisation and remodelling of the neuronal cytoskeleton. The three main components that make up the neuronal cytoskeleton are actin microfilaments, microtubules and neurofilaments. These three types of filaments all localise to distinct compartments of the neurons and play different roles which are important in developing and maintaining neuronal structure and synapse function.

The actin filaments provide support to cell protrusions such as filopodia and lamellipodia which are located at the edge of the growth cones. The polymerisation and depolymerisation of actin filaments also drives the protrusion of these structures. Microtubules are polymers of α and β-tubulin dimers organised in long hollow cylinders with an outer diameter of 25nm. Microtubules are present in the cell body and extend along both the axon and dendrites and into the growth cones at the tip of the neurites. These polymers function by supporting and strengthening these neuronal structures and are also involved in intracellular transport. Neurofilaments are intermediate filaments found specifically in axons of the neurons with a diameter of 10nm. These filaments are made up of filamentous proteins and function by regulating the diameter of an axon which in turn controls the rate of electrical signals that travel down this axon (summarised in Alberts *et al.*, 2002).

The actin filaments and microtubules play a part in regulating the growth cone structure. As the growth cone structure is a major dynamic structure of the neuron, the organisation of the growth cone will be discussed below.

1.4 The organisation of the growth cone

Growth cones are located at the tips of the developing neurons known as neurites and are one of the main dynamic structures of the neuron. These structures rely on a constant reorganisation of actin filaments to sense guidance cues and move accordingly towards or away from the cues. The ability to sense these cues and move is important as the dynamic nature of the growth cones determine the direction of neurite outgrowth.

The growth cone structure can be divided into three different regions, known as the peripheral, transitional and central regions (Figure 1.4). The peripheral region of the growth cone mainly consists of actin filaments arranged in actin meshwork and actin bundles. These two actin arrangements give shape and structure as well as motility to the filopodia and lamellipodia which are found at the periphery of the growth cone. The actin meshwork forms the veil-like lamellipodia while actin bundles extend into spike-like filopodia structures. The central region is located at the centre of the growth cone nearest to the neurite shaft. This region is mainly composed of microtubules and contains many organelles and vesicles. In between the central and peripheral regions is an

area known as the transitional zone. In this zone, both actin filaments and dynamic microtubules are found. These dynamic microtubules can periodically extend out into the peripheral region of the growth cone and into the filopodia structures (reviewed in Dent and Gertler, 2003).

The organisation of the actin filaments is important for the function of filopodia and lamellipodia. Disruption of F-actin by the drug cytochalasin prevents the formation of filopodia and shows that the growth cone can advance and extend normally but is highly disoriented (Bentley and Toroian-Raymond, 1986). Therefore while the lamellipodia is involved in motility, the filopodia has a sensory role to guide the direction of motility. Filopodia has actin bundles with the barbed ends orientated towards the tip for rapid polymerisation and hence protrusion of the structure.

This dynamic process of interaction between the three regions is critical for the growth cones to move in response to guidance cues in order to direct neurite outgrowth (reviewed in Rodriguez *et al.*, 2003). The process of neuritogenesis will be discussed next.

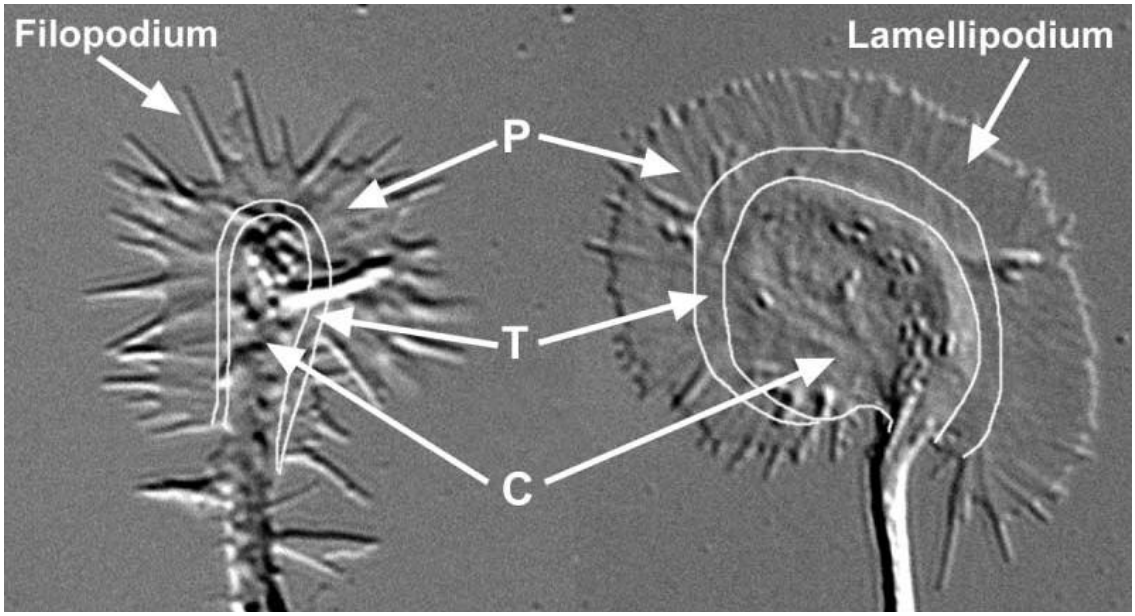

Figure 1.4 Three different regions within the growth cone structure. The three sections of the growth cone are known as the peripheral, transitional and central regions. On the left is an example of a "filopodial" growth cone and on the right is an example of a "lamellipodial" growth cone. Typically growth cone structures have both filopodia and lamellipodia located at the periphery. The periphery regions contain actin meshwork and actin bundles that give structure to the lamellipodia and filopodia respectively. The central region contains thick microtubules while in the transitional zone both actin filaments and dynamic microtubules are found (from Dent and Gertler, 2003).

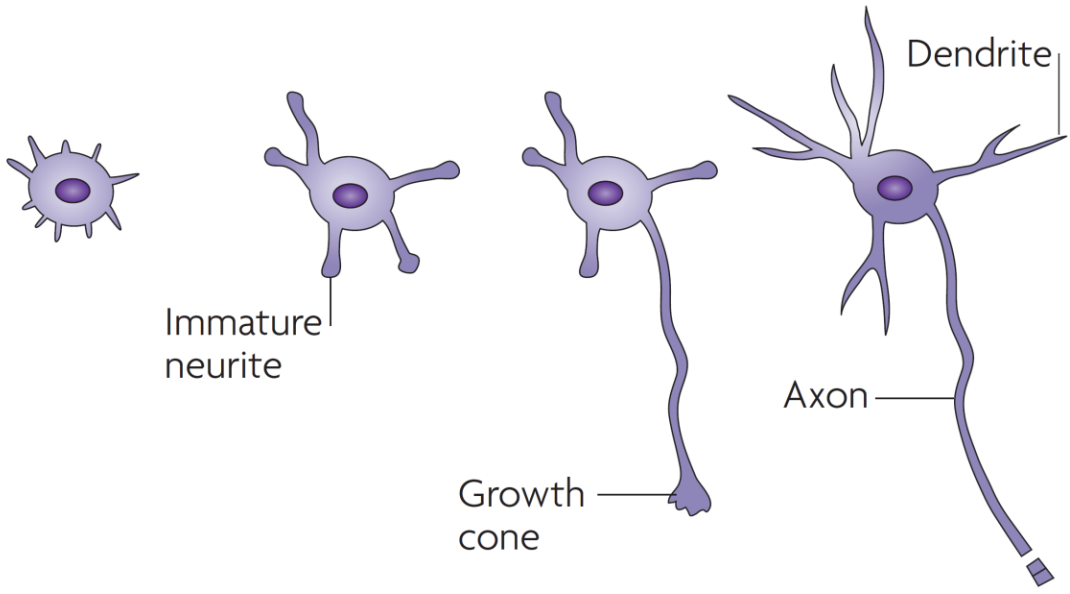

Figure 1.5 Neurite formation and elongation. Firstly, lamellipodia or buds are formed around the cell body. Secondly, neurite initiation occurs where these lamellipodia or buds are extended to form immature neurites with a nascent growth cone at the tips. Neurite elongation involves rapid extension of a single neurite and neurites have polarised when they become one long axon and many dendrites. The axon shaft is defined by the shrinking of growth cone structure due to depolymerisation of F-actin at the tips (from Arimura and Kaibuchi, 2007).

1.5 Neurite Formation and Elongation

The regulation of the actin filament network is important in many aspects of neuritogenesis including neurite formation and extension (Endo *et al.,* 2007; Korobova and Svitkina, 2008). Neuritogenesis is dependent on continuous actin filament reorganisation. Neuritogenesis involves firstly the formation of buds or lamellipodia at the cell surface, secondly the protrusion of immature neurites at the bud sites and finally these neurites polarise into one single axon and many dendrites (Figure 1.5). The latter steps are known as neurite outgrowth and polarisation (reviewed in Dent and Gertler, 2003).

Prior to neurite initiation, lamellipodia are formed around the cell body which has been observed in primary hippocampal neurons (Dehmelt *et al.*, 2003). These veil-like structures segregate to form distinct and individual lamellipodia which start to resemble the growth cone. Neurite initiation involves a reorganisation of microtubules and actin filaments to produce an immature neurite with a nascent growth cone at the tips (Figure 1.5). Microtubules align to produce a tight bundle which serves to stabilise and maintain the neurites while actin filaments drive the motility of lamellipodia and filopodia in response to guidance cues (reviewed in Da Silva and Dotti, 2002).

After neurite initiation, one neurite differentiates to form an axon. A current model of neurite extension is shown in three main stages (reviewed in Goldberg and Burmeister, 1986; Dent and Gertler, 2003). The first stage involves cycles of filopodial and lamellipodial protrusion where these dynamical structures are

extended out from the leading edge of the growth cone. The second stage concentrates around the central domain of the growth cone where it is engorged. In this process, microtubules move into the lamellipodia and filopodia of the growth cone, transporting vesicles and organelles to the structures. The last stage is known as the consolidation of the neurite. This involves depolymerisation of a majority of F-actin at the neck of the growth cone which causes the membrane to shrink around the microtubule bundles and subsequently the axon shaft is defined and formed (Figure 1.5). This final step is fundamentally essential in maintaining the polarity of the growth cone in order to restrict the protrusive activity of lamellipodia and filopodia structures to the distal tip of the axon.

1.6 Guidance cues and pathways that affect actin polymerisation

The actin cytoskeleton, as well as many other important cellular processes, is regulated by Rho GTPases. The most extensively studied RhoGTPases are Rac, Cdc42 and Rho. They function by responding to guidance cues by interacting with and regulating the activity of many downstream targets and effector proteins that alter the structure and function of the cytoskeleton.

The growth cone is a dynamic structure that can move in response to guidance cues. Filopodia and lamellipodia are specialised structures located at the periphery of the growth cone which protrude when attractant guidance cues are present or retract when repulsive cues are around. Filopodia are the environmental sensors that detect these guidance cues and both the filopodia and lamellipodia move in response to these cues as a result of altered actin filaments that support these structures. Distinct guidance cues trigger activation of different pathways which can in turn recruit and activate actin binding proteins that can subsequently turnover the actin structure of filopodia and lamellipodia.

There are attractive cues such as netrin-1 and neurotrophin that can promote actin polymerisation in filopodia. Netrin-1 attracts axons and fluorescent imaging techniques using cortical neurons revealed that netrin-1 increases actin filaments causing more axon branching and filopodia formation (Dent *et al.*, 2004). Netrin-1 has also been found to increase filopodia formation in

hippocampal neurons through a pathway involving the phosphorylation of Ena/VASP proteins and protein kinase A (PKA) activation (Lebrand *et al.*, 2004). A specific type of neurotrophin known as brain derived neurotrophic factor can also promote the number and length of filopodia and it has been shown to function via activating ADF/cofilin which is an actin binding protein that can increase actin dynamics (Gehler *et al.*, 2004b).

Inhibitory cues including Semphorin 3A (Sem3A) and ephrin can enhance actin depolymerisation. Sem3A can cause growth cone collapse by depolymerising actin filaments. This involves phosphorylation and inactivation of cofilin at serine 3 by LIM kinase (LIMK) (Aizawa *et al.*, 2001). LIMK is regulated by p21-activated kinase (PAK). The association of PAK with LIMK is enhanced by activated Rac or Cdc42 and LIMK is phosphorylated by PAK at threonine residue 508. This phosphorylation elevates LIMK activity and increases its subsequent phosphorylation and inactivation of cofilin by tenfold (Edwards *et al.*, 1999). Cofilin can also be reactivated by the protein phosphatase Slingshot-1, which contains multiple F-actin binding sites. The cofilin phosphatase activity can be greatly enhanced when F-actin is bound. Slingshot-1 also functions by stabilising and bundling F-actin which is independent of the cofilin phosphatase activity (Kurita *et al.*, 2007).

PAK has recently been shown to be a crucial factor in the polarisation and differentiation of neurites to become an axon or dendrite. Manipulation of PAK activity has resulted in disruption of neuronal morphology by influencing F-actin and microtubules partially through Rac1 and cofilin. Through PAK, Rac1 regulates both dynamic instability of microtubules and actin polymerisation.

Thus, this suggests that the PAK pathway may play a major role in regulating actin filaments as well as polarisation and differentiation of neurons (Jacobs *et al.*, 2007).

Another pathway downstream of Rac involves the WAVE (WASP (Wiskott - Aldrich Syndrome Protein)-family Verprolin homologous proteins) complex. WAVE is a protein complex that has a G-actin binding site, one Arp2/3 binding site and one profilin binding site and the activation of WAVE is mediated by Rac without any physical interaction (Eden *et al.*, 2002). As the WAVE complex contains an Arp2/3 binding site, WAVE can directly bind to and activate the Arp2/3 complex (Nakanishi *et al.*, 2007). Hence, WAVE can control the polymerisation process by regulating Arp2/3 activation.

A protein that has a C terminal domain that is homologous to WAVE is N-WASP. N-WASP is a neuronal specific protein that lies downstream of the Cdc42 pathway. It contains two G-actin binding sites, one Arp2/3 binding site and one profilin binding site (reviewed in Ishikawa and Kohama, 2007). N-WASP is activated when mammalian F-actin-binding protein 1 (Abp1) binds directly to this protein and in conjunction with Cdc42 can release the autoinhibition of N-WASP. This activates N-WASP and results in the subsequent binding of actin and Arp2/3 causing acceleration of actin polymerisation. Hence, the N-WASP, Abp1 and Cdc42 mediated Arp2/3 complex plays an important role in actin polymerisation and controlling the morphology of neurons (Pinyol *et al.*, 2007).

Colocalisation studies on fibroblasts have shown that WAVE localises to the tips of membrane ruffles while N-WASP localises to actin bundles in filopodia (Nakagawa *et al.*, 2001; reviewed in Takenawa and Miki, 2001). This suggests that WAVE has a role in lamellipodia formation while N-WASP plays a part in filopodia formation. Furthermore, WAVE and N-WASP may affect the action of Arp2/3 in lamellipodia and filopodia respectively.

Another inhibitory guidance cue is ephrin. In prostate carcinoma cells, when ephrinA1 receptor is stimulated by ephrin, the Src-FAK (focal adhesion kinase) pathway is activated. From studies of dominant negative mutants for FAK and Src, Rho activation by ephrinA1 requires formation of Src-FAK complex. EphrinA1-induced repulsive motility requires activation of Src-FAK complex to activate RhoA which is involved in retraction fibre formation (Parri *et al.*, 2007). RhoA is found to be active in growth cones and distal axons (Gehler *et al.*, 2004a) and is upstream of RhoA Kinase (ROCK). Both RhoA and ROCK have been shown to be required for controlling growth cone dynamics (Bito *et al.*, 2000). Dominant active RhoA significantly reduced the size of growth cones while inhibition of ROCK significantly increased growth cone size in cerebellar granule neurons. In addition, cells treated with Y-27632, a specific inhibitor of ROCK (Uehata *et al.*, 1997) has revealed that membrane ruffles and filopodia processes were initiated earlier and more frequently than WT controls (Bito *et al.*, 2000; Loudon *et al.*, 2006). These Y-27632 treated cells also have increased motility of membrane ruffles and higher turnover of filopodia processes (Bito *et al.*, 2000). As well as controlling growth cone dynamics, there is evidence to show that RhoA and ROCK initiate axon outgrowth. Cells cotransfected with C3, a RhoA inhibitor enzyme and similarly cells treated with

Y-27632 increased the number of processes without affecting the length (Bito *et al.*, 2000). These results strongly suggest that the Rho/ROCK pathway is important in regulating growth cone dynamics and initiating axon outgrowth.

Growth cones contain myosin II, an actin motor protein (Rochlin *et al.*, 1995). Myosin II activity is inhibited by myosin light chain phosphatase and can be activated by myosin light chain kinase. Alternatively, myosin II can be directly activated by ROCK through phosphorylation of serine 19 in the regulatory myosin light chain (Ueda *et al.*, 2002). Myosin II functions by promoting retrograde F-actin flow from the peripheral to the central regions of the growth cone (Lin *et al.*, 1997). However, it has been shown that ROCK does not regulate myosin II driven F-actin retrograde flow in growth cone lamellipodia (Zhang *et al.*, 2003). This suggests that lamellipodial retrograde flow is driven by myosin II in a ROCK independent pathway and that ROCK regulates the activity of myosin II in a different context. As well as suppressing protrusive activity of the growth cone, myosin II is also required for axon retraction but via a different pathway than the one that drives F-actin bundle formation and growth cone collapse (Gallo, 2006). Similar to the inhibition of ROCK, the suppression of myosin II activity by blebbistatin increased the initiation of lamellipodia and filopodia in axons (Loudon *et al.*, 2006), suggesting that ROCK and myosin II function in the same pathway to repress the protrusive activity of growth cones. In addition, inhibition of ROCK and myosin II disrupts growth cone polarity and impairs the turning behavior of growth cones towards an attractive cue (Loudon *et al.*, 2006). This indicates that ROCK and myosin II are important for axon consolidation and maintaining growth cone polarity.

Guidance cues are important in regulating actin polymerisation and depolymerisation in lamellipodial and filopodial structures as well as maintaining neuron and growth cone polarisation. In response to these guidance cues, there are a large number of actin binding proteins that impact on F-actin directly to influence the treadmilling process of the filament which will be discussed next.

1.7 Actin binding proteins that regulate actin filaments and affect early neuritogenesis and growth cone function

The actin filaments are important in many aspects of growth cone dynamics and neuritogenesis. As the treadmilling process of actin filaments are controlled and regulated by many actin binding proteins, the function of these actin binding proteins will be discussed in the context of growth cones and neuritogenesis.

As discussed earlier a variety of actin binding proteins including ADF/cofilin, Arp2/3, gelsolin and formin are regulated by different tropomyosin isoforms. ADF/cofilin enhances actin depolymerisation when bound to actin filaments. This protein appears to play a part in growth cone development and neurite

extension. In neurons, the expression level of ADF/cofilin is high and it colocalises to F-actin in growth cones (Bamburg and Bray, 1987). Adenovirus-mediated overexpression of *Xenopus* ADF in rat cortical neurons significantly enlarged growth cone size and increased the number of filopodia. Also, the overexpression of *Xenopus* ADF caused a significant increase in neurite length (Meberg and Bamburg, 2000). Studies in chick dorsal root ganglion neurons have shown that the phosphorylation of ADF/cofilin by LIMK and slingshot needs to be regulated as it is essential for proper neurite extension (Endo *et al.,* 2007). Therefore, this suggests that ADF/cofilin plays a part in growth cone development and neurite extension but these processes may require tight regulation by LIMK, slingshot and tropomyosin.

Another actin binding protein, Arp2/3 whose activity on actin filaments is influenced by the presence of tropomyosin appears to play a role in specific aspects of neuronal development. Arp2/3 enhances polymerisation by generating new branch points to existing actin filaments (reviewed in Amann and Pollard, 2001). In fibroblasts, Arp2/3 is located in the peripherial region and its inhibition severely disrupts actin organisation and membrane protrusion (Strasser *et al.*, 2004). Immunostaining studies showed that Arp2/3 was also located at the periphery in hippocampal neurons and neuroblastoma cell lines (Korobova and Svitkina, 2008). The elimination of Arp2/3 by small interfering RNA in primary neurons and neuroblastoma cell lines revealed that F-actin content is decreased, lamellipodial protrusion and retraction are inhibited and filopodia initiation and dynamics are disrupted (Korobova and Svitkina, 2008). Also, the depletion of Arp2/3 showed that RhoA activity is increased in these

cells. Arp2/3 is shown to be a downstream effector of Rac and Cdc42 (Rohatgi *et al.*, 1999; Klooster *et al.*, 2006). These results suggest that Arp2/3 may play a role in regulating the formation and dynamics of lamellipodia and filopodia by responding to Rac and Cdc42 as well as affecting RhoA activity.

The activity of gelsolin, an actin severing and capping protein on actin filaments is also impacted on by tropomyosin. This protein co-localises with actin filaments in the neurites and central region of the neuronal growth cones as well as the leading edge of lamellipodia and filopodia shown by immunostaining of fixed hippocampal neurons (Lu *et al.*, 1997). In gelsolin knockout (KO) mouse studies it has been shown that hippocampal neurons exhibit a greater number of filopodia in response to the lack of gelsolin which was due to a delayed retraction rate. Gelsolin also regulates the generation of filopodial dynamics (Lu *et al.*, 1997). This suggests that gelsolin plays a role in the formation and dynamics of filopodia.

Tropomyosin works in conjunction with formin as well as myosin to regulate elongation at the barbed end of the actin filament (Wawro *et al.*, 2007). At the barbed end of F-actin, mDir/formin which is the mammalian homologue of formin, enhances polymerisation by promoting actin nucleation (reviewed in Ishikawa and Kohama, 2007). The mDir/formin protein is found at the tip of filopodia, suggesting that it may play a role in regulating filopodial dynamics.

Myosin is part of a family of actin motor proteins and is involved in cell motility. Myosin II, which has been discussed earlier, can be recruited by certain

tropomyosin isoforms. The most prominent myosins in neuronal growth cones are myosin II and V. Myosin II drives retrograde flow of F-actin from the peripheral region of lamellipodia and filopodia to the central domain of growth cones (Lin *et al.*, 1997). In non-muscles, there are two subtypes of myosin II, myosin IIA and myosin IIB. Myosin IIB is more abundant in the growth cone than myosin IIA. Both myosin IIA and myosin IIB are found in the central regions of the growth cone with myosin IIB also located in the periphery of growth cones (Rochlin *et al.*, 1995). Studies using myosin IIB knockout mice have confirmed that myosin IIB is required for proper growth cone motility and that the rate of retrograde flow is increased in growth cones with the depletion of myosin IIB (Bridgman *et al.*, 2001; Brown and Bridgman, 2003). The increase in rate of retrograde flow suggests that myosin IIA may also play a role in this process and may functionally compensate for the loss of myosin IIB. The other myosin that is predominantly found in the growth cones is myosin V. Myosin V is also found in the cell body and colocalises with F-actin bundles in filopodial structures (Wang *et al.*, 1996). Chromophore-assisted laser inactivation (CALI) of myosin V in growth cones of chick dorsal root ganglion neurons significantly decreased the rate of filopodial extension without affecting the rate of filopodial retraction (Wang *et al.*, 1996). Taken together, myosin II and myosin V play different roles in controlling growth cone dynamics.

These studies demonstrate that tropomyosin isoforms regulate many actin binding proteins that affect the treadmilling of F-actin in growth cone dynamics and neuritogenesis.

1.8 Aims

The aim of this project is to investigate the role of Tm5NM1/2, isoforms containing exon 9d from the γTm gene, on growth cone function and the early stages of neuritogenesis. The effect of eliminating Tm5NM1/2 on growth cone dynamics and neurite formation including length and branching is investigated. Functional compensation by other neuronal tropomyosin isoforms for the loss of Tm5NM1/2 is analysed. Furthermore, the impact of Tm5NM1/2 depletion on the levels of active and inactive ADF/cofilin is examined.

1.9 Hypotheses

Growth cone structures in Tm5NM1 transgenics are larger (Schevzov *et al.*, 2005a) while growth cones of Tm5NM1/2 KO neurons are smaller in size as compared to WT controls (Fath *et al.,* manuscript in preparation). As the growth cone is a major dynamic structure of the neuron, the depletion of Tm5NM1/2 is hypothesised to also have an impact on the dynamic behaviour of growth cones.

In addition, the overexpression of Tm5NM1 increases neurite outgrowth (Schevzov *et al.*, 2005a). Therefore, it is predicted that the loss of Tm5NM1/2 will affect the regulation of neuritogenesis in neurons of Tm5NM1/2 KO mice. In Tm5NM1/2 depleted neurons, neurite outgrowth is hypothesised to be decreased.

On the molecular level, there is a significant decrease of ADF/cofilin activity while total ADF/cofilin is unaltered when Tm5NM1 is overexpressed (Bryce *et al.*, 2003). Therefore, it is hypothesised that with the depletion of Tm5NM1/2 the inactive form of ADF/cofilin is significantly decreased with unchanged total ADF/cofilin levels. As Tm5NM1 is a competitive inhibitor of active ADF/cofilin, the depletion of Tm5NM1/2 is predicted to alter the localisation of active ADF/cofilin in neurons.

Chapter 2

Materials and Methods

2.1 Materials

2.1.1 Mice deficient for Tm5NM1/2 isoforms (γ9d or Tm5NM1/2 KO mice)

For this study a mouse model was used which is deficient for products of the γTm gene containing exon 9d (γ9d or Tm5NM1/2 KO). All animal experiments were performed in accordance with institutional and National Health and Medical Research Council (NH&MRC) guidelines. The knockout construct used to delete the exon 9d containing isoforms from the γTm gene (Tm5NM1/2) as well as the generation of mice are described in detail (Fath *et al.*, manuscript in preparation).

2.1.2 List of Chemicals and Reagents

2.1.2.1 Media and sera for cell culture

Table 2.1 List of media and sera used in cell culture

MEDIA AND SERA	MANUFACTURER
Dulbecco's Modified Eagle's medium (DMEM)	Invitrogen, Carlsbad, CA, USA
Fetal bovine serum (FBS)	HyClone, Ogden, UT, USA
Neurobasal Medium (NB)	Invitrogen, Carlsbad, CA, USA
GlutaMax	Invitrogen, Carlsbad, CA, USA
B27 Supplement	Invitrogen, Carlsbad, CA, USA

2.1.2.2 Solutions and reagents for cell culture

Table 2.2 List of solutions and reagents used for cell culture

OTHER REAGENTS	MANUFACTURER
Water for Irrigation (ddH_2O)	Baxter Healthcare, Deerfield, IL, USA
Poly-D-lysine (PDL)	Sigma-Aldrich, Louis, MO, USA
Hanks Balanced Salt Solution (without Ca^{2+} and Mg^{2+})	Sigma-Aldrich, St. Louis, MO, USA
HEPES (4-(2-hydroxyethyl)-1-piperazineethanesulfonic acid)	Sigma-Aldrich, St. Louis, MO, USA
Trypsin solution from porcine pancreas	Sigma-Aldrich, St. Louis, MO, USA
Deoxyribonuclease I (DNase) from bovine pancreas	Sigma-Aldrich, St. Louis, MO, USA
Bovine Serum Albumin Fraction V IgG Free	Invitrogen, Carlsbad, CA, USA
Phosphate Buffered Saline (PBS) Tablets	MP Biomedicals, Aurora, OH, USA

2.1.2.3 Reagents for Immunofluorescence

Table 2.3 List of reagents for immunofluorescence

SOLUTIONS FOR IMMUNOFLUORESCENCE	MANUFACTURER
4,6-diamidino-2-phenylindole (DAPI)	Invitrogen, Carlsbad, CA, USA
Phalloidin Alexa Fluor 647 (Cy5)	Molecular Probes, Eugene, OR, USA
Immu-Mount	Thermo Electron Corporation, Waltham, MA, USA

2.1.2.4 Other Chemicals

Table 2.4 List of other chemicals used in experiments

OTHER CHEMICALS	MANUFACTURER
Micro-90	International Products Corporation, Burlington, NJ USA
Boric Acid	Selby-Biolab, Scoresby, Victoria, Australia
Sodium tetraborate	BDH, Poole, UK
Sodium Hydroxide	Amresco, Solon, OH, USA
Ethanol	Crown Scientific, Minto, NSW, Australia
Paraformaldehyde (PFA) powder	Sigma-Aldrich, St. Louis, MO, USA
Nonidet P-40 (NP40)	Calbiochem, La Jolla, CA, U.S.A
Methanol	Crown Scientific, Minto, NSW, Australia

2.1.3 Antibodies

2.1.3.1 Primary Antibodies

Table 2.5 List of primary antibodies used in experiments

ANTIBODIES	TARGETS	MANUFACTURER
γ9d	Tm5NM1/2	Chiron Mimotopes, Emeryville, CA, USA
CG3	All γTm gene products	Kind gift provided by Professor Jim Lin, IA, USA
α9b	TmBr2	Chiron Mimotopes, Emeryville, CA, USA
αf1b	TmBr2, TmBr3, Tm5a/b	Chiron Mimotopes, Emeryville, CA, USA
αf9d	Tm2, Tm3, Tm5a/b	Chiron Mimotopes, Emeryville, CA, USA
TUJ1	Neuronal β3 tubulin	Covance, Princeton, NJ, USA
Tau1	Microtubule associated protein Tau, dephosphorylated at serine 192-204 (Axonal marker) (Szendrei *et al.,* 1993)	Chemicon, Temecula, CA, USA
MAP2	Microtubule-associated protein 2 (Dendritic marker)	Chemicon, Temecula, CA, USA
pADF/cofilin	Phosphorylated ADF/cofilin (Inactive form)	Kind gift provided by Professor James R. Bamburg, CO, USA
Total ADF/cofilin	Total ADF/cofilin	Kind gift provided by Professor James R. Bamburg, CO, USA

2.1.3.2 Secondary Antibodies

Table 2.6 List of secondary antibodies used in experiments

ANTIBODIES	MANUFACTURER
Donkey Anti-Mouse Alexa Fluor 488 IgG	Molecular Probes, Eugene, OR, USA
Donkey Anti-Mouse Cy3 IgG	Jackson ImmunoResearch Laboratories, West Grove, PA, USA
Donkey Anti-Rabbit Alexa Fluor 488 IgG	Molecular Probes, Eugene, OR, USA
Donkey Anti-Rabbit Cy3 IgG	Jackson ImmunoResearch Laboratories, West Grove, PA, USA
Donkey Anti-Sheep Alexa Fluor 488 IgG	Molecular Probes, Eugene, OR, USA
Donkey Anti-Sheep Cy3 IgG	Jackson ImmunoResearch Laboratories, West Grove, PA, USA
Goat Anti-Mouse Alexa Fluor 488 IgM	Molecular Probes, Eugene, OR, USA
Goat Anti-Mouse Cy3 IgM	Jackson ImmunoResearch Laboratories, West Grove, PA, USA

2.1.4 Equipment and Software

2.1.4.1 List of Equipment used in experiments

Table 2.7 List of equipment used in experiments

EQUIPMENT	MANUFACTURER
13mm Glass Coverslips Circle Number 1	Menzel-Glaser, Braunschweig, Germany
8-well Lab-TekII Chambered Coverglass	Nalge Nunc International, Rochester, NY, USA
Multiwell 24 well tissue culture plates	Becton Dickinson Labware, Franklin Lakes, NJ, USA
Olympus BX50 Microscope (SPOT)	Olympus, Tokyo, Japan
Olympus IX81 Live Cell Microscope	Olympus, Tokyo, Japan
Sail Brand Microscope Slides	LOMB Scientific, Taren Point NSW, Australia

2.1.4.2 List of software used in experiments

Table 2.8 List of software used in experiments

SOFTWARE	MANUFACTURER
Adobe Photoshop	Adobe Systems, San Jose, CA, USA
MetaMorph Imaging Software 7.1	Molecular Devices, Sunnyvale, CA, USA
Microsoft Excel	Microsoft Corporation, Redmond, Washington, USA
SPSS Software	SPSS, Chicago, IL, USA

2.2 Methods

2.2.1 Preparing plates for cell culture

A detergent solution (2% MICRO-90 in milliQ water) was prepared and incubated in a 60ºC incubator for 15 mins. Round glass coverslips (Ø13mm) were placed into the heated detergent and incubated at 60ºC for 30 mins. After the incubation, the detergent was carefully decanted and the coverslips were washed thoroughly (more than 10x) with deionised water. After the washes, the water was replaced with 100% ethanol. The coverslips were washed twice with ethanol to ensure that no traces of water were left behind. Coverslips were left submerged in 100% ethanol in the cell culture hood until needed for plate preparation. The following steps for setting up cell culture plates were all performed under sterile conditions in class II cabinets.

2.2.1.1 Short-term cell culture plates

Cell culture plates (24 wells) were used for short-term cultures. In each well, 500µL of ddH_2O was added. Using forceps and an ethanol burner, each coverslip was flamed and cooled before being placed into separate wells. The water was aspirated off from each well and replaced with 0.1 mg mL^{-1} poly-D-lysine (PDL), which was diluted in borate buffer. The plates were incubated overnight at 37ºC in a humidified 5% CO_2 incubator. After the overnight incubation, the PDL solution was aspirated from each well. The plates were washed twice with water for irrigation for 1 hour in total. After the washes, the water was aspirated off and the plates were left to dry in the hood. Once the coverslips dried, the plates were sealed with parafilm and stored at 4ºC.

2.2.1.2 Long-term cell culture plates

The protocol for preparing and plating long-term cell culture plates have been previously described in detail (Fath *et al.*, 2009) (Figure 2.1). For this protocol 12-well cell culture plates were used. These plates were also used for short-term cultures as the resulting neuronal cells showed better morphology due to the presence of supporting cortical ring cultures. To prepare the plates, a drop of ddH_2O was placed into the middle of each well. Each glass coverslip was flamed with an ethanol burner, cooled and placed into the middle of the well, on top of the water droplet. Firstly at the edge of the bottom of the well, referred to as the "ring", 100µL of PDL solution was placed (Refer to section 2.2.1.1). This was done by dispensing the solution while tracing the edge at the bottom of the well. Another 100µL of PDL solution was then carefully placed on top of the coverslip, ensuring that the ring solution and the solution on the coverslip did not merge. The plates were incubated overnight at 37ºC in a humidified 5% CO_2 incubator. After the overnight incubation, the PDL solution was aspirated off from each well. The plates were washed 2x with ddH_2O for 1 hour in total. To wash, 100µL of ddH_2O was firstly added to the rings and then on top of the coverslip. After the two washes, the water was aspirated off and the plates were left to dry in the hood. The dried plates were sealed with parafilm and stored at 4ºC.

2.2.2 Dissecting and culturing hippocampal and cortical neuronal cells

Primary cells from dissected hippocampal and cortical tissues of 16.5 day embryos were cultured as described previously (Schevzov *et al.,* 2008; Fath *et al.,* 2009). Pregnant mice were sacrificed by cervical dislocation. Under sterile conditions, 16.5 day embryos were harvested and placed in petridishes on ice filled with HBSS. Brains were removed from these embryos and were cut longitudinally into two hemispheres. The meninges layer was peeled off from the brains and the cortical tissue was separated from the midbrain of each hemisphere. The hippocampal tissue was then dissected from the cortex. The dissected hippocampal and cortical tissues were incubated with 1x Trypsin for 30 mins and 1 hour respectively. The tissues were then treated with 1mg/mL DNAseI after which the cells were triturated 10x with wide and then narrow fire polished glass pipettes.

For short-term cultures, neuronal cells were plated onto PDL coated glass coverslips in 24-well cell culture plates (Fath *et al.*, 2009). The plating volume was adjusted to 500µL Dulbecco's Modified Eagle's medium (DMEM) containing 10% fetal bovine serum (FBS) per well. For plates using the long-term cell culture protocol, hippocampal or cortical cells were plated onto coverslips at a density of 2000 cells per mL in plating medium while $1x10^5$ cortical WT neurons were plated on the outside ring at a density of $1x10^6$ cells/mL in plating medium (Figure 2.1) (Fath *et al.*, 2009). These cultures were plated on the coverslip and the ring at 100µL volume per well. All cell culture

plates were incubated for two hours at 37ºC in a humidified 5% CO_2 incubator after which the medium was changed to growth medium (Neurobasal medium containing 2% B27 supplement and 0.5mM GlutaMax). For short-term culture plates, 500µL of plating medium was replaced with an equal amount of growth medium while for plates under the long-term culture protocol, the 100µL of culture on the coverslip and 100µL of culture in the ring were replaced by 1mL of growth medium added into the well (Figure 2.1).

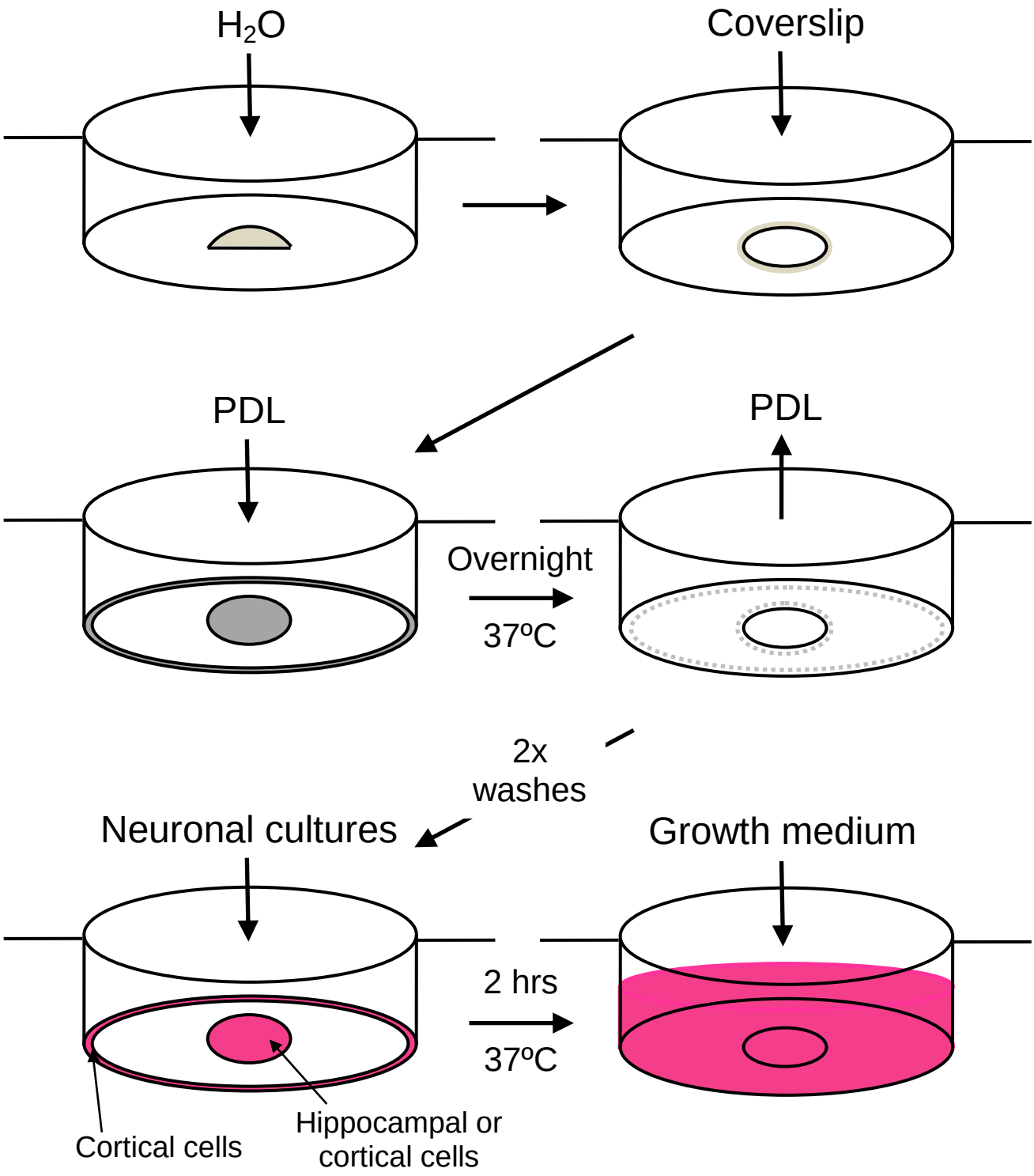

Figure 2.1 Protocol for plating long term cultures. A drop of water was placed in the middle of each well. A 13mm Ø round coverslip was placed on top of this water droplet. PDL was coated on the coverslip and at the edge of the bottom of the well, referred to as the "ring". After overnight incubation at 37ºC, the PDL solution was washed off and hippocampal and cortical neuronal cultures were plated onto the coverslip and the ring. After 2hrs at 37ºC, the neuronal cultures in plating medium were replaced with growth medium.

2.2.3 Immunofluorescence

Hippocampal and cortical neurons were cultured on PDL coated glass coverslips and fixed after 4 days with 4% PFA in PBS for 20 mins. After the fixation, the cells were washed 5x with PBS for 2 mins and permeabilised with 0.2% NP40 for 20 mins. The permeabilised cells were washed 5x with PBS for 2 mins and incubated with 2% FBS in PBS blocking solution for 30 mins. Cells were incubated with primary antibodies for 1 hour. After washing the cells 5x in PBS for 2 mins, the cells were incubated with fluorophore labelled secondary antibodies and DAPI for 30 mins. To avoid bleaching of the samples, the procedure was carried out in the dark at room temperature. Neuronal cells were washed 5x in PBS for 2 mins and then gently rinsed in distilled water before being mounted onto microscope slides using Immu-Mount. This protocol was followed by all immunofluorescence experiments unless otherwise stated.

2.2.3.1 Tropomyosin Localisation

Hippocampal and cortical neurons were cultured, fixed, permeabilised and stained as stated above. Primary antibodies used were the sheep polyclonal antibodies γ9d (Percival *et al.*, 2004), α9b, αf1b, αf9d (Schevzov *et al.*, 1997) and the mouse monoclonal antibodies TUJ1 and CG3 (Novy et al., 1993). The CG3 and γ9d antibodies detect isoforms from the γTm gene while the α9b, αf1b and αf9d antibodies detect isoforms from the αTm gene (Schevzov *et al.*, 2005b). The TUJ1 antibody detects neuron specific β3 tubulin.

All primary antibodies (except α9b) were diluted to 1:100 in 2% FBS in PBS blocking solution. α9b was used at a dilution of 1:200. Secondary antibodies used were the fluorophore-conjugated donkey anti-mouse and sheep antibodies at 1:250, diluted in 2% FBS in PBS blocking solution. DAPI was used at 1:1000, diluted in 2% FBS in PBS blocking solution. Cells were incubated with the secondary antibodies and DAPI for 30 mins in the dark at room temperature. After the secondary antibody staining, the cells were incubated with phalloidin far red (Alexa 647) which was used at 60U/mL, diluted in 1% FBS in PBS. The cells were washed 5x in PBS for 2 mins before being gently rinsed in distilled water and mounted onto microscope slides using Immu-Mount.

2.2.3.2 Neurite Outgrowth

Primary antibodies used to identify the axonal and dendritic compartments were the mouse monoclonal Tau1 and the rabbit polyclonal MAP2 antibodies. The Tau1 and MAP2 antibodies were used at 1:250, diluted in 2% FBS in PBS blocking solution. The secondary antibodies used were the fluorophore-conjugated donkey anti-mouse and rabbit antibodies. These were used at 1:250, diluted in 2% FBS in PBS blocking solution. DAPI was used at 1:1000, diluted in 2% FBS in PBS blocking solution.

2.2.3.3 Determining the inactive and total levels of ADF/cofilin

Hippocampal and cortical neurons were cultured and fixed as stated above. Fixed cells were washed 2x with PBS and permeabilised with ice cold methanol for 10 mins at room temperature. Neuronal cells were washed once with PBS and incubated 3x for 5 mins with 0.5% BSA in PBS blocking solution. The cells were stained with the primary antibodies for overnight at 4ºC in a humidified container. After 3x washes with 0.5% BSA in PBS cells were stained with the secondary antibodies for 1 hour in the dark at room temperature. The cells were then washed 2x in PBS and incubated with DAPI for 10 mins at room temperature in the dark. Following DAPI staining, the cells were washed 2x with PBS and mounted onto microscope slides using Immu-Mount.

Primary antibodies used were the rabbit polyclonal ser3 phospho-ADF/cofilin (pADF/cofilin) and mouse monoclonal ADF/cofilin, diluted to 1:500 in 0.5% BSA in PBS blocking solution. Secondary antibodies used were the fluorophore-conjugated donkey anti-mouse and rabbit antibodies, diluted 1:2000 in 0.5% BSA in PBS blocking solution. DAPI was used at 1:10,000, diluted in PBS.

2.2.4 Generation and analysis of kymographs

Hippocampal neurons were plated in 8-well chamber slides at a density of $2x10^3$ cells per chamber. A number of experiments represented by three different chamber slides were set up. Neurons were cultured for 1 day and imaged on an Olympus IX81 live cell microscope equipped with an environmental chamber. Neurons were imaged for 8 mins and 20 secs at 37ºC and 5% CO_2 with a picture captured every 1.4 secs. Images were assembled in a stack using MetaMorph software version 7.1. Lines of 1 pixel thickness were selected at various positions perpendicular to the cell edge of growth cones in between two filopodia. Using MetaMorph software, kymographs were generated from growth cone depicted along those lines. Protrusions of growth cones are represented by positive slope lines on the kymographs while retractions are shown as negative slope lines. When the growth cone is pausing this is depicted by a horizontal line (Figure 2.2). Protrusion and retraction rates of growth cones were analysed from kymographs. For each growth cone analysed, an average of 4 kymographs were collected and the mean was determined. The protrusion and retraction rates as well as the frequency at which the growth cone changes between protrusion and retraction were analysed.

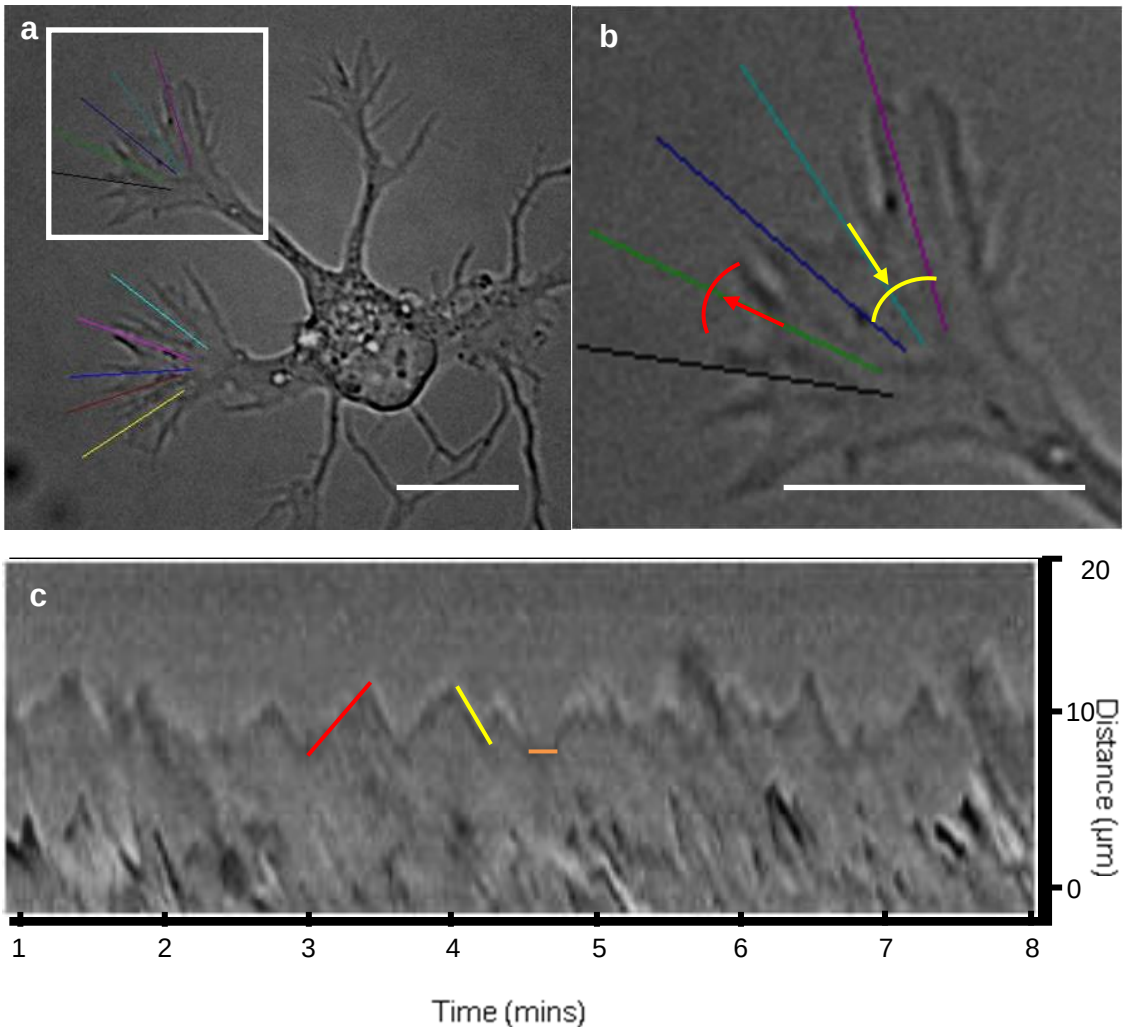

Figure 2.2 Analysis of growth cone dynamics using kymographs. Hippocampal neurons were cultured for 1 day and imaged every 1.4 secs for 8 mins and 20 secs. A still image of a hippocampal neuron is shown (a) and boxed in white is a growth cone which is enlarged (b). Lines of 1 pixel thickness were selected at various positions on growth cones perpendicular to the cell edge in between two filopodia. Kymographs were generated along that line using MetaMorph software (c). The advancement and retraction of the lamellipodial membrane are depicted as red and yellow curved lines. The red positive slope line represents growth cone protrusion while the yellow negative slope line depicts growth cone retraction. The horizontal line shown in orange corresponds to the pausing of the growth cone. Scale bar 20µm.

2.2.5 Analysis of Tropomyosin Localisation

Hippocampal and cortical neurons were cultured for 4 days at a density of 5000 cells or 10,000 cells per well. Two to three coverslips were stained per condition for each experiment. Two independent experiments were performed. In each experiment, 5 neurons per coverslip were imaged using an Olympus IX81 live cell microscope with a 40x oil objective. The relative intensity level and the location of the signals from the two antibodies used to stain each coverslip were analysed using MetaMorph Software version 7.1.

2.2.6 Analysis of Neurite outgrowth

To determine the optimal conditions for comparing neurite outgrowth of Tm5NM1/2 KO neurons with WT controls, primary hippocampal and cortical neurons were plated at $50x10^3$ cells per well and fixed every day from 1 day to 10 days. For each time point, 50 neurons were imaged either on an Olympus BX50 SPOT or Olympus IX81 live cell microscopes using 20x objectives. Neurite lengths were measured using MetaMorph software and the rate of neurite outgrowth (length vs time) was plotted in Microsoft Excel. The optimal conditions for comparing neurite outgrowth between Tm5NM1/2 KO and WT neurons were determined to be at $50x10^3$ cells per well cultured for 4 days.

To compare neurite outgrowth between Tm5NM1/2 KO neurons and WT controls, hippocampal and cortical neurons were plated at a density of $50x10^3$ cells per well and at an optimal time of 4 days. Images of 50 fixed neurons were taken from each coverslip either on the Olympus BX50 SPOT or Olympus IX81

live cell microscope using the 20x objective. For each condition, 3 coverslips were stained and three independent experiments were performed. Neurite lengths were determined by outlining the entire extension or protrusion using MetaMorph software version 7.1. The data were collated in Microsoft Excel. These data for both Tm5NM1/2 KO and WT neurons were first separated into primary, secondary and tertiary neurites (Figure 2.3) and secondly divided into axons and dendrites (Figure 2.4). From these results, axon and dendrite primary and secondary branching were determined and analysed between Tm5NM1/2 KO and WT neurons (Figure 2.3).

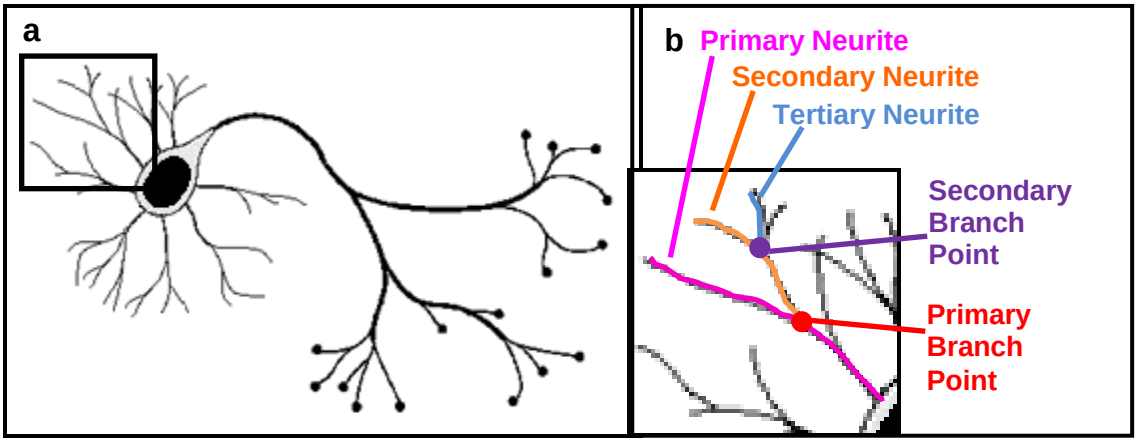

Figure 2.3 Classification of neurites and branch points. A schematic diagram of a neuron (a) with a neurite section enlarged (b). A primary neurite protrudes from the cell body while a secondary neurite extends from the primary neurite. Similarly, tertiary neurites originate from the secondary neurite. Neurite lengths were measured by outlining the length of the protrusion using MetaMorph. Branching was determined using these results. A primary branch point is the junction between primary and secondary neurite whilst a secondary branch point is the link between secondary and tertiary neurites.

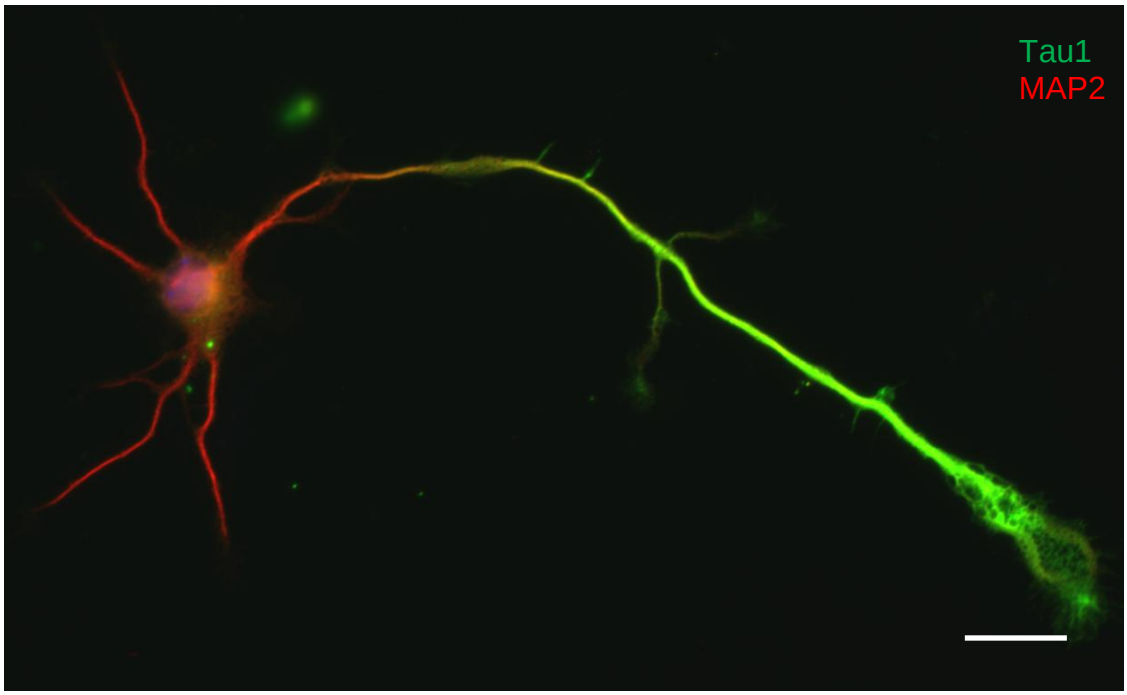

Figure 2.4 Immunofluorescence staining of a polarised neuron. Neurons have been stained using Tau1 (green) and MAP2 (red) antibodies that detect axons and dendrites respectively. A polarised neuron has distinct green staining at one single axon. Scale bar 20µm.

2.2.7 Analysis of inactive pADF/cofilin as a ratio of the total ADF/cofilin

Hippocampal and cortical neurons were cultured for 4 days. A total of 2 coverslips were stained and two independent experiments were performed. For each experiment, 10 images were taken on the Olympus IX81 live cell microscope.

The intensity of pADF/cofilin was quantified as a ratio to total ADF/cofilin using MetaMorph software. The divide function was used to determine the intensity of pADF/cofilin staining over total ADF/cofilin in neuronal growth cones. The ratios were collated in Microsoft Excel and compared between WT and Tm5NM1/2 KO neurons.

2.2.8 Statistical Analysis

Statistical analyses were performed on growth cone dynamics and neurite outgrowth data using the parametric 2 sample independent T test or non parametric Mann Whitney U Test from the SPSS software.

Chapter 3

Effect of Tm5NM1/2 depletion on growth cone dynamics

3.1 Introduction

Tm5NM1 localises to growth cones of developing neurons which indicates that it may play a role in growth cone development (Schevzov *et al.,* 1997; Schevzov *et al.,* 2005a). When Tm5NM1 is overexpressed the growth cone sizes of cultured hippocampal and cortical neurons from these mice are significantly increased (Schevzov *et al.*, 2005a; Schevzov *et al.*, 2008). Furthermore, Tm5NM1 alters growth cone size via increasing the F-actin pool (Schevzov *et al.*, 2008). This strongly suggests that Tm5NM1 regulates the amount of microfilaments in these structures. As tropomyosins are actin stabilising proteins, Tm5NM1 may also influence the actin dynamics of these microfilaments. Hence, the depletion of Tm5NM1/2 was hypothesised to have an impact on growth cone dynamics via its regulation of F-actin.

Results showed that the protrusion rates of homozygous Tm5NM1/2 KO growth cones were significantly increased compared to WT samples while retraction rates and rate of directional change were comparable to WT mice. From

hemizygous Tm5NM1/2 KO growth cones, protrusion and retraction rates were similar to WT controls while the rate of directional change was significantly decreased when compared to WT neurons.

3.2 Results

Growth cone dynamics in neurons from hemizygous and homozygous Tm5NM1/2 KO mice were analysed by generating kymographs at the leading edge of growth cones (Figure 3.1). From these kymographs, the mean protrusion and retraction rates as well as rate of directional change were determined.

Growth cone dynamics were analysed from kymographs of 3 independent experiments and these results were represented in separate graphs (Figures 3.2a, 3.2b and 3.2c). Slight variations were observed between these three experiments. The data from these 3 experiments were pooled together into a single graph (Figure 3.3). Protrusion rates in hemizygous and homozygous Tm5NM1/2 KO growth cones were both increased when compared to WT samples, however only the increase in Tm5NM1/2 KO growth cones was found to be significant ($p=0.007$). Retraction rates in both hemizygous and homozygous Tm5NM1/2 samples were comparable to WT samples. The rate of directional change was significantly decreased in hemizygous Tm5NM1/2 KO growth cones ($p<0.0001$) while in homozygous KO samples there was a trend towards an increased rate of directional change when compared to WT samples.

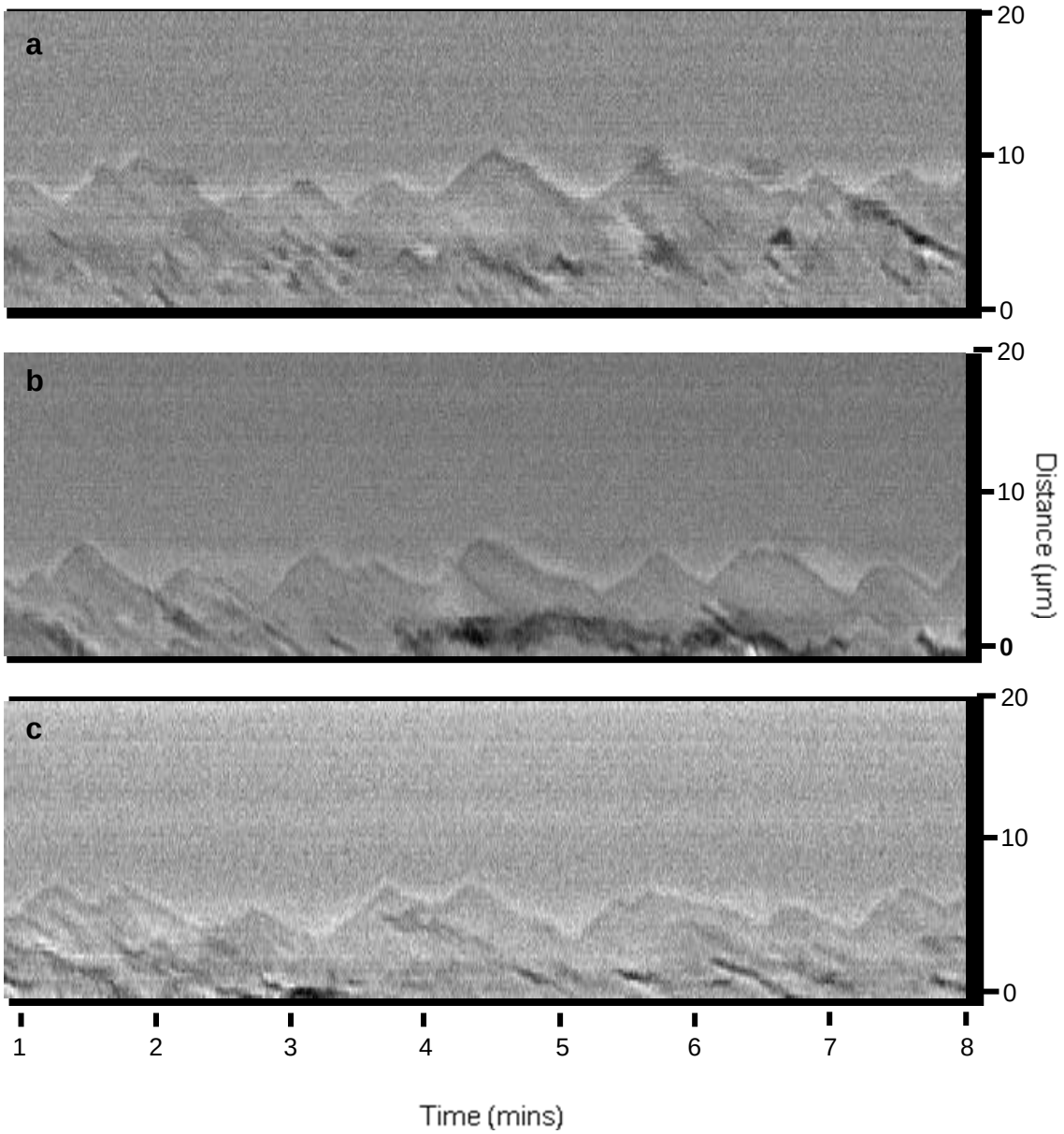

Figure 3.1 Kymographs of WT, hemizygous and homozygous Tm5NM1/2 KO neurons. These kymographs, depicting the dynamics of growth cones, appear similar between WT (a), hemizygous Tm5NM1/2 (b) and homozygous Tm5NM1/2 KO (c) neurons.

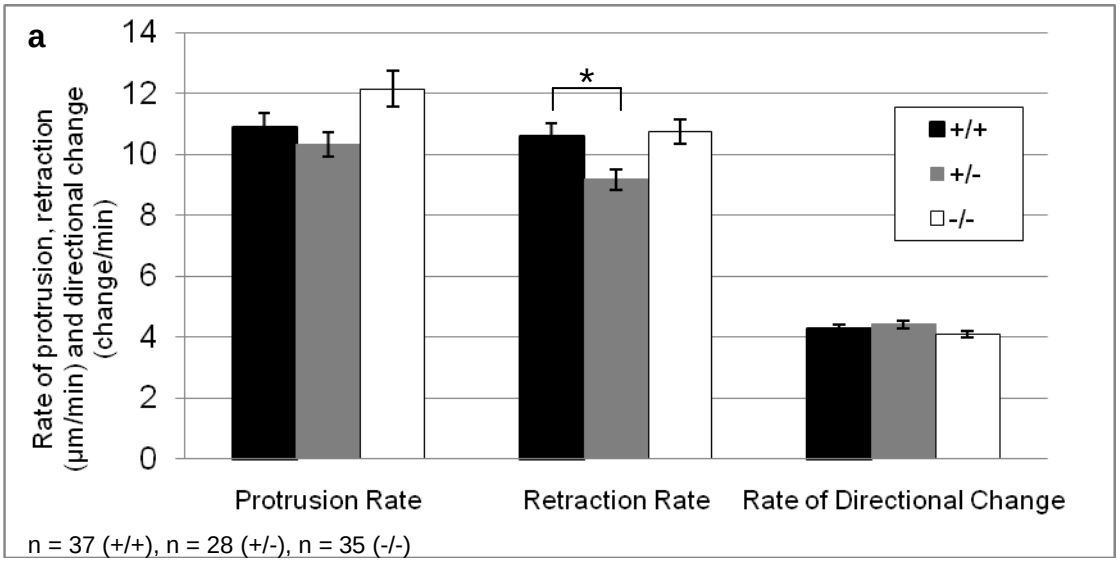

n = 37 (+/+), n = 28 (+/-), n = 35 (-/-)

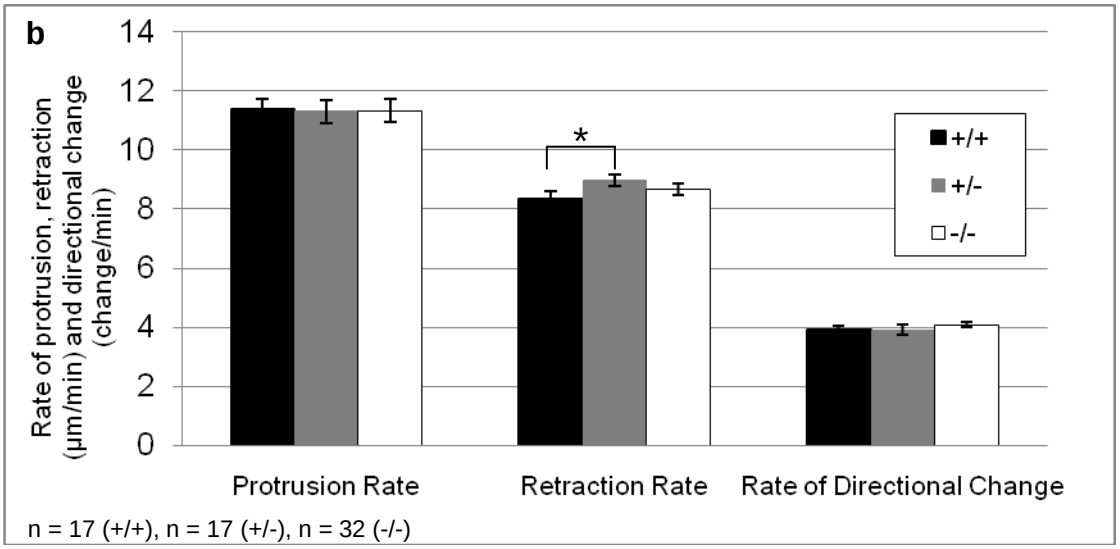

n = 17 (+/+), n = 17 (+/-), n = 32 (-/-)

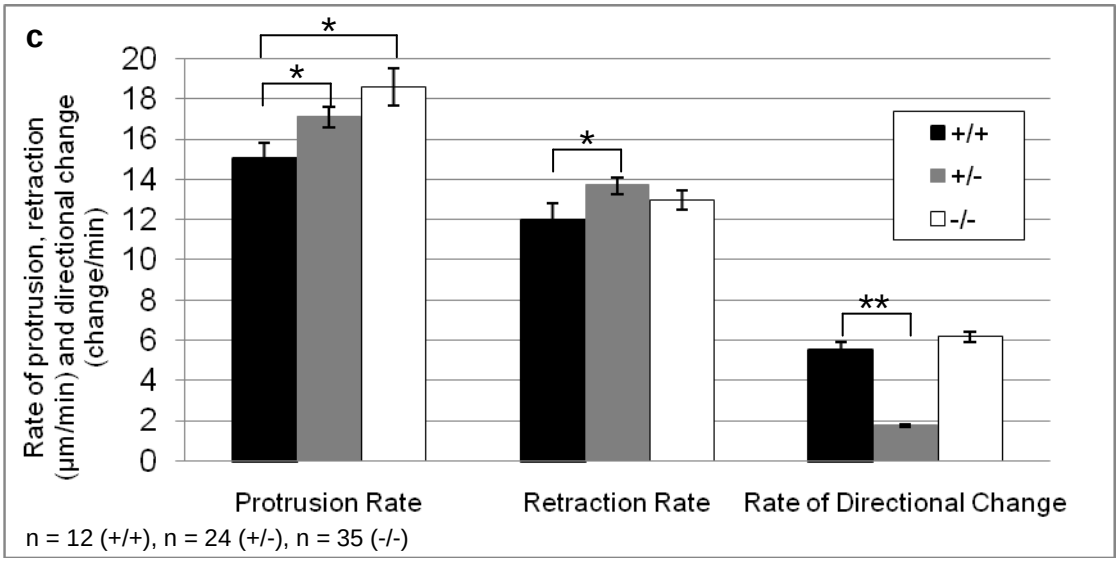

n = 12 (+/+), n = 24 (+/-), n = 35 (-/-)

Figure 3.2 Growth cone dynamics of WT, hemizygous and homozygous Tm5NM1/2 KO hippocampal neurons from three independent experiments. Each graph represents a separate experiment (a, b, c). Protrusion rates were only significantly different in experiment 3. There was a significant increase in protrusion rates from both hemizygous Tm5NM1/2 KO growth cones (p=0.035) and homozygous KO growth cones (p=0.02) when compared to WT controls. Retraction rates of hemizygous Tm5NM1/2 KO growth cones were all significantly different when compared to WT samples (Experiment 1 – p=0.017, Experiment 2 – p=0.038, Experiment 3 – p=0.02) but not from homozygous KO growth cones. Rate of directional change was only significantly different in hemizygous Tm5NM1/2 KO growth cones in experiment 3 (p<0.0001) Mean protrusion, retraction rates and rate of directional change for all growth cones are shown. n represents the total number of kymographs analysed. Error bars represent standard error of the mean. *p<0.05, **p<0.0001

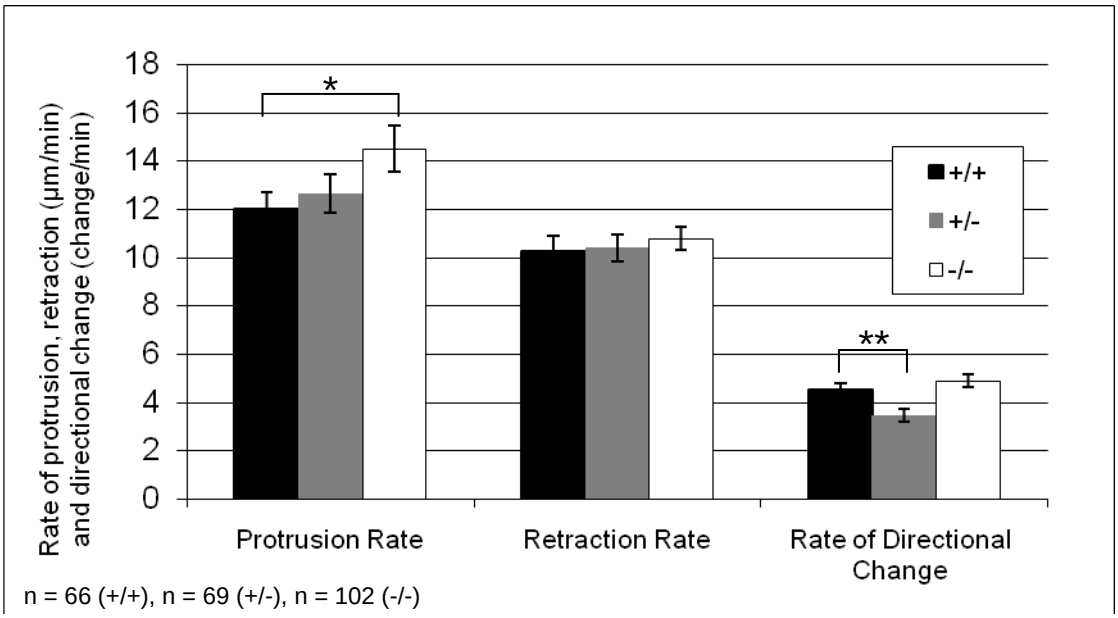

Figure 3.3 Effect of Tm5NM1/2 depletion on protrusion, retraction rates and rate of directional change in hippocampal neurons. Protrusion rates of homozygous KO growth cones are significantly increased (p=0.007) while rate of directional change from hemizygous KO growth cones are significantly decreased (p<0.0001) when compared to WT counterparts. Mean protrusion, retraction rates and rate of directional change for all growth cones are shown. n represents the total number of kymographs analysed. Error bars represent standard error of the mean. *p<0.05, **p<0.0001

3.3 Discussion

3.3.1 Variability between experiments

There are small variabilities between the three experiments. This could be due to slight alterations in the conditions under which these neurons have been cultured. Even though the number of days in culture and the density at which these cultures are plated are controlled, there are some conditions that cannot be completely controlled between experiments. The neuronal cultures have been cultured and imaged at 37ºC and 5% CO_2 however these cultures are very sensitive and react to small changes in culture conditions. The temperature and CO_2 levels may be altered with the opening of the incubator which is necessary for medium changes. The number of times and the duration each time the incubator is opened cannot be strictly controlled. As these are live cultures that are imaged, the fluctuating conditions inside the environmental chamber of the microscope may add another factor of variation in the results between these experiments.

3.3.2 Tm5NM1/2 isoforms are not essential for the formation of growth cones and regulation of dynamics

Previous immunofluorescence images showed that Tm5NM1 is present in the peripheral regions of growth cones of developing neurons (Schevzov *et al.*, 2005a). This suggests that this isoform may be involved in the regulation of dynamic structures of the growth cone. However, results show that neurons lacking Tm5NM1/2 exhibit only a subtle change in their phenotype with regards to growth cone dynamics as compared to neurons from WT control mice. This indicates that Tm5NM1/2, products from the γTm gene, may not be essential for growth cone function.

Alternatively Tm5NM1/2 could be required for growth cone function but are rescued by compensating tropomyosin isoforms. Previously, western blot analysis has shown that with the loss of Tm5NM1/2, expression of exon 9c containing isoforms of the γTm gene (Tm5NM4/7) is upregulated. However, it is unlikely that the amount of isoform product would be sufficient to rescue the loss of Tm5NM1/2 in neurons cultured for 1 day from Tm5NM1/2 KO mice. Less than 1% of the depleted Tm5NM1/2 is compensated by total γTm gene products at 1DIV and this compensation peaks at about 15% at 4DIV (Fath *et al.* manuscript in preparation). Another candidate is Tm4. This appears to be more likely as Tm4 sorts to the growth cone structure and may play a role in the stabilisation of the actin filaments in this region (Had *et al.*, 1994).

3.3.3 Partial functional compensation by other tropomyosin isoforms influence actin filament dynamics in neuronal growth cones

Results presented here show that with regards to growth cone dynamics, the protrusion and retraction rates were similar between hemizygous Tm5NM1/2 KO and WT neurons. As the effects were comparable to WT controls, this suggests that the stability and turnover rate of actin filaments within the growth cone is similar to WT controls. The partial loss of Tm5NM1/2 may have affected the stability of the actin filaments. However, in the hemizygous Tm5NM1/2 KO mice, only half of Tm5NM1/2 isoform product is knocked out leaving behind a pool of Tm5NM1/2 isoforms which can either homodimerise or heterodimerise with other tropomyosin isoforms. Even though non-muscle tropomyosin isoforms have been found to prefer homodimerisation over heterodimerisation (Gimona *et al.,* 1995), Tm5NM1/2 can also form heterodimers. *In vitro* data show heterodimer formation of Tm5NM1/2 with Tm5a, Tm5b and Tm4, preferentially in that order (Temm-Grove *et al.,* 1996; Araya *et al.,* 2002). Hence, a potential impact on actin filament instability due to the hemizygous loss of Tm5NM1/2 may be restored by the dimerisation of Tm5NM1/2 with Tm4 or Tm5a/5b. Tm4 localises to the central part of the growth cone and to the base of filopodia (Had *et al.*, 1994). Tm5a/5b isoforms localise to growth cone structures when they form at the end of neurites (Schevzov *et al.*, 1997). Tm5a/5b isoforms also have the highest affinity to F-

actin compared to any other tropomyosin isoforms that have been studied (Moraczewska *et al.,* 1999). As Tm5NM1/2 preferentially associates with Tm4 and Tm5a/5b, isoforms which are found in growth cones, they are likely candidates to functionally compensate for the hemizygous loss of Tm5NM1/2.

In homozygous Tm5NM1/2 KO neurons, protrusion rates were significantly increased while retraction rates were comparable to WT samples. These results suggest that the stability of actin filaments in growth cones from homozygous Tm5NM1/2 KO neurons is different to WT controls. A potential difference in stability of actin filaments due to the depletion of Tm5NM1/2 can be explained by two possible scenarios. Firstly, the loss of Tm5NM1/2 may be compensated at a functional level by other tropomyosin isoforms. As discussed earlier, it appears unlikely that Tm5NM4/7 isoforms are functionally compensating as it only corresponds to less than 1% of the level of Tm5NM1/2 product (Fath *et al.* manuscript in preparation). Instead, other tropomyosin isoforms could functionally compensate by localising to specific regions within the growth cone structures where Tm5NM1/2 is lost while the overall protein levels are unchanged. Tm4 and Tm5a/5b appear to be likely candidates as they are found in growth cone structures of developing neurons (Had *et al.*, 1994; Schevzov *et al.*, 1997). Therefore, it is possible that unattached Tm4 or Tm5a/5b can associate with F-actin in the growth cones that have now been depleted of Tm5NM1/2. The resulting actin filament dynamics may differ from WT controls as it depends on its association with specific tropomyosin isoforms. Previously, it has been shown that the association of Tm5NM1/2 with actin filaments results in more stable filaments while the association of another

isoform, TmBr3, with actin filaments results in higher turnover rate of the filaments (Bryce *et al.*, 2003). Hence, actin filaments decorated by Tm4 or Tm5a/5b in homozygous Tm5NM1/2 KO neurons may have different dynamics to actin filaments associated with Tm5NM1/2 in WT controls. Another possibility is that Tm5NM1/2 are not functionally compensated by Tm4 or Tm5a/5b as they may bind to different actin filament populations within growth cones. The actin filaments depleted of Tm5NM1/2 will have an altered stability compared to actin filaments associated with Tm5NM1/2. The two possible scenarios may be revealed by examining the levels of unattached Tm4 or Tm5a/5b associating with actin filaments. This may be determined by analysing the size of the soluble and insoluble pools of Tm4 and Tm5a/5b isoforms. If the soluble pool of Tm4 or Tm5a/5b is unchanged then this suggests that Tm4 or Tm5a/5b are not associating with actin filaments to compensate for the lack of Tm5NM1/2. A decrease in the soluble pool of Tm4 or Tm5a/5b indicates that Tm4 or Tm5a/5b is recruited to actin filaments. However, this does not necessarily mean that the corresponding tropomyosin isoforms have associated with F-actin which lacks Tm5NM1/2. To determine whether the tropomyosin has bound specifically to F-actin that has been depleted of Tm5NM1/2, immuno-electron microscopy needs to be performed. This will allow the visualisation of individual actin filaments and their association with particular tropomyosin isoforms by immuno-labelling.

Chapter 4

Localisation of tropomyosin isoforms in Tm5NM1/2 depleted neurons

4.1 Introduction

Previous analysis of neuronal tissue from Tm5NM1/2 KO mice revealed a partial upregulation of γTm products containing exon 9c, Tm5NM4/7. However a recent study using immunofluorescence staining on neurons cultured at 4DIV from Tm5NM1/2 deficient mice have shown that only about 15% of total γTm gene product is formed compared to WT controls (Fath *et al.,* manuscript in preparation). The aim of this section is to investigate the localisation of the compensatory isoforms Tm5NM4/7 and products from other tropomyosin genes.

Results of immunofluorescence analysis show that isoforms from the γTm gene are not present at neurite tips at detectable levels in Tm5NM1/2 KO neurons where Tm5NM1/2 are normally found. In addition, other neuronal tropomyosin isoforms from the αTm gene including Tm5a/5b, TmBr2 and TmBr3 show no

difference in their localisation in homozygous Tm5NM1/2 KO neurons compared to WT control, with the isoforms colocalising to neurite tips and growth cone structures in hippocampal and cortical neurons. The low levels of Tm5NM4/7 detected by western blot analysis are also unlikely to functionally compensate for the loss of Tm5NM1/2. However, a single isoform or a combination of Tm5a/5b, TmBr2 and/or TmBr3 isoforms may increase its localisation to growth cone structures therefore compensating at a functional level for the loss of Tm5NM1/2.

4.2 Results

4.2.1 Confirmation of the lack of Tm5NM1/2 expression in Tm5NM1/2 KO neurons

Firstly, it was confirmed that neurons from Tm5NM1/2 KO mice used in these experiments lack Tm5NM1/2 expression. Hippocampal and cortical neurons from both WT and Tm5NM1/2 KO mice were stained using the γ9d antibody which detects the isoforms Tm5NM1/2. In WT neurons, Tm5NM1/2 have a prominent localisation at neurite tips and within the growth cone structure. The deficiency of Tm5NM1/2 in neurons from Tm5NM1/2 KO mice is confirmed by the lack of γ9d signal throughout the neurons (Figure 4.1). Neurons derived from these mice were then used to determine whether other tropomyosin isoforms functionally compensate for the lack of Tm5NM1/2.

4.2.2 γTm gene products are not functionally compensating for the loss of Tm5NM1/2

As Tm5NM1/2 are isoforms from the γTm gene, functional compensation by other isoforms from the same gene was investigated. The CG3 antibody was used as it detects all products from the γTm gene. Results show that the CG3 signal is present at neurite tips and growth cone structures of WT neurons while no signal is detected in Tm5NM1/2 KO neurons (Figure 4.1). The complete lack of detectable CG3 signal in Tm5NM1/2 KO neurons indicates that other isoforms from the γTm gene are not likely to functionally compensate for the loss of Tm5NM1/2.

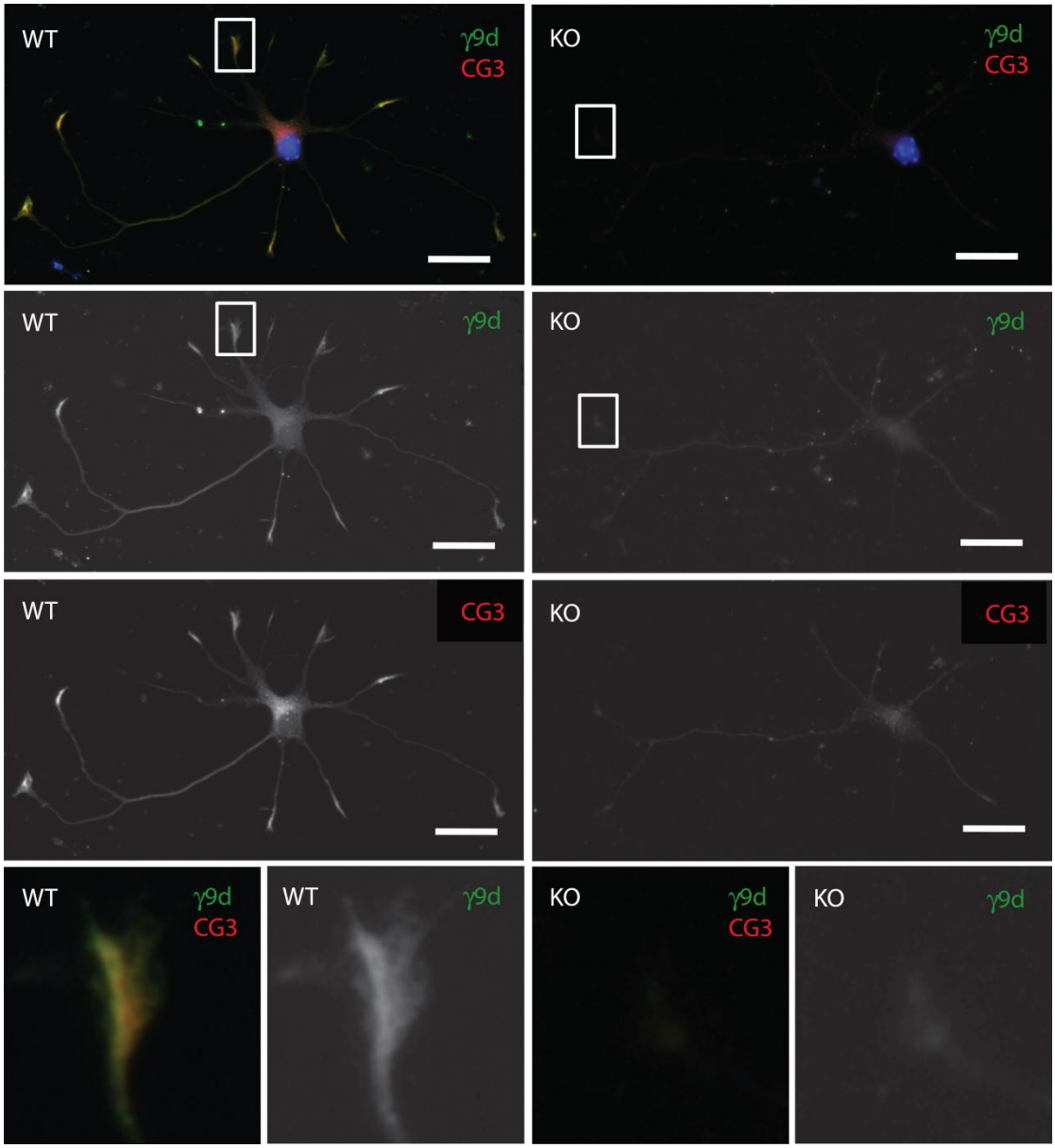

Figure 4.1 Alternative isoforms from the γTm gene are not compensating at a functional level for the loss of Tm5NM1/2. Hippocampal WT and Tm5NM1/2 KO neurons have been costained with the CG3 and γ9d antibodies. The use of the γ9d antibody specific for Tm5NM1/2 showed signal at the neurite tips and growth cone structures in WT samples. As expected, Tm5NM1/2 signal was not detected at any neuronal structures in Tm5NM1/2 KO neurons. The CG3 antibody detects all isoforms from the γTm gene. The CG3 antibody colocalises to neurite tips and growth cone structures in WT neurons but no signal was detected in any neuronal structures in Tm5NM1/2 KO neurons. This indicates that the remaining products from the γTm gene were not functionally compensating for the loss of Tm5NM1/2. Scale bar 20µm.

4.2.3 Other neuronal tropomyosins may functionally compensate for the lack of Tm5NM1/2

As isoforms from the γTm gene were not functionally compensating for the lack of Tm5NM1/2, altered localisation of tropomyosins from other tropomyosin genes were analysed. Stainings using the α9b (Figure 4.2), αf1b (Figure 4.3) and αf9d (Figure 4.4) antibodies were analysed. Samples were co-stained using the TUJ1 antibody to visualise neurite structures. The TUJ1 antibody targets β3 tubulin which is present in the soma, dendrites and axons. The α9b antibody specifically detects the isoform TmBr2 while the αf1b antibody targets the isoforms Tm5a, Tm5b, TmBr2 and TmBr3. In addition, the αf9d antibody detects the isoforms Tm6, Tm2, Tm3, Tm5a and Tm5b. In neurons, the only expressed isoforms that are detected by the αf9d antibody are Tm5a/5b. Immunostaining using the α9b, αf1b and αf9d antibodies showed signal at some but not all neurite tips and growth cone structures in both WT and Tm5NM1/2 KO neurons (Figure 4.2, 4.3, 4.4). Therefore either a single isoform or a combination of these tropomyosin isoforms, TmBr2, TmBr3 and Tm5a/5b, from the αTm gene may be able provide functional compensation for the lack of Tm5NM1/2.

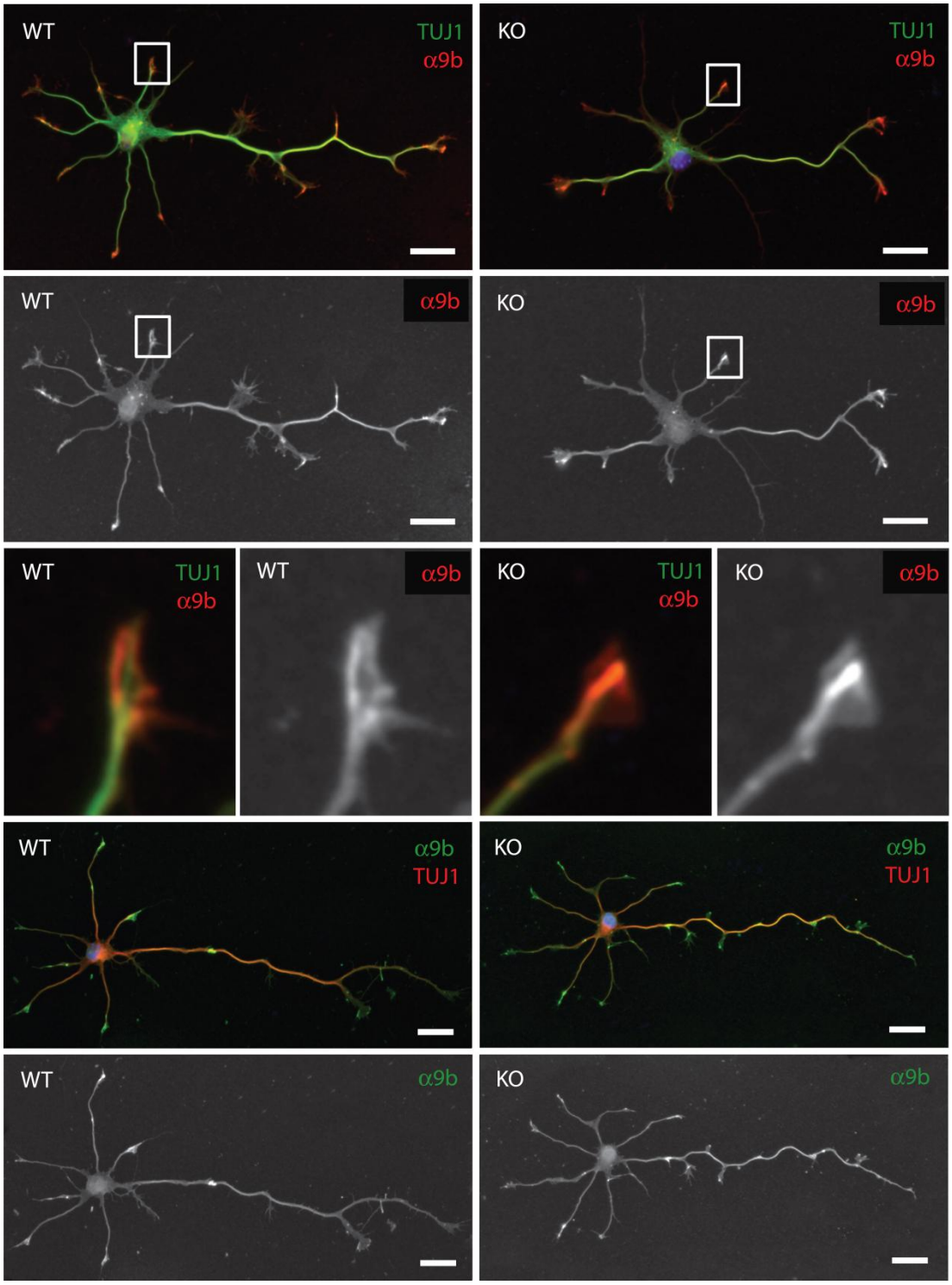

Figure 4.2 TmBr2 localises to growth cones and may functionally compensate for the loss of Tm5NM1/2. Hippocampal WT and Tm5NM1/2 KO neurons have been stained using the α9b and TUJ1 antibodies. The TUJ1 antibody detects β3 tubulin in all regions of the neuron except the growth cones. The α9b antibody targets TmBr2. Results using the α9b antibody showed that TmBr2 localises to some neurite tips and growth cone structures in both Tm5NM1/2 KO neurons and WT samples. Scale bar 20µm.

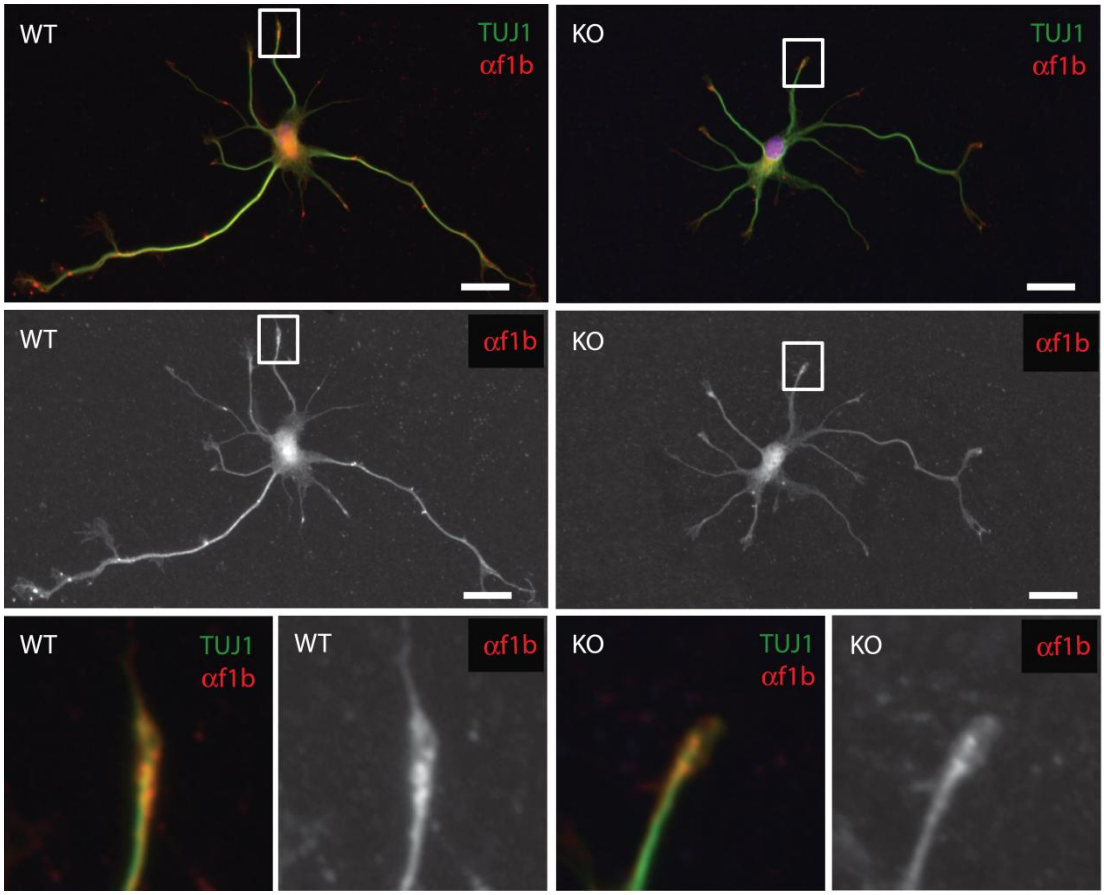

Figure 4.3 TmBr2, TmBr3 and/or Tm5a/5b isoforms localise to the growth cone structures and may functionally compensate for the loss of Tm5NM1/2. Hippocampal WT and Tm5NM1/2 KO neurons have been stained using the αf1b and TUJ1 antibodies. The TUJ1 antibody detects β3 tubulin in every structure of the neuron except growth cones. The αf1b antibody detects TmBr2, TmBr3 and Tm5a/5b isoforms. Staining using the αf1b antibody showed that TmBr2, TmBr3 and/or Tm5a/5b localises to some neurite tips and growth cone structures in both WT and Tm5NM1/2 KO neurons. Scale bar 20µm.

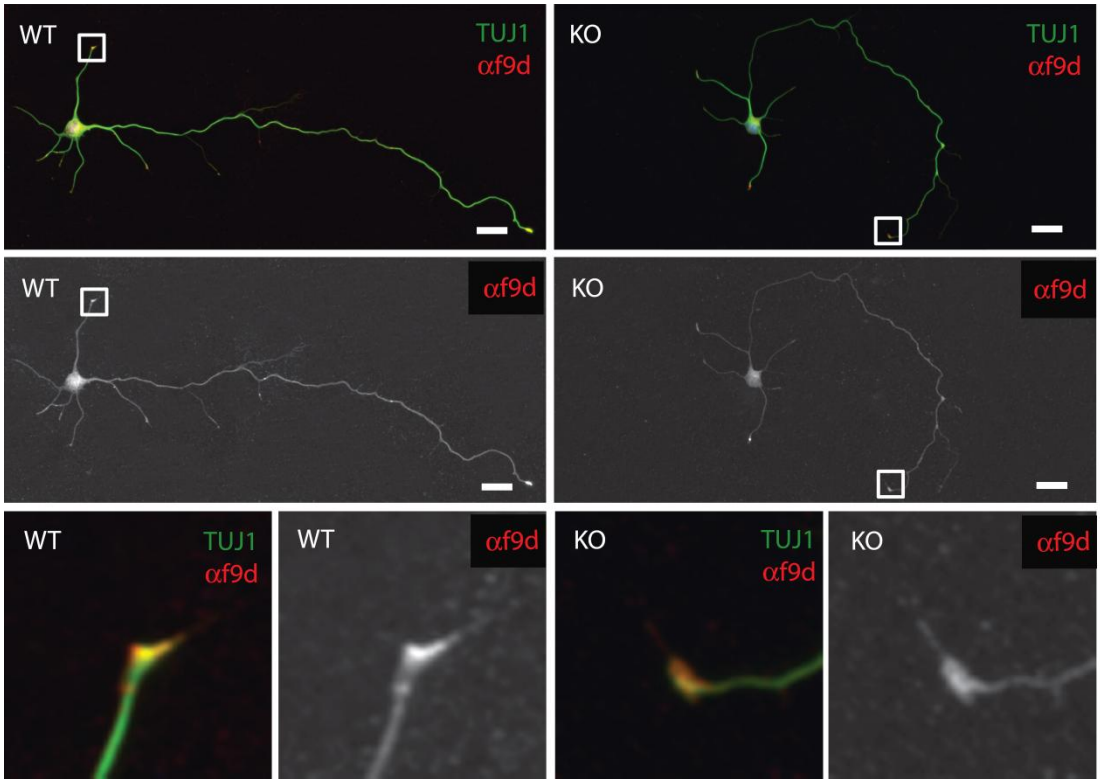

Figure 4.4 Tm5a/5b isoforms localise to the growth cones and may functionally compensate for the loss of Tm5NM1/2. Hippocampal WT and Tm5NM1/2 KO neurons have been stained with the αf9d and TUJ1 antibodies. The TUJ1 antibody detects β3 tubulin in all regions of the neuron except the growth cones. The αf1b antibody only detects Tm5a/5b isoforms in neurons. The localisations of the αf9d signal depicting Tm5a/5b isoforms are found in some neurite tips and growth cone structures in both Tm5NM1/2 KO neurons and WT samples. Scale bar 20μm.

4.3 Discussion

Western blot analysis of neuronal tissue from homozygous Tm5NM1/2 KO embryonal mice has shown that there is a partial upregulation of Tm5NM4/7, exon 9c products from the γTm gene. The aim was to determine whether these γTm gene products translate to partial functional compensation for the loss of Tm5NM1/2. Results presented here have shown that the γTm gene products are not present at detectable levels in growth cone structures of Tm5NM1/2 KO neurons. However, previous immunofluorescence studies on neuronal cultures have revealed that there were 15% of total γTm gene products present in Tm5NM1/2 KO neurons at 4DIV. Therefore, about 15% of the total Tm5NM1/2 KO neuronal population are compensated by Tm5NM4/7 at 4DIV. The compensation by Tm5NM4/7 to the small population of Tm5NM1/2 KO neurons may be undetected as only a small sample size was analysed in this experiment. Nevertheless, the formation of other γTm gene products, including the low levels of Tm5NM4/7, may only be partially compensating at a functional level for the loss of Tm5NM1/2.

4.3.1 Other tropomyosin isoforms may functionally compensate for the lack of Tm5NM1/2 in growth cone structures

As Tm5NM4/7 and other γTm gene products are not likely to fully compensate at a functional level for the loss of Tm5NM1/2, other neuronal tropomyosins have been analysed. Using the α9b, αf1b and αf9d antibodies, the localisation patterns of the neuronal tropomyosin isoforms, Tm5a/5b, TmBr2, TmBr3 in Tm5NM1/2 KO neurons were shown to be similar to WT controls. Signals from the α9b, αf1b and αf9d antibodies were found in some neurite tips and growth cones in both WT and Tm5NM1/2 KO neurons, structures where Tm5NM1/2 are normally located (Figure 4.2, 4.3 and 4.4). As Tm5a/5b, TmBr2 or TmBr3 and Tm5NM1/2 locate to growth cone structures, it is possible that a single isoform or a combination of Tm5a/5b, TmBr2 or TmBr3 isoforms may functionally compensate for the loss of Tm5NM1/2. However, more experiments need to be performed to determine whether these isoforms are associating with F-actin depleted of Tm5NM1/2.

The signal obtained using the αf1b antibody detects all Tm5a/5b, TmBr2 and TmBr3 neuronal tropomyosin isoforms and an antibody that exclusively detects TmBr3 has not been used. Hence, it cannot be conclusively determined that TmBr3 is detected in both WT and homozygous Tm5NM1/2 KO cultures. Nevertheless, TmBr3 appears to be an unlikely candidate as expression is normally upregulated later in neuronal development, replacing Tm5NM1/2 when the isoforms relocate to somatodendritic compartments (Weinberger *et*

al., 1996). On the other hand, signals obtained using the α9b and αf9d antibodies exclusively detect the isoforms TmBr2 and Tm5a/5b respectively. The localisation pattern of Tm5a/5b in growth cones was expected as an earlier study has shown that these isoforms localise to the central region of growth cones and also at the base of some filopodia (Schevzo*v et al.*, 1997). Tm5a/5b relocate to the cell body and neurites when growth cones diminish in size. Hence, Tm5a/5b may play a role in the early stages of neuronal development. In contrast, the function of TmBr2 is not yet known. Results presented here show that the TmBr2 protein is present in growth cone structures of both WT and Tm5NM1/2 KO neurons, indicating that this isoform may functionally compensate for the loss of Tm5NM1/2. Another tropomyosin isoform that may compensate for the loss of Tm5NM1/2 is Tm4, the only product from the δTm gene. Tm4 is present in the growth cone of neurons and may play a role in stabilising actin filaments found in this region (Had *et al.*, 1994).

The likely candidates that may functionally compensate for the loss of Tm5NM1/2 by virtue of their presence in the growth cones of KO neurons are neuronal tropomyosin isoforms, TmBr2, Tm5a/5b and Tm4. Even though there is an upregulation of Tm5NM4/7, the protein levels of isoforms from other tropomyosin genes including TmBr2, Tm5a/5b and Tm4 are not altered in Tm5NM1/2 KO neurons (Fath *et al.,* manuscript in preparation). As the protein levels are unchanged, TmBr2, Tm5a/5b and Tm4 may relocate from other regions of the neuron to growth cone structures and associate with F-actin polymers that are depleted of Tm5NM1/2. However, this appears unlikely as the localisation patterns of these isoforms are similar in Tm5NM1/2 KO and WT

neurons. Another alternative is that these isoforms TmBr2, Tm5a/5b and Tm4 may be recruited from the soluble pool of tropomyosins to associate with F-actin depleted of Tm5NM1/2. This may be determined by analysing the size of the soluble and insoluble pools of these tropomyosins. A decrease in the soluble pool of TmBr2, Tm5a/5b or Tm4 and a subsequent increase in the insoluble pool may indicate that these soluble isoforms have become insoluble by associating with F-actin, potentially those depleted of Tm5NM1/2. Another experiment is to quantify the signal intensities of the isoforms TmBr2, Tm5a/5b or Tm4 at growth cone structures from immunofluorescent images and to compare these levels between Tm5NM1/2 KO neurons and WT controls. Higher signal intensities at growth cone structures in Tm5NM1/2 KO neurons would indicate that there is an increased recruitment of TmBr2, Tm5a/5b or Tm4 located at those growth cones. To conclusively determine whether TmBr2, Tm5a/5b and Tm4 have been recruited from the soluble pool and associated with F-actin lacking Tm5NM1/2 immuno-electron microscopy will be performed in future experiments. This enables individual actin filaments to be analysed as specific tropomyosin isoforms that have associated with these actin filaments can be viewed by immuno-labelling.

Chapter 5

Elimination of Tm5NM1/2 on neurite outgrowth

5.1 Introduction

Previous studies have demonstrated an isoform specific effect of tropomyosin overexpression on neurite outgrowth. The overexpression of Tm5NM1, a low molecular weight tropomyosin, resulted in a significant increase in the number and total length of dendrites. Furthermore, the number of axonal branches as well as the total axon length was significantly increased when compared to WT mice. In contrast, the overexpression of a high molecular weight tropomyosin, Tm3 resulted in an initial inhibition of neurite outgrowth and later a significant decrease in the number and total length of dendrites (Schevzov *et al.*, 2005a). This indicates that the expression of tropomyosin isoforms is not functionally redundant and that distinct tropomyosin isoforms may regulate different aspects of neurite formation.

The aim of this section is to analyse the effect of Tm5NM1/2 depletion on neurite outgrowth. Results presented here show that neurite outgrowth is affected by the loss of Tm5NM1/2. Furthermore, the effect of Tm5NM1/2 depletion on neurite outgrowth is different in both hippocampal and cortical neurons. These results suggest that Tm5NM1/2 may play a role in neurite

outgrowth. In addition, Tm5NM1/2 may be used differently by unique types of neurons for neuritogenesis.

5.2 Results

5.2.1 Neurite Outgrowth Optimisation Experiment

The purpose of performing an optimisation experiment was to determine the optimal time window and growth conditions to examine neurite outgrowth. In order to determine these optimal conditions there are two factors that need to be considered; density and timecourse.

5.2.1.1 Density

Firstly, the density at which neurons were cultured was selected based on neurons having clear morphologies for morphometric analysis. A different density of neurons determines the amount of support provided by surrounding neurons. Neurons in culture are supported by each other and by secreted neurotrophic factors from non-neuronal cells. Therefore, neurons are better supported at higher densities than lower ones. However, neurons at higher densities which are well supported by the elevated levels of growth factors could potentially be too dense for clear morphometric analysis.

Therefore, the density 50,000 cells per well was selected as it was dense enough to allow good survival and growth of neurons (Figure 5.1 and Figure 5.3). Also it was a good density as both cortical and hippocampal neurons had clear morphology for morphometric analysis (Figure 5.1 and Figure 5.3).

5.2.1.2 Timecourse

A timecourse analysis was performed to determine the exact timepoint at which to compare neurite outgrowth between WT and Tm5NM1/2 KO neurons. The timecourse analysis allows the time point of maximal rate of neurite growth to be determined. This allowed one to select a timepoint at which an altered outgrowth rate, in response to changed tropomyosin protein levels, is most likely to be detected.

To determine the optimal timepoint at which to compare WT and Tm5NM1/2 KO neurons, the cultures were plated at the density of 50,000 cells per well over a period of 1DIV to 10DIV. Firstly, from this timecourse it is clearly shown by distinct Tau1 staining of the longest neurite that neuronal polarisation has occurred, starting at 2DIV in both cortical and hippocampal neurons (Figures 5.1 and 5.3). During polarisation, neurites differentiate into axons and dendrites. Therefore, measurements in all neurites (Figures 5.2a and 5.4a) have been divided into axons (Figures 5.2b and 5.4b) and dendrites (Figures 5.2c and 5.4c).

Results show that the mean primary neurite length of cortical neurons rapidly increased between 1DIV and 4DIV after which the rate of neurite outgrowth plateaued (Figure 5.2a). Data on neurite length were collected for axons and dendrites. The length of primary axons in cortical neurons followed the trend of total primary length with fast extensions until 4DIV after which the elongation rate plateaued (Figure 5.2b). Continuous growth was observed in the dendrites (Figure 5.2c). At 9DIV, mean neurite lengths were unusually higher than at

adjacent time points of 8DIV and 10DIV and this was also shown in axons and dendrites at the corresponding time point. At this stage of development, the neurons have reached a high level of complexity. The complex network makes it challenging to differentiate the neurites that originate from individual neurons. At 9DIV a smaller sample number of neurons were analysed resulting in higher standard error of the mean.

In the optimisation experiment of hippocampal neurons, neurite lengths including axons and dendrites were measured within the timewindow from 2DIV to 5DIV (Figure 5.4). This timewindow of 2DIV to 5DIV was determined based on results from the optimisation experiment of cortical neurons as maximal growth rate of neurite lengths was determined to be between 1DIV to 4DIV. Also, neuronal polarisation determined by the presence of axons and dendrites did not occur until 2DIV in cortical neurons (Figure 5.1). Results show that neuronal polarisation also occurred at 2DIV for hippocampal neurons (Figure 5.3). Therefore, neurite length data for hippocampal neurons were also collected for axons and dendrites. Analysis of primary neurite length shows that there is continuous growth between 2DIV to 5DIV (Figure 5.4a). The increase in neurite length in hippocampal neurons follows the same trend as cortical neurons but is less pronounced in hippocampal neurons. The continuous growth observed between 2DIV to 3DIV and 4DIV to 5DIV (Figure 5.4a) are reflected in axons (Figure 5.4b) and dendrites (Figure 5.4c).

From both optimisation experiments of cortical and hippocampal neurons, the best time to compare neurite length of homozygous KO Tm5NM1/2 growth cones with WT samples at 50,000 cells per well was determined to be at 4DIV.

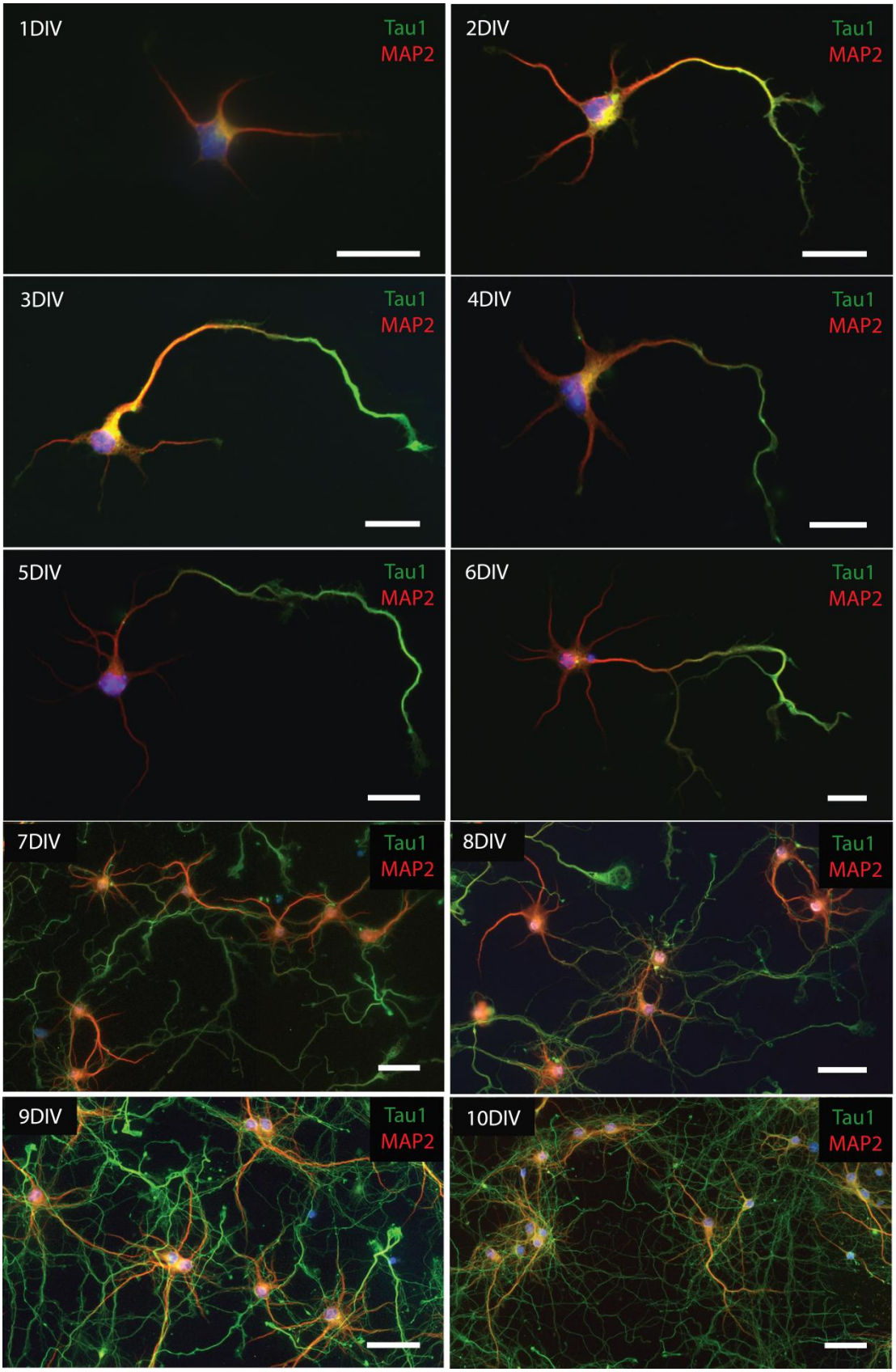

Figure 5.1 Development of cortical neurons in culture from 1DIV to 10DIV. Clear polarisation, shown by the distinct green staining at the longest neurite shaft which represents the axon, occurs from 2DIV. The Tau1 antibody in green was used to stain for axons while the MAP2 antibody shown in red were used to stain for dendrites. Scale bar 20µm for images from 1DIV to 6DIV. Scale bar 100µm for images from 7DIV to 10DIV.

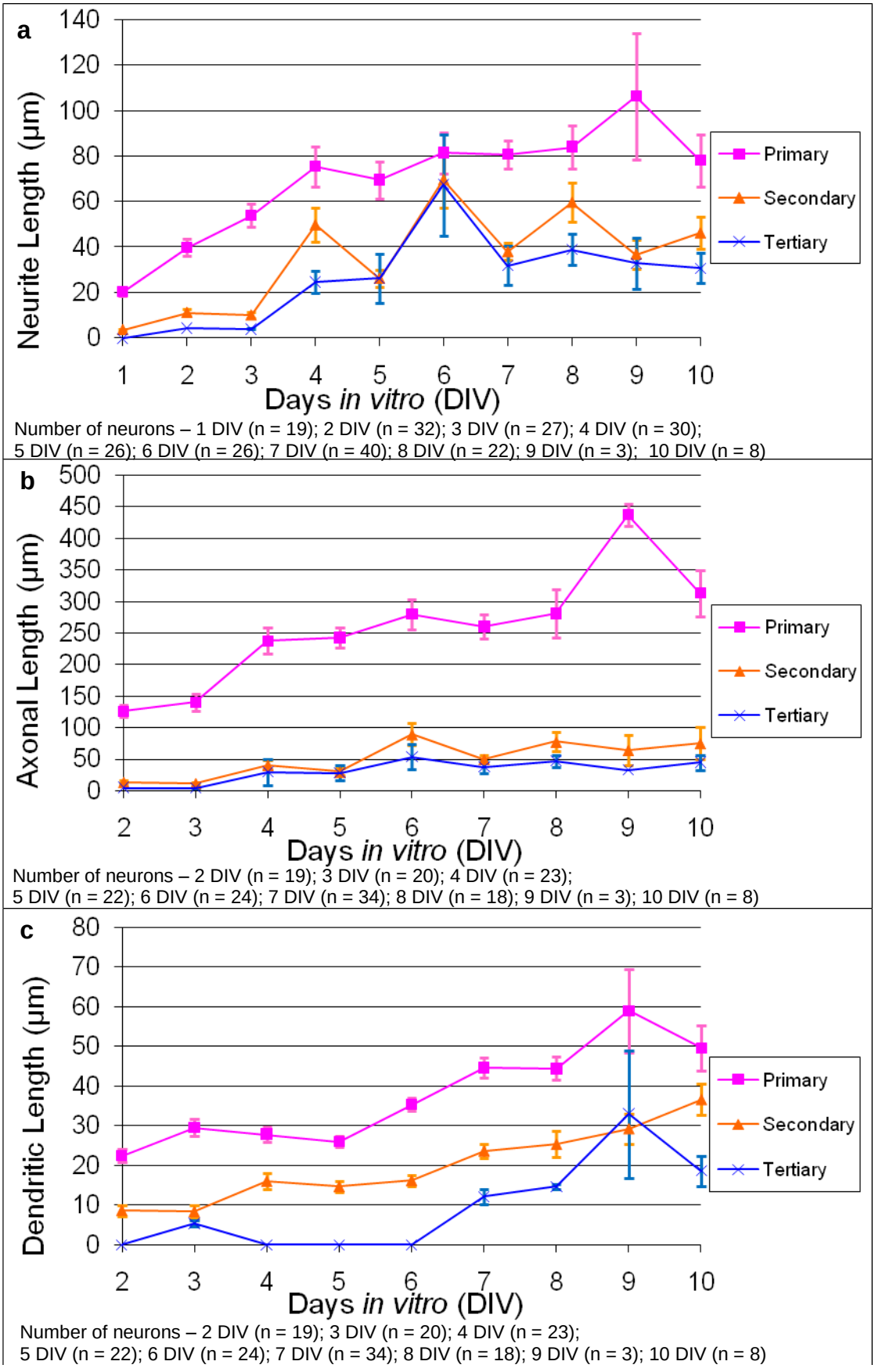

Figure 5.2 Neurite length of cultured cortical neurons from 1DIV to 10DIV. There was rapid growth in the length of primary neurites until 4DIV from all neurites (a) and axons (b) after which the length plateaus. Continuous growth was observed in dendrites (c). Optimal time to measure neurite length from cortical neurons was determined to be at 4DIV. Error bars represent standard error of the mean.

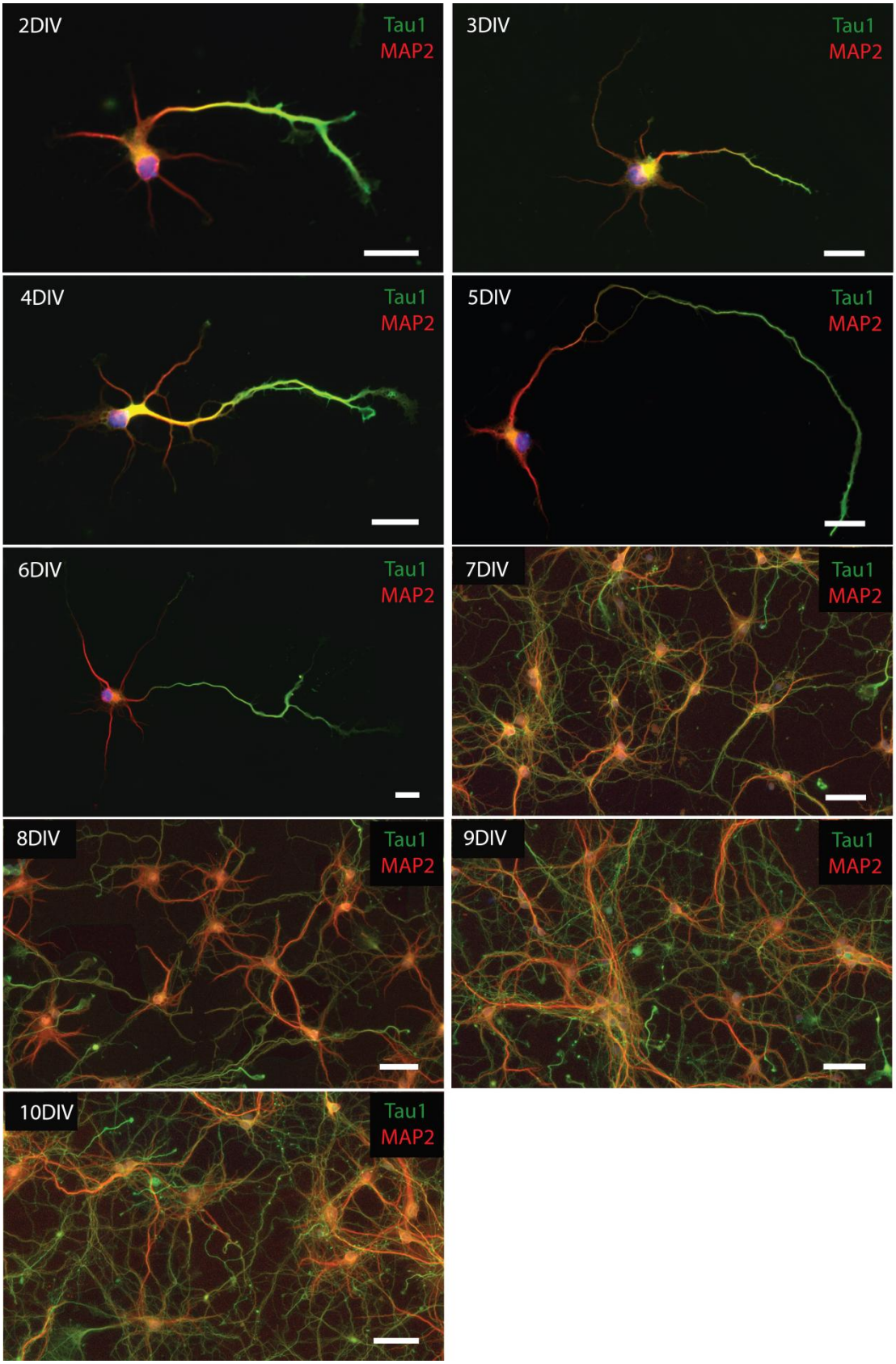

Figure 5.3 Development of hippocampal neurons in culture from 2DIV to 10DIV. The Tau1 antibody in green was used to stain for axons while the MAP2 antibody shown in red was used to stain for dendrites. Clear polarisation, shown by the distinct green staining at the longest neurite shaft which represents the axon, occurs from 2DIV. Scale bar 20µm for images from 2DIV to 6DIV. Scale bar 100µm for images from 7DIV to 10DIV.

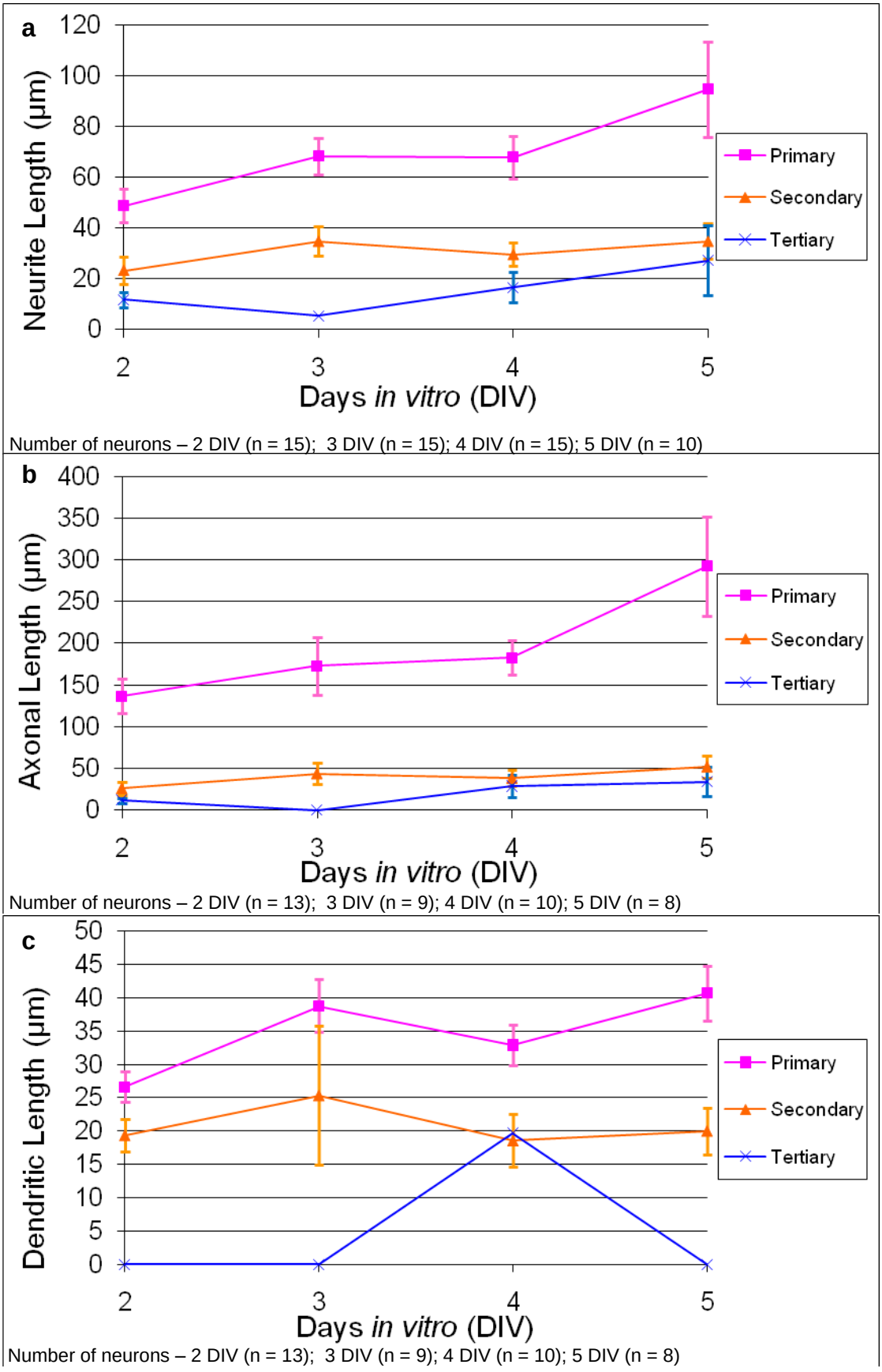

Figure 5.4 Neurite length of cultured hippocampal neurons from 2DIV to 5DIV. Continuous growth in length was observed from all neurites (a), axons (b) and dendrites (c). Optimal time to measure neurite length from cortical neurons was determined to be at 4DIV. n represents the amount of neurons analysed. Error bars represent standard error of the mean.

5.2.2 Neurite Length

Results from neurite length measurements of homozygous Tm5NM1/2 KO and WT control cortical neurons showed that the mean primary neurite length was not significantly different between the two groups (Figure 5.5a) which was reflected in the axonal length (Figure 5.5b). However the length of primary dendrites was significantly decreased ($p=0.04$) in Tm5NM1/2 KO neurons even though this decrease was small (Figure 5.5c). The decrease in neurite length from secondary neurites was highly significant ($p<0.0001$) when comparing Tm5NM1/2 KO neurons to WT controls (Figure 5.5a). This change was present in both axons ($p<0.0001$) (Figure 5.5b) and dendrites ($p=0.005$) (Figure 5.5c) where secondary neurites were significantly shortened in Tm5NM1/2 KO cortical neurons. The decrease of tertiary neurite length was highly significant ($p<0.0001$) when comparing Tm5NM1/2 KO neurons to WT controls (Figure 5.5a) which was similar in axons ($p<0.0001$) (Figure 5.5b). In contrast, the analysis of tertiary neurites in the dendritic compartment showed a trend towards increased neurite lengths when comparing Tm5NM1/2 KO neurons to WT controls (Figure 5.5c).

The mean length of primary neurites was not significantly different between homozygous Tm5NM1/2 KO neurons and WT controls in hippocampal neurons (Figure 5.6a). However, primary neurite lengths from axons ($p<0.0001$) (Figure 5.6b) and dendrites ($p=0.021$) (Figure 5.6c) were shown to be significantly decreased. Neurite length from secondary neurites was significantly shortened in Tm5NM1/2 KO neurons compared to WT samples ($p=0.006$) (Figure 5.6a) which was reflected in axons ($p<0.0001$) (Figure 5.6b). Secondary neurite

length from dendrites was not significantly different in Tm5NM1/2 KO neurons as compared to WT controls (Figure 5.6c). Mean length from tertiary neurites was significantly decreased in length when comparing Tm5NM1/2 KO neurons to WT samples (p=0.018) (Figure 5.6a) which was similar in axons (p=0.001) (Figure 5.6b). In contrast, the length of tertiary neurites from dendrites was shown to be comparable between Tm5NM1/2 KO neurons and WT controls (Figure 5.6c).

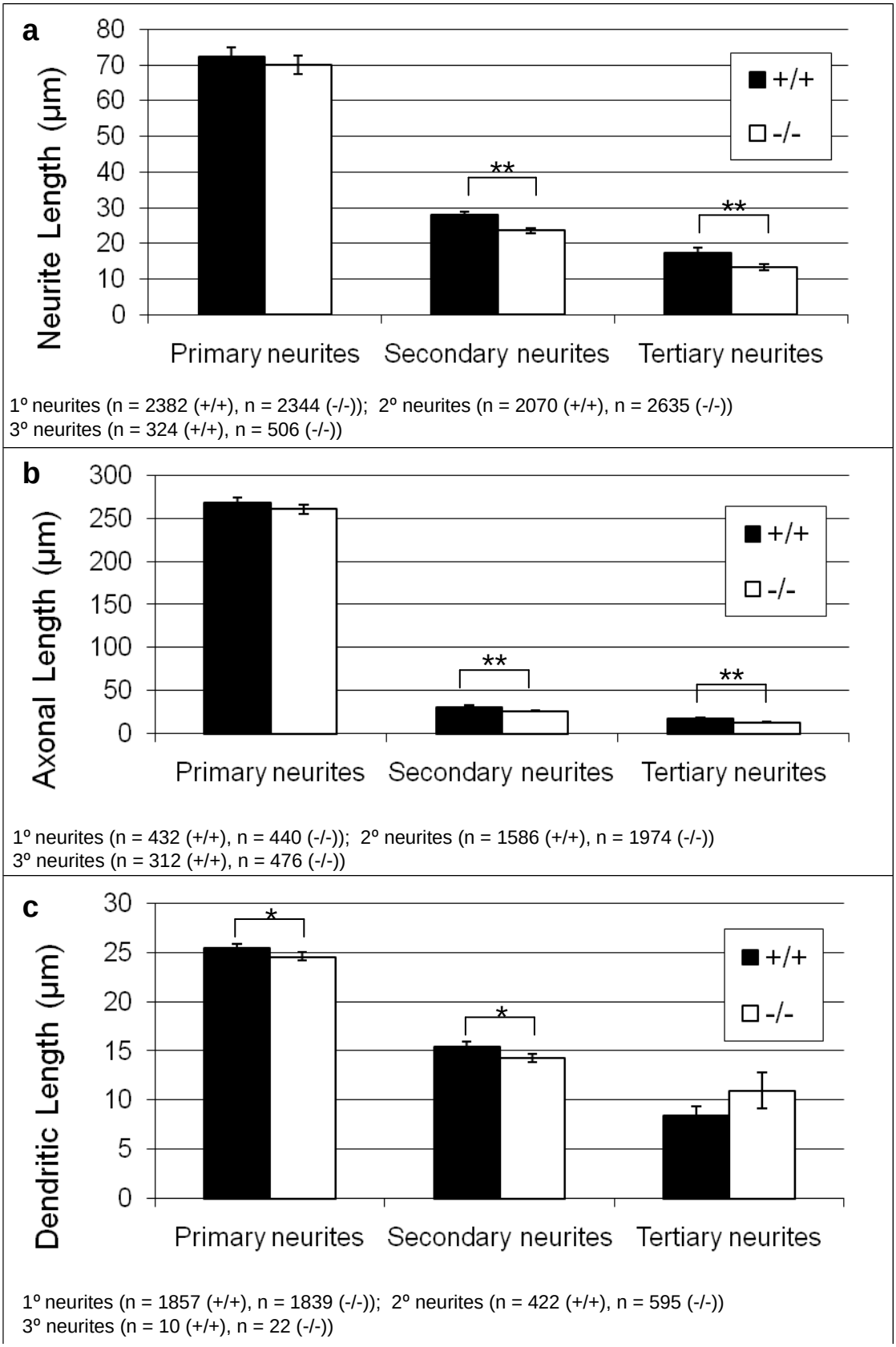

Figure 5.5 Effect of Tm5NM1/2 elimination on neurite length in cortical neurons. Primary neurites from Tm5NM1/2 KO neurons were not affected in pooled data (a) and axons (b) but were significantly decreased in dendrites ($p=0.04$) compared to WT controls (c). Secondary neurites were significantly decreased in length from pooled data ($p<0.0001$) (a), axons ($p<0.0001$) (b) and dendrites ($p=0.005$) in Tm5NM1/2 KO neurons(c). Tertiary neurites from Tm5NM1/2 KO neurons were significantly shortened in pooled data ($p<0.0001$) (a) and axons ($p<0.0001$) (b) but were not significantly different in dendrites (c). n represents the number of neurites measured. Error bars represent standard error of the mean. *$p<0.05$, **$p<0.0001$

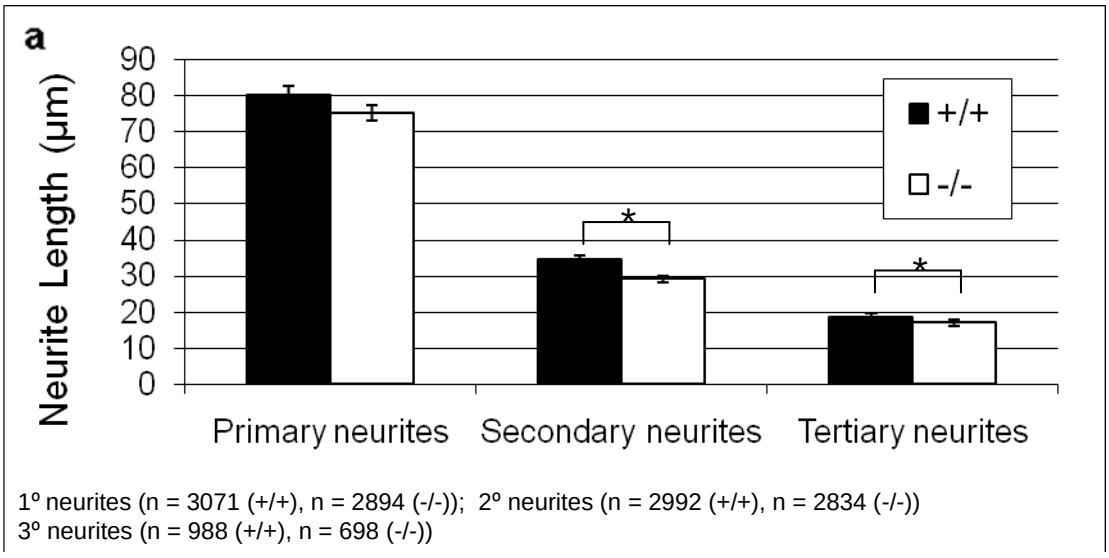

1º neurites (n = 3071 (+/+), n = 2894 (-/-)); 2º neurites (n = 2992 (+/+), n = 2834 (-/-))
3º neurites (n = 988 (+/+), n = 698 (-/-))

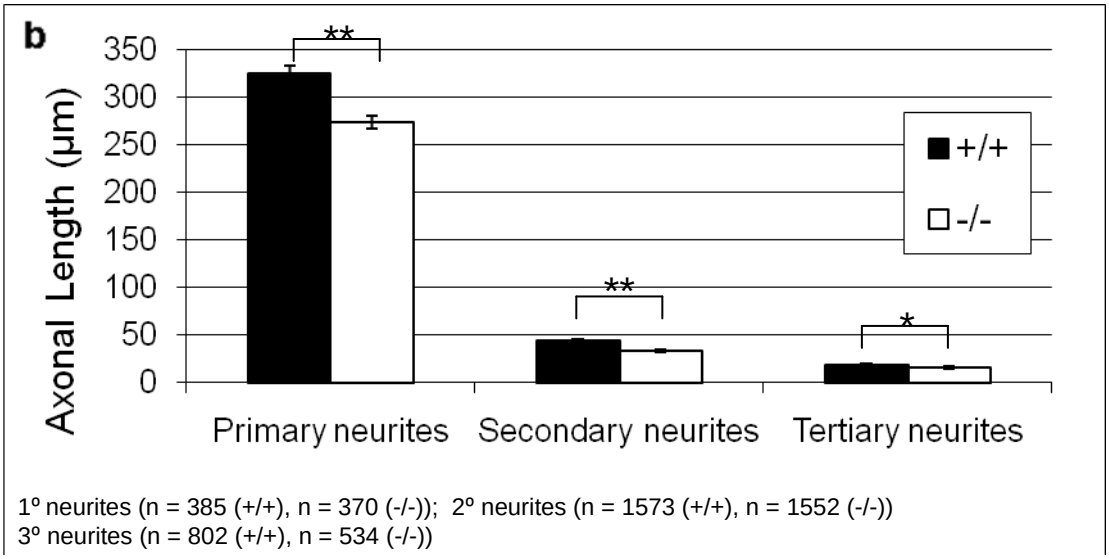

1º neurites (n = 385 (+/+), n = 370 (-/-)); 2º neurites (n = 1573 (+/+), n = 1552 (-/-))
3º neurites (n = 802 (+/+), n = 534 (-/-))

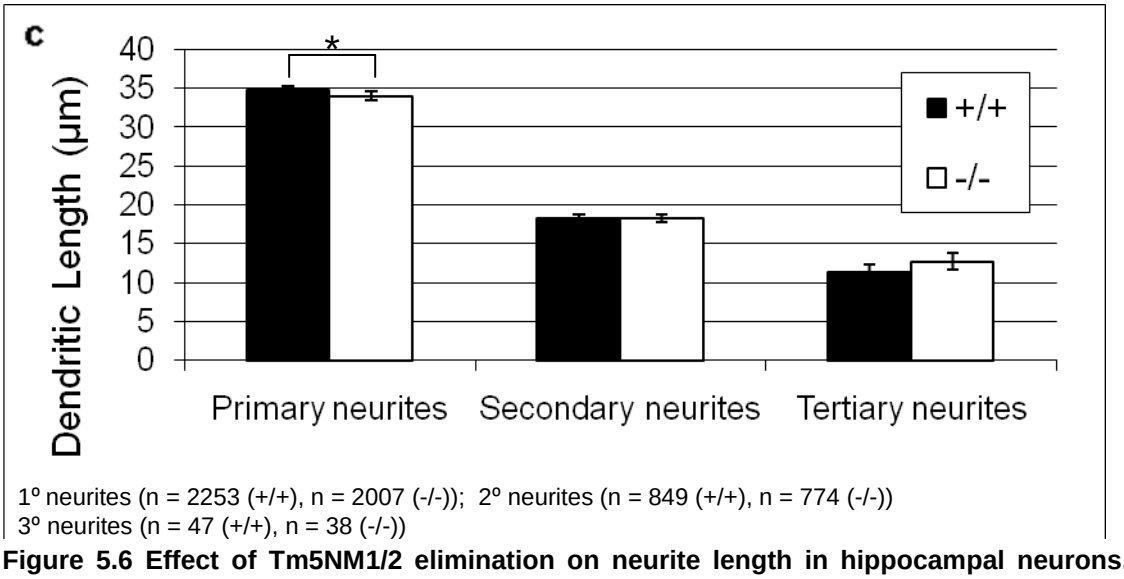

1º neurites (n = 2253 (+/+), n = 2007 (-/-)); 2º neurites (n = 849 (+/+), n = 774 (-/-))
3º neurites (n = 47 (+/+), n = 38 (-/-))

Figure 5.6 Effect of Tm5NM1/2 elimination on neurite length in hippocampal neurons. Primary neurites from pooled data (a) of Tm5NM1/2 KO neurons was comparable in length to WT samples while lengths were significantly shortened from axons ($p<0.0001$) (a) and dendrites ($p=0.021$) (b). Mean length of secondary neurites was significantly decreased in pooled data ($p=0.006$) (a) and axons ($p<0.0001$) (b) from Tm5NM1/2 KO neurons but were comparable to WT controls in dendrites (c). Tertiary neurites from Tm5NM1/2 KO neurons were significantly shortened in pooled data ($p=0.018$) (a) and axons ($p=0.001$) (b) while lengths were comparable to WT samples in dendrites (c). n represents the number of neurites measured. Error bars represent standard error of the mean. *$p<0.05$, **$p<0.0001$

5.2.3 Neurite Branching

The number of primary branches from homozygous Tm5NM1/2 KO cortical neurons was significantly increased in both axons ($p<0.0001$) (Figure 5.7a) and dendrites ($p<0.0001$) (Figure 5.7b) when compared to WT controls. Also, the number of secondary branches of axons was significantly increased ($p<0.0001$) (Figure 5.7a) but not those of dendrites (Figure 5.7b).

In hippocampal neurons, the number of primary branches from axons (Figure 5.8a) and dendrites (Figure 5.8b) were not significantly different between homozygous Tm5NM1/2 KO neurons and WT controls. The number of secondary branches was significantly decreased in axons ($p=0.005$) (Figure 5.8a) while in dendrites the number was similar between Tm5NM1/2 KO neurons and WT samples (Figure 5.8b).

5.2.4 Number of Dendrites

The number of dendrites from homozygous Tm5NM1/2 KO cortical neurons was comparable to WT controls (Figure 5.9a). In homozygous Tm5NM1/2 KO hippocampal neurons, the number of dendrites was significantly decreased while the effect was subtle (Figure 5.9b).

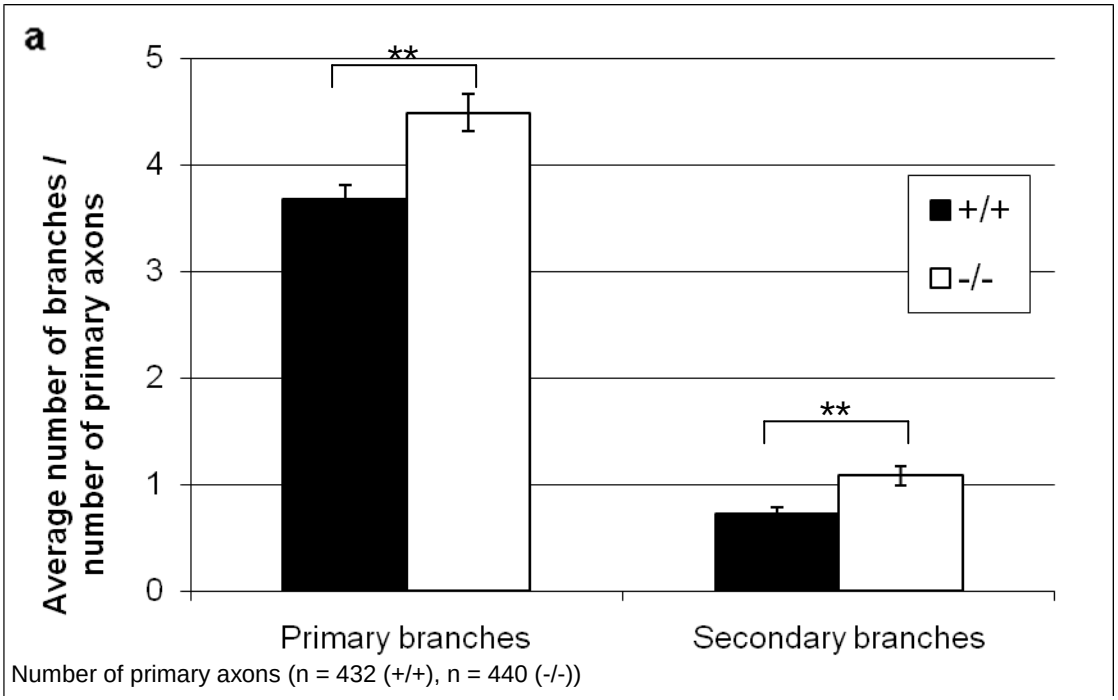

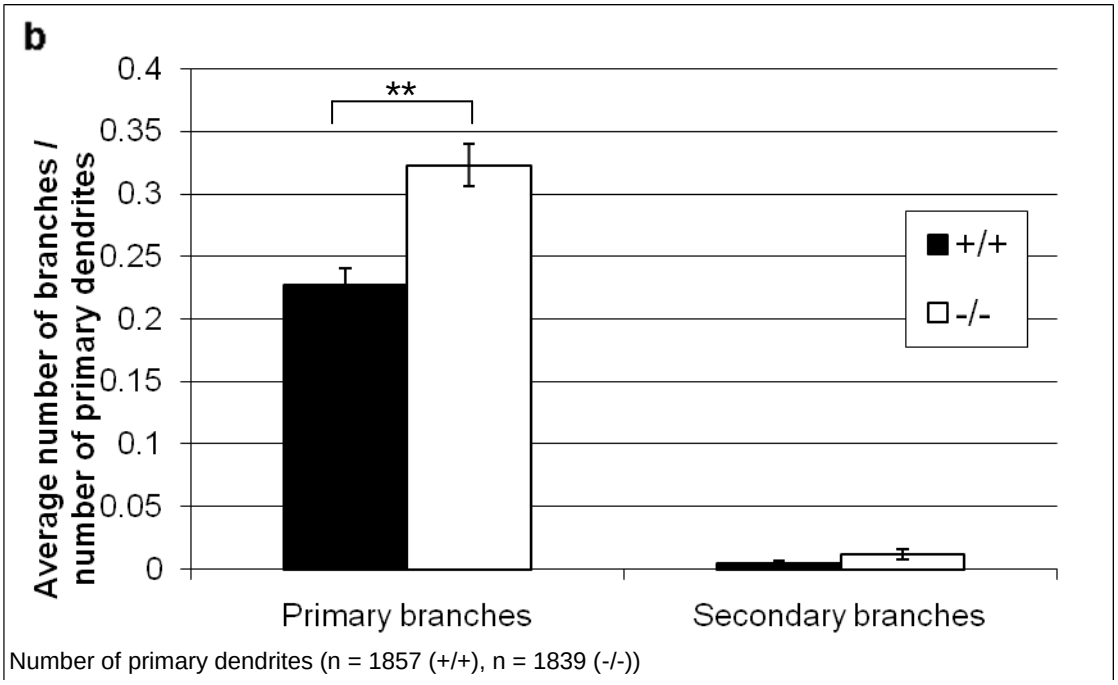

Figure 5.7 Elimination of Tm5NM1/2 has an impact on the number of axonal and dendritic branches in cortical neurons. Both the number of primary branches from axons ($p<0.0001$) (a) and dendrites ($p<0.0001$) (b) was significantly increased in homozygous Tm5NM1/2 KO neurons compared to WT samples. The number of secondary branches in axons from homozygous Tm5NM1/2 KO neurons was significantly increased compared to WT controls ($p<0.0001$) (a) while from dendrites the number were similar to WT samples (b). n represents the number of primary axons (a) or primary dendrites (b) that were analysed. Error bars represent standard error of the mean. **$p<0.0001$

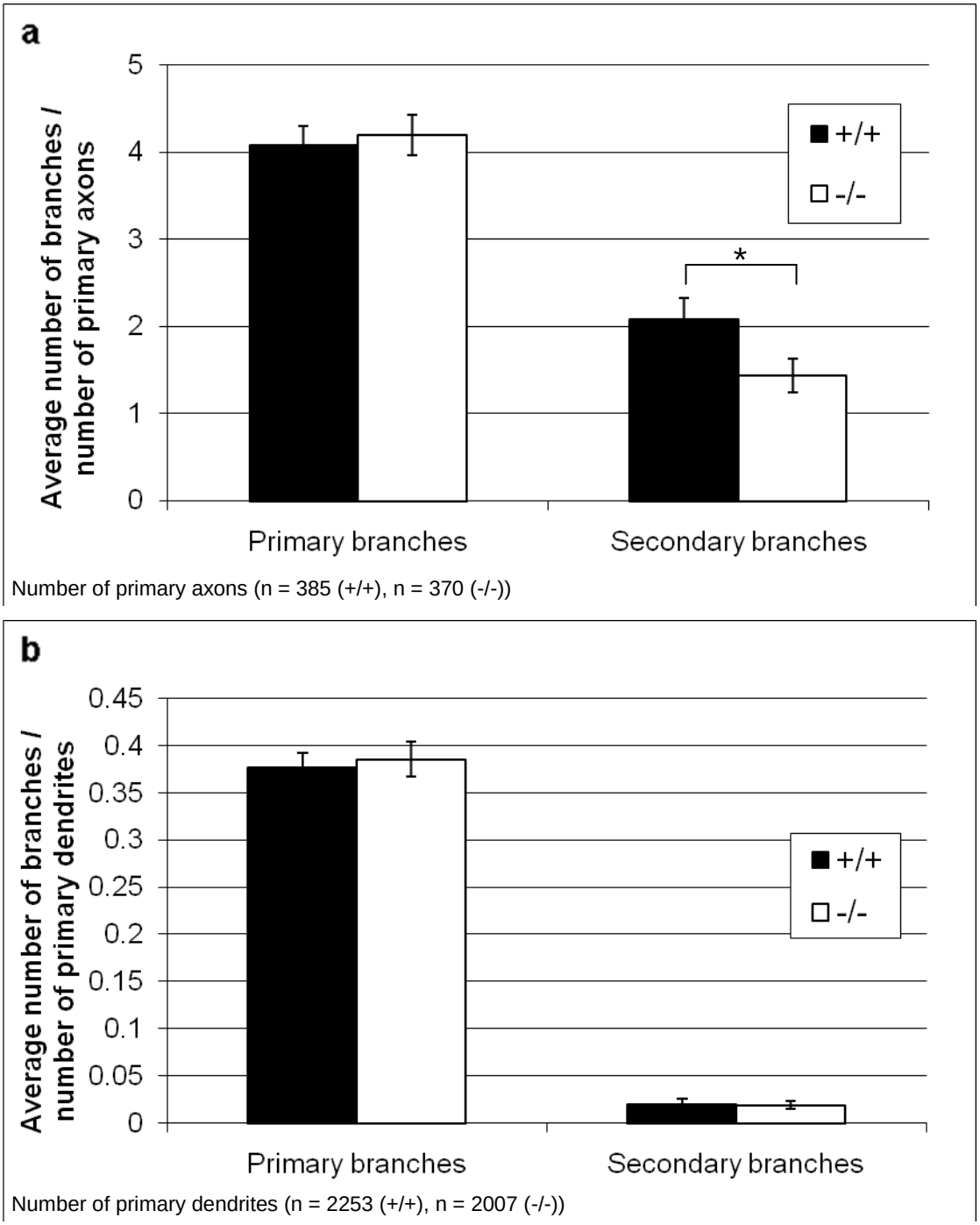

Figure 5.8 Loss of Tm5NM1/2 reduces the number of secondary branches in axons from hippocampal neurons. The number of primary branches in axons (a) and dendrites (b) from homozygous Tm5NM1/2 KO neurons were comparable to WT controls. The number of secondary branches from axons were significantly decreased (p=0.005) (a) from Tm5NM1/2 KO neurons while in dendrites, the number was similar to WT controls (b). n represents the number of primary axons (a) or primary dendrites (b) that were analysed. Error bars represent standard error of the mean. *p<0.05

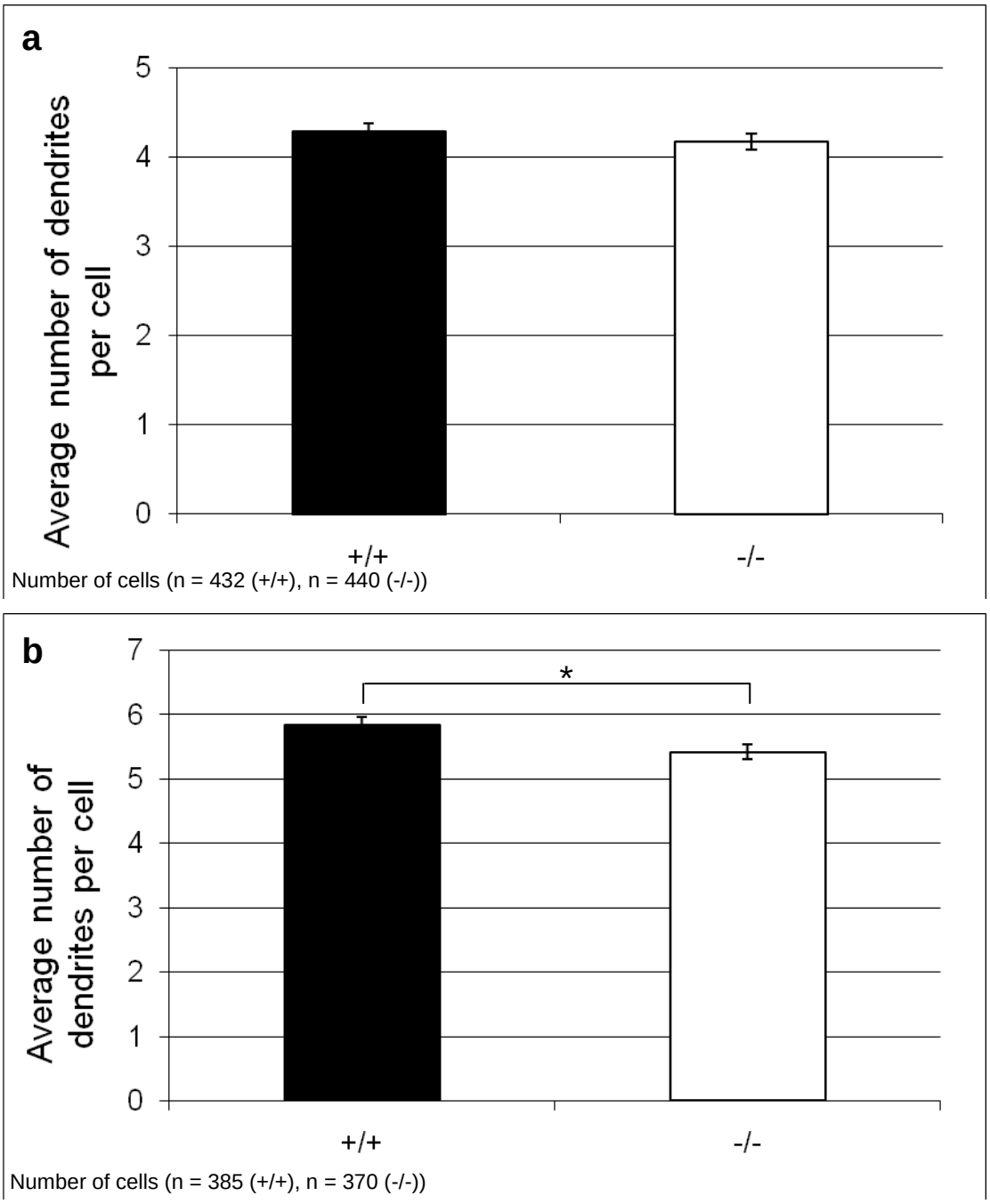

Figure 5.9 Depletion of Tm5NM1/2 affects the number of dendrites from hippocampal neurons but not cortical neurons. The number of dendrites from homozygous Tm5NM1/2 KO cortical neurons was comparable to WT controls (a). While from Tm5NM1/2 KO hippocampal neurons, the number of dendrites was significantly decreased compared with WT samples although the effect was small (p=0.002) (b). n represents the number of cells that were analysed. Error bars represent standard error of the mean. *p<0.05

5.2.5 Neuronal Polarisation

The percentage of polarised neurons was similar between both cortical and hippocampal homozygous Tm5NM1/2 KO neurons and WT controls (Figure 5.10). The data show a slight and insignificant increase in the percentage of neuronal polarisation when comparing Tm5NM1/2 KO neurons to WT controls in cortical neurons ($p=0.184$) (Figure 5.10a). In contrast, the percentage of neuronal polarisation in hippocampal neurons was slightly decreased when comparing Tm5NM1/2 KO neurons to WT controls but this difference was found to be not significant ($p=0.268$) (Figure 5.10b).

The effect of eliminating Tm5NM1/2 on neurite length, the number of branches and dendrites in both cortical and hippocampal neurons have been summarised in Tables 5.1 and 5.2.

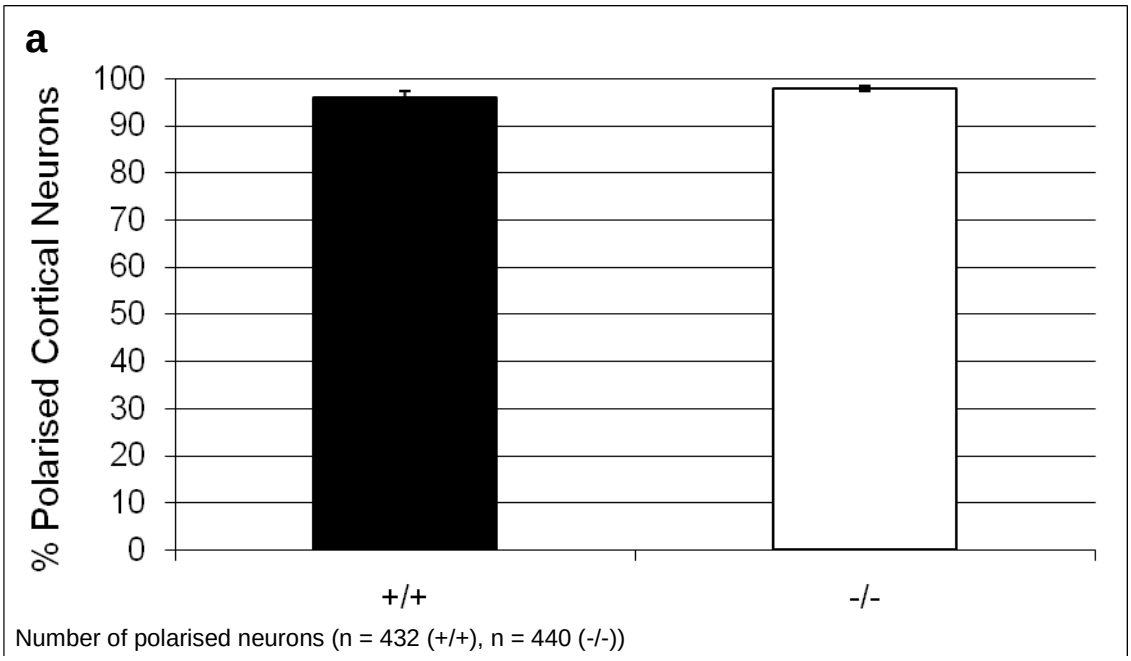

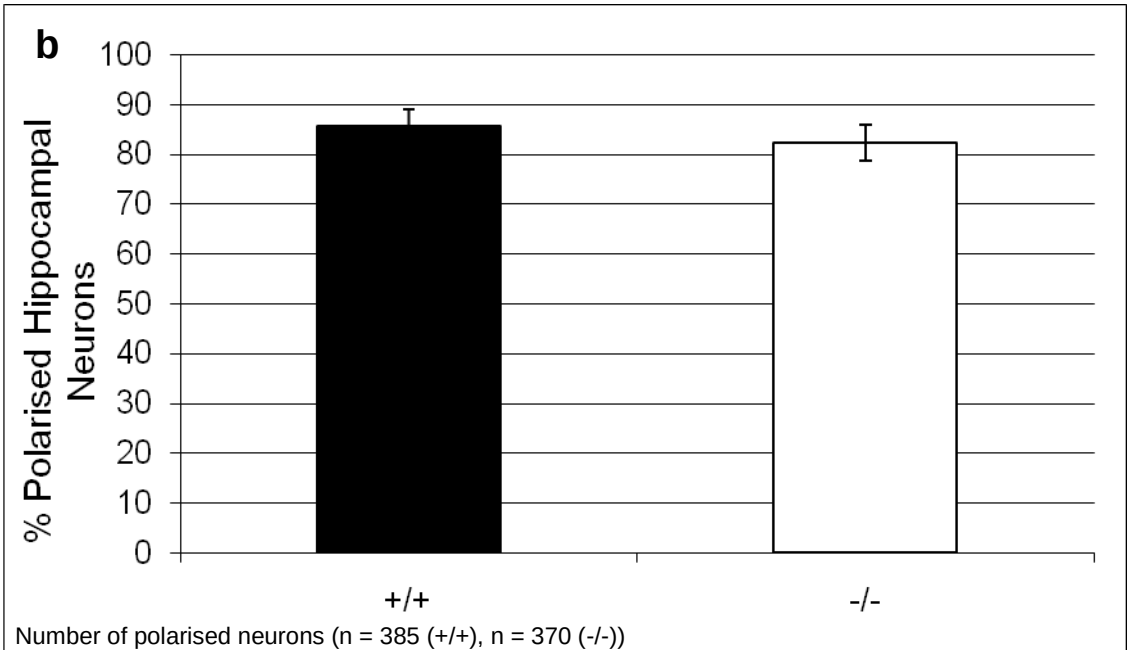

Figure 5.10 Depletion of Tm5NM1/2 has no effect on neuronal polarisation in cultured cortical and hippocampal neurons. The percentage of polarised neurons were slightly increased in homozygous Tm5NM1/2 KO cortical neurons (a) (p=0.184) and subtly decreased in hippocampal (b) neurons when compared to WT samples (p=0.268) and these differences were found to be not significant. n represents the number of polarised neurons analysed. Error bars represent standard error of the mean.

Table 5.1 Neurite length of cortical and hippocampal neurons is affected by the elimination of Tm5NM1/2

			Cortical Neurons	Hippocampal Neurons
Neurite Length		Primary	-	-
		Secondary	↓	↓
		Tertiary	↓	↓
Length	Axon	Primary	-	↓
		Secondary	↓	↓
		Tertiary	↓	↓
	Dendrite	Primary	↓	↓
		Secondary	↓	-
		Tertiary	-	-

Table 5.2 Loss of Tm5NM1/2 has an impact on the number of branches and dendrites in cortical and hippocampal neurons

			Cortical Neurons	Hippocampal Neurons
Branching	Axon	Primary	↑	-
		Secondary	↑	↓
	Dendrite	Primary	↑	-
		Secondary	-	-
Number of Dendrites			-	↓

5.3 Discussion

5.3.1 Tm5NM1/2 are not essential for early stages of neuritogenesis

Results presented here show that there are no obvious alterations in neuronal morphology between homozygous Tm5NM1/2 KO and WT controls. The presence of protrusions and neurites from neurons lacking Tm5NM1/2 indicate that Tm5NM1/2 are not absolutely required for the initial stages of neuritogenesis. Although Tm5NM1/2 are not needed for early neuritogenesis, there is evidence to suggest that Tm5NM1/2 may still play a role in the early stages of neuronal development. Earlier studies have shown that Tm5NM1/2 localise to the immature shafts of axons. The localisation pattern of Tm5NM1/2 suggests that these isoforms may have a role in regulating the formation of axons. Furthermore, cortical neurons overexpressing Tm5NM1 exhibited significant increase in the number of dendrites and axonal branches as well as significant overall lengthening of dendrites and axons. As overexpression of Tm5NM1 in neurons has affected both axonal and dendritic length and branches, Tm5NM1 may play a role in regulating and maintaining these processes (Schevzov *et al.,* 2005a).

5.3.2 Loss of Tm5NM1/2 affects neuritogenesis in both axons and dendrites

The neurite lengths including axons and dendrites from both Tm5NM1/2 KO cortical and hippocampal neurons are significantly but subtly decreased when compared to WT controls (Figure 5.5, Figure 5.6 and Table 5.1). The number of dendrites is also significantly decreased in Tm5NM1/2 KO hippocampal neurons while it was unaltered in cortical neurons (Figure 5.9 and Table 5.2). In contrast, previous results have shown that the overexpression of Tm5NM1 in cortical neurons significantly increased the overall lengthening of axons and dendrites as well as the number of dendrites (Schevzov *et al.,* 2005a). Taken together, this indicates that Tm5NM1/2 plays a role in neurite extension.

Studies have shown that the regulation of the actin filament network is important in many aspects of neuritogenesis including neurite formation and extension (Endo *et al.,* 2007; Korobova and Svitkina*,* 2008). As Tm5NM1 stabilises actin (Bryce *et al.,* 2003), the Tm5NM1/2 depleted actin filament populations will be unstable which may affect neurite extension. The subtle phenotype of neurite shortening from Tm5NM1/2 KO neurons at 4DIV may be explained by partial functional compensation from Tm5a/5b, TmBr2 and Tm4 isoforms, as discussed earlier in Chapter 4. The instability formed by the loss of Tm5NM1/2 in F-actin may be stabilised and partially compensated by associating with other tropomyosin isoforms such as Tm5a/5b, TmBr2 and Tm4. The effect of each tropomyosin isoform is unique to every actin filament population that it associates with (Bryce *et al.,* 2003; Schevzov *et al.,* 2005a). For example, while Tm5NM1 stabilises actin, overexpressed Tm3, a high

molecular weight tropomyosin that is not normally found in neuronal cells, associates with less stable filaments and causes delayed, as well as reduced neuritogenesis (Schevzov *et al.,* 2005a; Creed *et al.,* 2008). Even though TmBr3 locates to neurite tips in Tm5NM1/2 KO neurons as shown in Chapter 4, it is unlikely for TmBr3 to functionally compensate for the loss of Tm5NM1/2 as it has been shown to give less stable actin filament populations (Bryce *et al.,* 2003) and one would expect a phenotype similar to Tm3 overexpression. Tm5a/5b on the other hand are the most likely candidates because they have the greatest affinity for actin filaments from all the characterised tropomyosins (Moraczewska *et al.,* 1999). Therefore, Tm5a/5b isoforms could associate with actin filament populations in Tm5NM1/2 depleted neurons to generate similar but still subtly reduced stability than actin populations in WT neurons. In addition, other possible tropomyosin isoforms for functional compensation are TmBr2 and Tm4, as discussed earlier in Chapter 4. Although the stabilities that these two isoforms confer on actin filaments are unknown, it is still possible that a combination of Tm5a/5b, TmBr2 and Tm4 isoforms may associate with actin filament populations depleted of Tm5NM1/2 that would explain the mild phenotype observed in Tm5NM1/2 KO neurons.

Another aspect of neurite outgrowth that was analysed in Tm5NM1/2 KO hippocampal and cortical neurons was branching. Overexpression of Tm5NM1 in cortical neurons significantly increased the number of axonal branches (Schevzov *et al.*, 2005a). Interestingly, the numbers of both axonal and dendritic branches are significantly increased in Tm5NM1/2 KO cortical neurons when compared to WT controls, which is similar to effects observed in

response to Tm5NM1 overexpression (Figure 5.7). In contrast, the number of axonal branches is significantly decreased in Tm5NM1/2 KO hippocampal neurons (Figure 5.8). The different phenotypes observed between cortical and hippocampal neurons are discussed below.

5.3.3 Loss of Tm5NM1/2 has different effect on neuritogenesis in hippocampal and cortical neurons

The elimination of Tm5NM1/2 affects neuritogenesis differently in cortical and hippocampal neurons. Even though overall the neurite lengths in axons and dendrites are reduced, the decreased lengths of primary, secondary and tertiary neurites differ between cortical and hippocampal neurons. In addition, the number of branches from cortical neurons is increased whereas it is decreased for axons in hippocampal neurons.

The unique phenotypes observed may be due to the different tropomyosin pools that are present in cortical and hippocampal neurons. Western blot analyses of neuronal tissue have shown that the pool of tropomyosin isoforms is different between these two types of neurons (Vrhovski *et al.,* 2003). Therefore when Tm5NM1/2 are eliminated, neuritogenesis may be impacted differently as the remaining pool of tropomyosins will be unique to each type of neuron. The remaining pool of tropomyosin will affect the actin filament

population differently because as mentioned earlier, the stability of actin filament populations are unique due to associations with distinct tropomyosin isoforms (Bryce *et al.,* 2003; Schevzov *et al.,* 2005a). Previously it has been shown that the level of Tm5NM1/2 is different in various regions of the adult brain including cortex and hippocampus (Vrhovski *et al.,* 2003). Therefore it is possible that the normal Tm5NM1/2 protein level is different in cortical and hippocampal neurons at the embryonic stage of development. Hence, the elimination of Tm5NM1/2 in neurons with higher Tm5NM1/2 levels may cause greater impact on neuritogenesis compared to neurons with lower Tm5NM1/2 levels.

5.3.4 Lack of Tm5NM1/2 has no detectable effect on neuronal polarisation

Tm5NM1/2 mRNA is an early polarity marker (Hannan *et al.,* 1995). Also, Tm5NM1/2 protein is present in axons of developing neurons but relocates to the somatodendritic compartment after maturation (Hannan *et al.,* 1995; Vrhovski *et al.,* 2003). This suggests that Tm5NM1/2 may play a role in polarisation of neurons. However, results presented here show that with the elimination of Tm5NM1/2, neuronal polarisation does not appear to be altered (Figure 5.10). This indicates that Tm5NM1/2 are not required for neuronal polarisation but rather may assist in this process. Alternatively, Tm5a/5b or TmBr2 may functionally compensate for this process however the role of these isoforms in neuronal polarisation is not known.

Chapter 6

Levels of ADF/cofilin in Tm5NM1/2 depleted neurons

6.1 Introduction

Tropomyosins are known to protect actin filaments from the severing activity by ADF/cofilin (Bernstein and Bamburg, 1982; reviewed in Cooper, 2002; Ono and Ono, 2002). Previous studies have shown that distinct tropomyosin isoforms have different protective effects against the action of ADF/cofilin (Bryce *et al.*, 2003; Schevzov *et al.*, 2005a) When Tm5NM1, a low molecular weight tropomyosin is overexpressed, a significant increase in the phosporylated or inactive form of ADF/cofilin is observed. However, when a high molecular weight tropomyosin Tm3 is overexpressed, the levels of inactive ADF/cofilin were comparable to WT controls (Bryce *et al.*, 2003). This suggests that certain tropomyosin isoforms such as Tm5NM1 are strong inhibitors of ADF/cofilin activity.

The aim is to examine the levels of active and inactive ADF/cofilin between homozygous Tm5NM1/2 KO and WT mice. As Tm5NM1 is a competitive inhibitor of active ADF/cofilin, it was hypothesised that with the loss of Tm5NM1/2 from actin, more active ADF/cofilin is present to depolymerise the actin filament causing higher turnover.

Results show that both cortical and hippocampal KO neurons have a small decrease in the level of phosphorylated (inactive) ADF/cofilin compared to WT, however only results from cortical neurons were significant.

6.2 Results

6.2.1 Loss of Tm5NM1/2 significantly increases ADF/cofilin activity in cortical neurons

The ratio of phosphorylated ADF/cofilin (pADF/cofilin) to total ADF/cofilin was analysed by using phosphorylation specific and unspecific antibodies in cortical neurons. Both inactive and total ADF/cofilin were present in the growth cone and neurite tips of homozygous Tm5NM1/2 KO and WT neurons, which is shown in the ratio images. Overall, the level of inactive ADF/cofilin from homozygous Tm5NM1/2 KO neurons appears similar to WT controls (Figure 6.1). Further analysis was performed on the growth cone regions where the staining colocalised. The ratio of staining intensity for pADF/cofilin and total ADF/cofilin was quantified and the mean intensity was plotted (Figure 6.2). Results show that the staining intensity ratio from Tm5NM1/2 KO neurons was significantly decreased ($p<0.0001$) when compared to WT controls although the difference was small (0.9593 ± 0.0105 (WT) vs 0.8977 ± 0.0073 (KO)) (Figure 6.2).

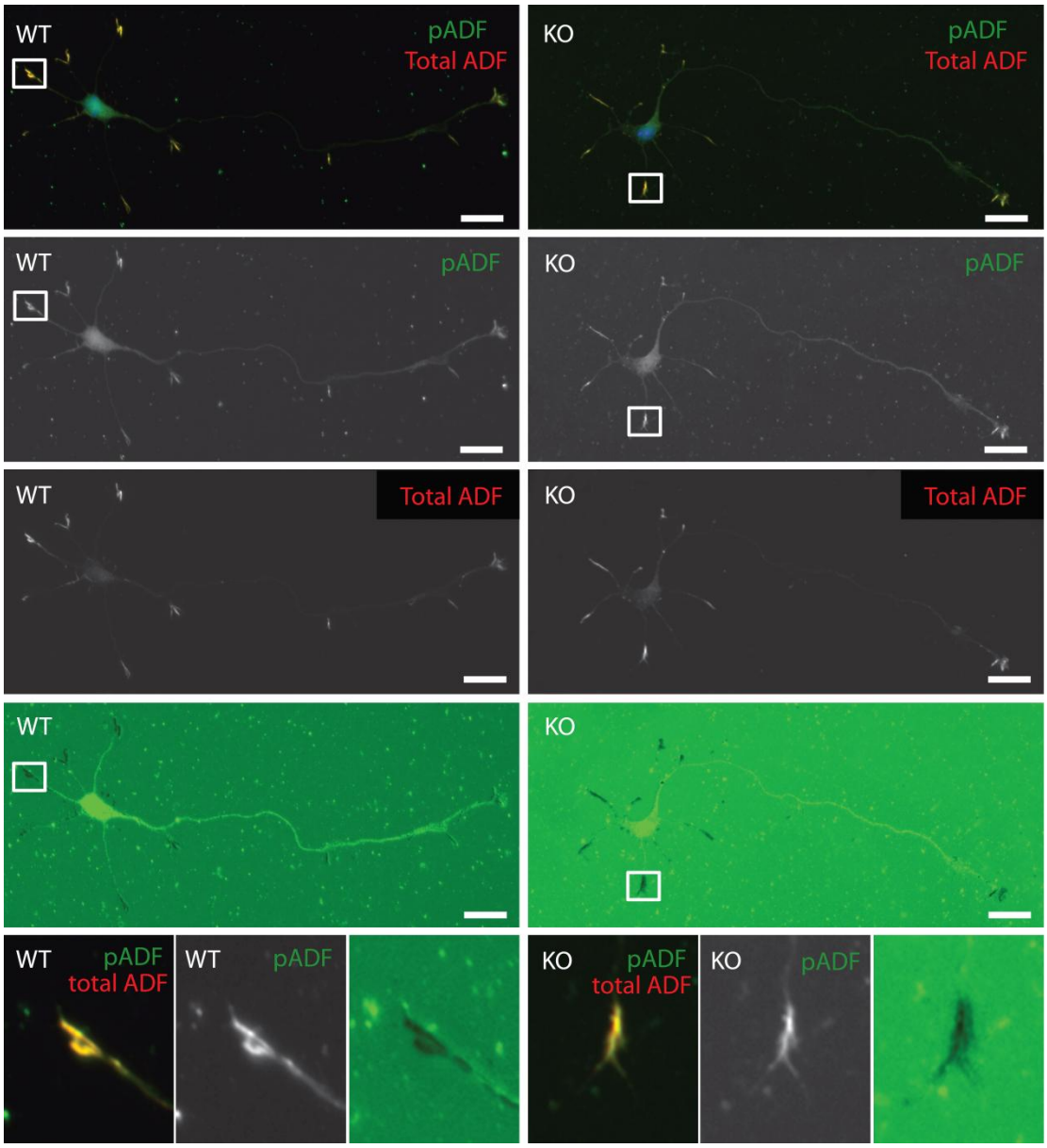

Figure 6.1 Effect of Tm5NM1/2 depletion on levels of inactive ADF/cofilin in growth cones of cortical neurons. Cortical WT and homozygous Tm5NM1/2 KO neurons have been stained using the pADF and total ADF antibodies. The pADF antibody detects the inactive form of ADF/cofilin. Ratio of staining intensity for the pADF and total ADF/cofilin antibodies are shown. Levels of inactive ADF/cofilin in growth cone structures of homozygous Tm5NM1/2 KO cortical neurons appear comparable to WT controls. The growth cone regions where the staining colocalised are highlighted.

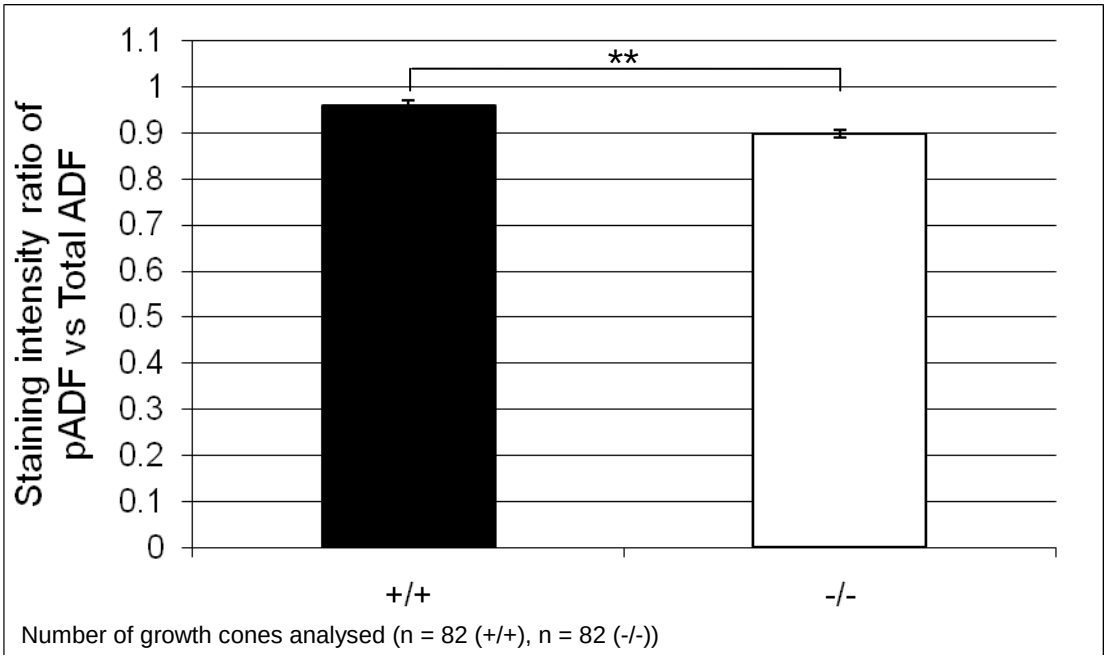

Figure 6.2 Depletion of Tm5NM1/2 increases levels of active ADF/cofilin in growth cones of cortical neurons. Mean staining intensity of pADF/cofilin over total ADF/cofilin was plotted for homozygous Tm5NM1/2 KO and WT neurons. The staining intensity levels of inactive ADF/cofilin were significantly lower in homozygous Tm5NM1/2 KO neurons compared to WT samples ($p<0.0001$). n represents the number of growth cones analysed. Error bars represent standard error of the mean. **$p<0.0001$

6.2.2 Level of inactive ADF/cofilin in Tm5NM1/2 KO hippocampal neurons are comparable to WT controls

Staining results show that the inactive and total ADF/cofilin also colocalised to neurite tips and growth cone regions in hippocampal neurons. At a qualitative level, the amount of inactive ADF/cofilin from homozygous Tm5NM1/2 KO appears comparable to WT neurons (Figure 6.3). Quantitative analysis was performed on the staining intensity of pADF/cofilin vs total ADF/cofilin in the growth cone regions. Results show that inactive ADF/cofilin from homozygous Tm5NM1/2 KO neurons were similar to WT controls (Figure 6.4).

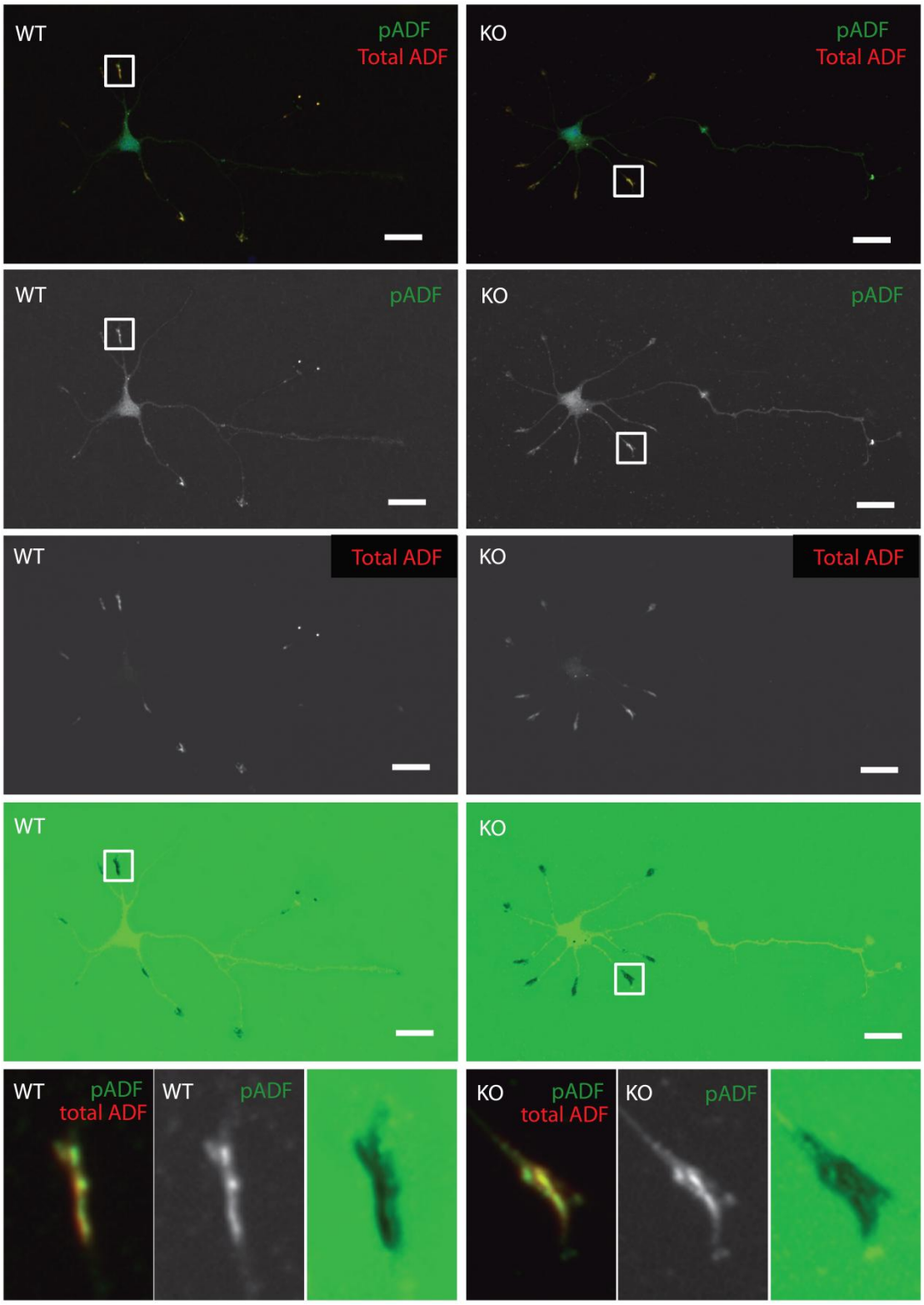

Figure 6.3 Effect of Tm5NM1/2 depletion on levels of inactive ADF/cofilin in growth cones of hippocampal neurons. Hippocampal WT and homozygous Tm5NM1/2 KO neurons have been stained using the pADF and total ADF antibodies. The pADF antibody detects the inactive form of ADF/cofilin. Ratio of staining intensity for the pADF and total ADF/cofilin antibodies are shown. Levels of inactive ADF/cofilin in growth cone structures of homozygous Tm5NM1/2 KO hippocampal neurons appear comparable to WT controls. The growth cone regions where the staining colocalised are highlighted.

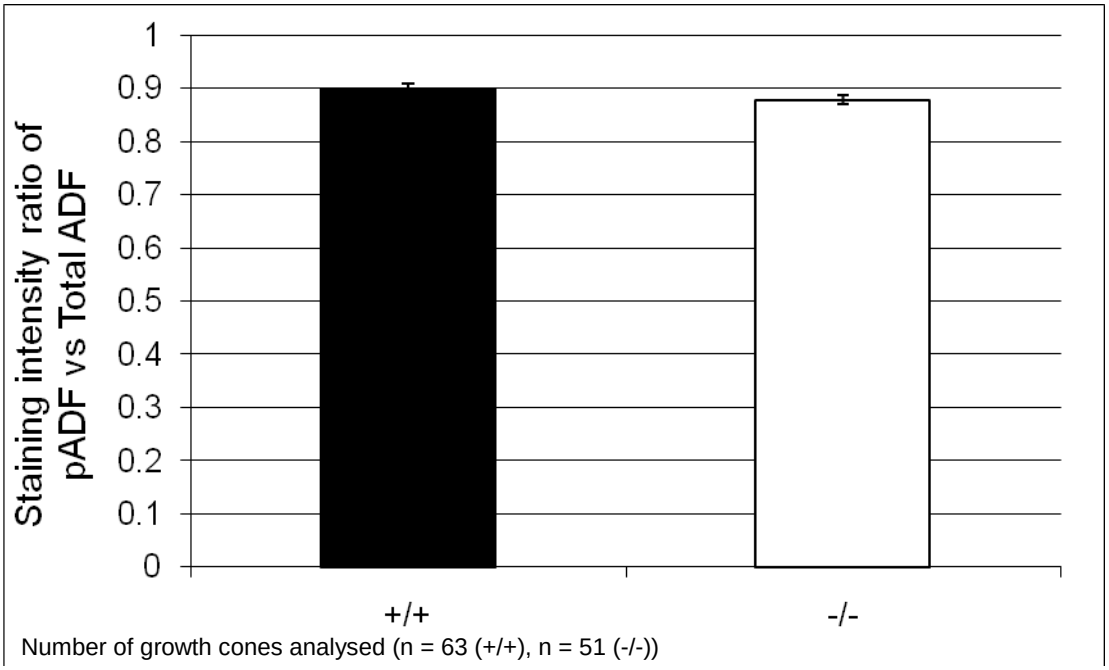

Figure 6.4 Elimination of Tm5NM1/2 has no effect on the levels of ADF/cofilin in growth cones of hippocampal neurons. Mean staining intensity of pADF/cofilin over total ADF/cofilin was plotted for homozygous Tm5NM1/2 KO and WT neurons. Staining intensity levels of inactive ADF/cofilin were similar in homozygous Tm5NM1/2 KO neurons compared to WT samples (p=0.131). n represents the number of growth cones analysed. Error bars represent standard error of the mean.

6.3 Discussion

6.3.1 Loss of Tm5NM1/2 expression significantly increases ADF/cofilin activity in growth cones of cortical neurons

Tm5NM1/2 provides stability to actin filaments by competing with ADF/cofilin for actin association (Bernstein and Bamburg, 1982; Ono and Ono, 2002; Bryce *et al.,* 2003). Therefore as expected, the lack of Tm5NM1/2 caused a significant increase in active ADF/cofilin within growth cones of cortical neurons even though the effect was small (Figure 6.2). Also, active ADF/cofilin was increased by a small margin in hippocampal neurons although this was not significant (Figure 6.4). The marginal effects observed in both cortical and hippocampal neurons may be due to functional compensation by Tm5a/5b. Even though Tm5a/5b have not been proven to be an inhibitor of ADF/cofilin, their strong affinity for actin filaments suggest that ADF/cofilin may not have an opportunity to associate.

6.3.2 Increase in ADF/cofilin activity has significant but minor impact on actin filament dynamics in growth cones

Results presented here have shown that with the depletion of Tm5NM1/2 there is a significant but small increase in active ADF/cofilin in cortical neurons (Figure 6.2) while in hippocampal neurons the levels of active ADF/cofilin is unaltered (Figure 6.4). An earlier study has shown that with the overexpression of active ADF/cofilin, neurite outgrowth and extension are enhanced (Meberg and Bamburg, 2000). Therefore intuitively, an increase in active cofilin is expected to promote neurite outgrowth. However, the significant but subtle increase in active ADF/cofilin by the loss of Tm5NM1/2 in cortical neurons has resulted in a repression of neurite outgrowth. In hippocampal neurons, even though the levels of active ADF/cofilin are not significantly altered in Tm5NM1/2 KO neurons, neurite outgrowth is overall decreased. These interesting results where ADF/cofilin is increased while neurite outgrowth is decreased suggest that other parameters must be involved and this is discussed below.

6.3.3 The effect of tropomyosin on the activity of other actin binding proteins and neuritogenesis

Different tropomyosin isoforms have been shown to inhibit the function of Arp2/3 (Blanchoin *et al.*, 2001) and the severing activity of gelsolin (Ishikawa *et al.*, 1989b) on actin filaments and the degree of protection provided by tropomyosin is isoform specific. The Arp2/3 complex initiates new branch points in existing actin filaments thereby promoting actin polymerisation (reviewed in Amann and Pollard, 2001). Depletion of Arp2/3 has significantly shortened neurite lengths in B35 cells while neurite lengths were unchanged in rat hippocampal neurons (Korobova and Svitkina, 2008). The latter may be due to the timing of Arp2/3 protein knocked down by siRNA as it may have occurred after significant extension of neurites. Hence, Arp2/3 may play a role in neurite extension in primary neurons. The action of the Arp2/3 complex is partially inhibited by different tropomyosin isoforms and out of all the tropomyosins that have been studied, Tm5a has been shown to be the most effective inhibitor (Blanchoin *et al.*, 2001). As Tm5NM1/2 KO neurons may be partially compensated by Tm5a/5b, the association of Tm5a with Tm5NM1/2 depleted actin filaments will protect those filaments from the action of Arp2/3. Therefore, the level of Arp2/3 complex may be decreased from Tm5NM1/2 KO neurons causing a repression of neurite outgrowth. However, this is only a speculation and the level of Arp2/3 complex in Tm5NM1/2 KO neurons is unknown, but this will be subject to further investigation.

Another possible actin binding protein that may influence neurite outgrowth is gelsolin and it has been shown to be inhibited by tropomyosin isoforms. However, the actin-severing activity of gelsolin is only directly inhibited by HMW (high molecular weight) tropomyosins and not LMW (low molecular weight) tropomyosins (Ishikawa *et al.*, 1989b). As all tropomyosin isoforms analysed in this project, Tm5NM1/2, Tm5a/5b, TmBr2 and Tm4 are LMW tropomyosins, the levels of gelsolin may not be altered in Tm5NM1/2 KO neurons.

Interestingly, both HMW and LMW tropomyosins can collaborate with non muscle caldesmon to block the severing effect of gelsolin on actin filaments. Caldesmon and LMW tropomyosin alone when bound to actin filaments does not inhibit the action of gelsolin. However, when caldesmon works in conjunction with LMW tropomyosin, caldesmon promotes the binding of tropomyosin to the actin filament thereby increasing the protection of tropomyosin against the severing effect of gelsolin (Ishikawa *et al.*, 1989b). Therefore, the loss of Tm5NM1/2 with no upregulation of other tropomyosin isoforms at this early stage of development may result in a decrease of the tropomyosin pool. Lower levels of tropomyosin isoforms in neurons may cause less collaboration with caldesmon which may result in higher levels of gelsolin at those actin filaments. The increase in gelsolin levels will result in a rise in its severing effect of actin filaments which may potentially influence neurite outgrowth. This effect cannot be ruled out and the levels of caldesmon as well as gelsolin in Tm5NM1/2 KO neurons and WT controls will be quantified in future experiments.

Chapter 7

General Discussion & Future Directions

7.1 Summary

Previous studies have shown that the γTm gene products are essential for cell survival and embryonic development (Hook *et al.*, 2004). However, Tm5NM1/2 which are products of the γTm gene containing exon 9d, are not absolutely required (Fath *et al.*, manuscript in preparation). In this project, the role of Tm5NM1/2 in neuronal development has been examined. When examining growth cone dynamics, neurons lacking Tm5NM1/2 showed a significant increase in protrusion rates. Also, neurite outgrowth was affected by the loss of Tm5NM1/2 in both hippocampal and cortical neurons. At the molecular level, the elimination of Tm5NM1/2 had little impact on the levels of ADF/cofilin in hippocampal neurons while in cortical neurons a significant but subtle increase in active levels of this actin binding protein was observed. These results reveal that the early stages of neuritogenesis are largely independent of the presence of Tm5NM1/2. Other tropomyosins such as Tm5a/5b, TmBr2 and Tm4 may

functionally compensate for the loss of Tm5NM1/2 which may explain the mild phenotypes observed. These results have shown that the initial stages of neuritogenesis are not greatly impacted on by the loss of Tm5NM1/2. To determine the role of Tm5NM1/2 at later stages of neuronal development and understand how they impact on brain function, studies analysing synaptic function as well as *in vivo* analysis on Tm5NM1/2 KO mice including behavioural studies will be investigated in future experiments.

7.2 Significance of Project Findings

7.2.1 Tm5NM1/2 are not required for early stages of neuritogenesis

Results presented here on neurons from embryonal brain tissues have revealed that growth cone dynamics and neurite outgrowth were mildly affected by the loss of Tm5NM1/2, products containing exon 9d from the γTm gene (Figure 3.3, Table 5.1 and 5.2). The mild phenotype observed in response to the elimination of Tm5NM1/2 shows that these early stages of neuritogenesis are able to proceed in the absence of Tm5NM1/2. As discussed in earlier chapters, this mild phenotype observed from Tm5NM1/2 KO neurons may be due to functional compensation by other isoforms. The upregulation of Tm5NM4/7 are unlikely to functionally compensate for the loss of Tm5NM1/2 since only less than 1% and 15% of total γTm gene products at 1DIV and 4DIV respectively are compensated by these isoforms (Fath *et al.,* manuscript in preparation). However other neuronal tropomyosins Tm5a/5b, TmBr2 and TmBr3 may be able to compensate for the depletion of Tm5NM1/2. While no upregulation of these isoforms was observed, they are present in growth cone structures where Tm5NM1/2 are found. These isoforms may bind to actin filaments which are depleted of Tm5NM1/2 in the knockout mice.

Although the results show that Tm5NM1/2 are not essential for early neuritogenesis they may play a role in fine-tuning these processes. The role of Tm5NM1/2 may involve the translation of signals from the environment and

responding to those signals by recruiting specific actin-binding proteins to the actin filaments (reviewed in O'Neill *et al.,* 2008). Also as discussed in section 6.3.2, different tropomyosin isoforms can regulate and protect the actin filaments from the action of actin binding proteins such as Arp2/3 and gelsolin (Ishikawa *et al.*, 1989b; Blanchoin *et al.*, 2001). Hence, various tropomyosin isoforms will confer functionally distinct actin filaments, thereby exerting different effects on early neuritogenesis.

As the tropomyosin profile changes over time, the role of different tropomyosin isoforms may also differ during development. A recent study on cortical neurons using immunofluorescence has shown that the level of total γTm gene products gene products compensate for less than 1% of the loss of Tm5NM1/2 at 1DIV and the protein level of other γTm gene products including Tm5NM4/7 gradually changes over time, covering for 15% of the loss of Tm5NM1/2 at 4DIV. In support of these results, western blot analyses of brain lysates have revealed that total γTm gene products including Tm5NM4/7 isoforms are only partially compensating for the loss of Tm5NM1/2 at 1DIV and the level of expression increases over time where it is at a level equal to Tm5NM1/2 at 4 weeks old (Fath *et al.,* manuscript in preparation). Therefore as other γTm gene products including Tm5NM4//7 are completely compensating at a quantitative level for the lack of Tm5NM1/2 in adult mice, these γTm gene isoforms may provide functional compensation for the depletion of Tm5NM1/2 at later stages of neuronal development. Functional compensation by γTm gene products during neuronal development in adult Tm5NM1/2 KO mice is likely and will be investigated in future experiments.

7.2.2 Loss of Tm5NM1/2 increases the protrusion rates of lamellipodia

Growth cones from neurons of Tm5NM1 transgenic mice showed a significant enlargement in size which correlates with an increase in F-actin content (Schevzov *et al.*, 2008). Following on from this study, the significant but subtle decrease in growth cone size observed from Tm5NM1/2 KO neurons (Fath *et al.,* manuscript in preparation) may also be associated with a small reduction in the F-actin pool. As growth cone dynamics depend on the polymerisation and depolymerisation of F-actin, a subtle decrease in the pool of F-actin in Tm5NM1/2 KO neurons may therefore influence the dynamic structures of the growth cone.

Previously it has been shown that the filopodia, which are one of the dynamic structures of the growth cone were not altered in length or number in Tm5NM1/2 KO mice (Fath *et al.*, manuscript in preparation). In this study, the loss of Tm5NM1/2 has significantly increased the protrusion rates of lamellipodia, which are the other major dynamic structure in the growth cone (Figure 3.3). The increase in protrusion rates with no change in retraction rates, as a result of depleting Tm5NM1/2 indicates that the regulation of lamellipodia dynamics by tropomyosin expression may be a complex process. Tm5NM1/2 are known to inhibit the severing activity of ADF/cofilin (Bryce *et al.*, 2003) and may also impact on the action of other actin binding proteins such as Arp2/3 (Blanchoin *et al.*, 2001) and gelsolin (Ishikawa *et al.*, 1989b). Actin filament decoration by different tropomyosin isoforms generate distinct filament

populations which are protected from the activity of these actin binding proteins (Ishikawa *et al.*, 1989b; Blanchoin *et al.*, 2001; Bryce *et al.*, 2003). Hence, functional compensation by tropomyosin isoforms, such as Tm5a/5b, TmBr2 and Tm4 by binding to actin filaments depleted of Tm5NM1/2, may result in different degrees of inhibition from the activity of ADF/cofilin, Arp2/3 and gelsolin to those actin filaments. Therefore, the lamellipodia protrusion and retraction rates may involve a combination of these actin binding proteins and their effect on the polymerisation and depolymerisation process of actin filaments will depend on the local signalling pathways (Refer to section 7.2.3.1).

Another compartment of the growth cone that is dependent on F-actin pool size as well as polymerisation and depolymerisation rates are filopodia. An altered pool of tropomyosins in the growth cone may therefore impact on the structure and dynamics of filopodia. The structure of filopodia has been examined and it was found that the length and number of filopodia were not affected by the loss of Tm5NM1/2 (Fath *et al.*, manuscript in preparation). However, the dynamics of filopodia have not yet been analysed in Tm5NM1/2 KO neurons. The advancement and retraction of filopodia are important in the navigation of growth cones. When growth cones are deprived of filopodia by disruption of F-actin, the growth cone can advance and extend normally but are highly disoriented (Bentley and Toroian-Raymond, 1986). Hence, filopodia are important as sensory structures and effectors of motility. Therefore, it is critical for filopodia to function properly so they can act as sensors of their environment in order to direct neurite outgrowth.

7.2.3 RhoGTPase pathways and their effectors that regulate early neuritogenesis

Early neuritogenesis including growth cone dynamics and neurite outgrowth are regulated by RhoGTPases. The most extensively characterised RhoGTPases are Cdc42, Rac and Rho. They are active when bound to GTP and function by interacting with downstream effector proteins to regulate actin cytoskeleton dynamics and neuritogenesis (reviewed in Govek *et al.,* 2005; Heasman and Ridley, 2008).

7.2.3.1 RhoGTPases and their impact on growth cones

Each RhoGTPase, Cell division cycle 42, GTP binding protein (Cdc42), Rac and Rho, is important in different aspects of growth cone function. A study has revealed a role for Cdc42 in filopodia formation (Garvalov *et al.,* 2007). Elimination of Cdc42 has shown that the number and length of filopodia are suppressed in neurons. As the filopodia structure including length and number is not affected by the loss of Tm5NM1/2 (Fath *et al.,* manuscript in preparation), this suggests that Tm5NM1/2 is not involved in the Cdc42 signalling pathway in filopodia. Rac on the other hand is important in the formation of lamellipodia and in the regulation of membrane ruffles. Dominant negative Rac has been shown to inhibit lamellipodia and membrane ruffling (Ridley *et al.,* 1992). Therefore, as growth cone protrusion rates, mainly dependent on lamellipodia dynamics, are significantly increased by the depletion of Tm5NM1/2 (Figure 3.3), this suggests that Tm5NM1/2 may play a role in the Rac signalling

pathway in lamellipodia and this is discussed in detail below. The third RhoGTPase known as Rho appears to be important in regulating the formation of stress fibres and focal adhesions in fibroblasts (Ridley and Hall, 1992). Although neurons do not display classical focal adhesions and actin stress fibres, the navigation of the growth cone and the direction of neurite extension depend on three distinct adhesions in filopodia (Steketee and Tosney, 2002). These are the tip, shaft and basal adhesions which perform different functions. The tip adhesions initiate guidance signal cascades which can alter shaft adhesions to control veil advance of the lamellipodia. The basal adhesions are essential for filopodial formation and dynamics but do not have an impact on veil advance. Hence, Rho may play a role in regulating the formation of these different adhesions in growth cones. This idea will be subject to further investigation.

The complexity of lamellipodia dynamics may be due to the presence of multiple downstream targets such as WAVE (WASP (Wiskott-Aldrich Syndrome Protein)-family Verprolin homologous proteins) and p21-activated kinase (PAK), found in the Rac signalling pathway. WAVE is activated when it is dissociated from its inhibitory complex and this is mediated by Rac without directly binding to WAVE (Eden *et al.*, 2002). WAVE can then directly bind and activate the Arp2/3 complex, as it contains an Arp2/3 binding site within its structure (Nakanishi *et al.*, 2007). As tropomyosins inhibit the action of Arp2/3 in an isoform specific manner (Blanchoin *et al.*, 2001), the Arp2/3 complex may compete with some tropomyosins including Tm5NM1/2 which is dependent on the local signalling activity and its impact on Rac and WAVE.

A downstream target of Rac as well as Cdc42 is PAK (Edwards *et al.*, 1999). PAK1 localises to membrane ruffles in fibroblasts (Sells *et al.*, 2000) as well as lamellipodia and has been shown to phosphorylate and inactivate LIM kinase (LIMK). LIMK in turn also phosphorylates and inactivates ADF/cofilin, leading to actin filament stabilisation (Edwards *et al.*, 1999). The competition of ADF/cofilin with some tropomyosin isoforms for binding to actin filaments will be influenced by Rac, PAK and their impact on the local activity of LIMK. For example, active LIMK will cause an increase in inactive ADF/cofilin. The level of active ADF/cofilin will therefore decrease causing less of this actin binding protein to compete with tropomyosin isoforms such as Tm5NM1/2 for actin filament binding, thereby increasing the stability of the actin filament population. In Tm5NM1/2 KO neurons, actin filaments depleted of Tm5NM1/2 may associate with TmBr3. This could allow more ADF/cofilin to access the actin filaments which may result in a more dynamic filament population.

In another pathway downstream of Rac, PAK can inactivate myosin light chain (MLC) kinase which decreases MLC phosphorylation and reduces actomyosin assembly (Sanders *et al.*, 1999). Studies have also shown that Rac and PAK1 can regulate the phosphorylation of myosin II heavy chain (van Leeuwen *et al.,* 1999; Even-Faitelson *et al.,* 2005). Furthermore, the Rho pathway is also implicated in myosin II phosporylation via regulating myosin regulatory light chain (MRLC) and myosin phosphatase (Ueda *et al.*, 2002). ROCK phosphorylates the myosin binding site of myosin phosphatase thereby inactivating its activity. Also, inhibition of Rho kinase (ROCK), a direct target of Rho, has caused a reduction in the dephosphorylation of MRLC even in the

presence of myosin phosphatase inhibitor, suggesting that ROCK directly dephosphorylates MRLC. The inhibition of myosin phosphatase and direct dephosphorylation of MRLC by ROCK indicates that the Rho pathway plays a role in regulating myosin II assembly.

The regulation of myosins, which are actin associated motor proteins, is important for growth cone dynamics. Myosin IIB has been shown to be required for growth cone dynamics (Bridgman *et al.,* 2001). It is normally found in the central region of the growth cone as well as at the base of the filopodia and is involved in cell spreading. In neurons from transgenic mice overexpressing Tm5NM1, the exogenous isoform was able to recruit Tm5a and myosin IIB into the peripheral region of the growth cones (Schevzov *et al.*, 2005a). This recruitment of myosin IIB also led to an increase in growth cone size. As the loss of Tm5NM1/2 significantly decreased growth cone size, cell spreading in these neurons may be affected due to alterations in active myosin IIB.

Therefore, the polymerisation and depolymerisation rates of actin filaments in growth cones and lamellipodia dynamics may be impacted by a combination of these pathways depending on the local activity of downstream targets, especially from Rac. To gain more insight into the role of Tm5NM1/2 in lamellipodia dynamics, the local activity of WAVE, LIMK and MLC kinase from Tm5NM1/2 KO neurons will be the subject of further studies.

7.2.3.2 RhoGTPases and their effect on neurite outgrowth

Both RhoGTPases and tropomyosin are regulated spatially and temporally (Schevzov *et al.*, 1997; reviewed in Bar-Sagi and Hall, 2000; O'Kane *et al.*, 2003). As growth cone dynamics is examined at 1DIV and neurite outgrowth is analysed at 4DIV, the levels of Cdc42, Rac and Rho as well as the tropomyosin pool may differ at these timepoints. As the molecular switches influence local changes in downstream targets and affect tropomyosin association with actin filaments, differences in Cdc42, Rac and Rho as well as the tropomyosin pool may impact on actin polymerisation and depolymerisation differently for growth cone development and early neurite development.

In terms of neurite outgrowth, generally Cdc42 and Rac appear to be positive regulators while there is evidence to suggest that Rho is a negative regulator of this process (reviewed in Luo, 2000). Constitiutively active Cdc42 signficantly increased neurite length in primary chick spinal cord neurons (Brown *et al.*, 2000). Similarly, constitutively active Rac1 increased while dominant negative Rac1 decreased neurite extension in rat hippocampal neurons (Schwamborn and Puschel, 2004). In contrast, Rho displayed opposite effects to Rac1 as constititutively active Rho decreased while dominant negative Rho increased neurite extension in hippocampal neurons.

Previously, the overexpression of Tm5NM1 in cortical neurons has revealed significant increase in axonal and dendritic lengths. In contrast, the overall results presented here show that the loss of Tm5NM1/2 significantly but subtly

repress neurite outgrowth (Tables 5.1 and 5.2). This suggests that Tm5NM1/2 may have an impact on the mechanisms that affect neurite length. Intuitively, as neurite outgrowth is inhibited, the level of Rho is expected to be increased in Tm5NM1/2 KO neurons. However, it may not be that simple, as neurite outgrowth is a complex process. Many downstream targets such as PAK, LIMK and myosin II are regulated by a combination of Cdc42, Rac and Rho (reviewed in Luo, 2000). For example, one of the important common effectors of Cdc42 and Rac is PAK (Edwards *et al.*, 1999). Activated PAK phosphorylates LIMK and interestingly LIMK is also regulated by Rho through ROCK (Ng and Luo, 2004). Myosin II on the other hand is regulated by MLC kinase which is downstream of Rac and MRLC which is a target of the Rho signalling pathway (Sanders *et al.*, 1999; Ueda *et al.*, 2002). There are also pathways which are only regulated by one RhoGTPase. Cdc42 can activate Arp2/3 via N-WASP WASP (Wiskott-Aldrich Syndrome Protein) while Rac can also activate Arp2/3 but only through the WAVE complex (Rohatgi *et al.*, 1999; Klooster *et al.*, 2006). Rho can regulate profilin, a capping protein (Watanabe *et al.*, 1997). Thus, polymerisation and depolymerisation of F-actin that determine neurite outgrowth may be regulated by a variety of overlapping and distinct pathways.

Therefore, the different effects in axon and dendrites as well as neurite length and branching, from depleting Tm5NM1/2 (Tables 5.1 and 5.2) indicate that different aspects of neuritogenesis may be regulated by a combination of overlapping as well as distinct mechanisms and pathways. The depletion of Tm5NM1/2 has a greater impact on axon outgrowth than dendritic outgrowth in hippocampal neurons (Tables 5.1 and 5.2). Rac, Cdc42 and Rho have been

shown to affect axon and dendritic growth differently. A study has shown that downregulation of Rac1 by siRNA affects dendritic outgrowth but not the outgrowth of axon in mouse hippocampal neurons (Gualdoni *et al.,* 2007). Also, the Cdc42 signalling pathway is important for promoting both axon extension and dendritic growth (Brown *et al.*, 2000; Scott *et al.*, 2003). Furthermore, RhoA has been shown to affect the growth of axons and dendrites differently. Dominant negative RhoA inhibited axon growth while dendritic growth was promoted and the opposite effect was observed in constitutively active RhoA in hippocampal neurons (Ahnert-Hilger *et al.*, 2004). This suggests that RhoA activation increases axon outgrowth and decreases dendritic growth. Taken together, the greater impact on axonal outgrowth in hippocampal neurons suggest that Cdc42 and RhoA levels may be altered in Tm5NM1/2 KO neurons but further research needs to be performed to interpret this result.

In addition to distinct effects shown by axons and dendrites, the data in this study also shows that the neurite length and branching is affected differently by the loss of Tm5NM1/2 (Tables 5.1 and 5.2). While neurite length is decreased (Figure 5.5), neurite branching is increased (Figure 5.7) in Tm5NM1/2 KO cortical neurons. Also, interestingly the axon branching results in Tm5NM1/2 KO neurons are similar to cortical neurons which overexpress Tm5NM1. This indicates that Tm5NM1/2 may not be directly impacting on neurite branching and that other pathways or mechanisms may be involved. Studies have shown that two RhoGTPases, RhoA and Rnd2 can induce neurite branching (Fujita *et al.*, 2002; Chen and Firestein, 2007). Rnd2 is a new branch of the RhoGTPase

family and is specifically expressed in neurons (Fujita *et al.,* 2002). Both RhoA and Rnd2 interacts with microtubules to influence neurite branching (Fujita *et al.*, 2002; Chen and Firestein, 2007). As neurite outgrowth involves the assembly of microtubules and remodelling of actin filaments, Rac, Cdc42 and Rho may still play a role in neurite branching by regulating the polymerisation and depolymerisation of actin filaments. However, Rnd2 and RhoA may be the driving force in regulating neurite branching. To gain further insight into the role of Tm5NM1/2 in neurite branching, it will be interesting to analyse the levels of Rnd2 and RhoA in neurons from Tm5NM1/2 KO mice.

7.3 Future directions

In this project, growth cone function has only been analysed with respect to the lamellipodial compartment. Other important aspects of growth cone function are regulated by the filopodia. The filopodia are important for sensing local cues and directing growth cone migration and also neurite outgrowth (Bentley and Toroian-Raymond, 1986). Filopodia extend and retract in order to explore the environment for chemo-attractants and chemo-repellents, and in turn alter the direction of growth cone advance in response to these cues. Therefore, as filopodia dynamics are important for growth cone function this will be subject to further investigation. For this, chemotaxis experiments will be performed to determine the proper function of filopodia to sense different cues and the migration of growth cones towards these cues will be investigated. On a molecular level, the localisation and activity of RhoGTPases, such as Cdc42, Rac, Rho and Rnd2, as well as their effector proteins, including LIMK and PAK1, will be examined in neurons from Tm5NM1/2 KO mice to gain further insight into the role that Tm5NM1/2 play in these RhoGTPase signalling pathways with respect to early neuritogenesis.

As a complete knockout of the γTm gene is embryonic lethal (Hook *et al.,* 2004) and as adult Tm5NM1/2 KO mice show complete compensation by Tm5NM4/7, analysis using a conditional KO of the γTm gene will provide more insight into the function of γTm gene products in neuronal cells. A conditional γTm gene KO mouse model is currently being generated and will be the subject of future studies.

7.3.1 Implications for tropomyosin dysfunction

The effect of depleting Tm5NM1/2 in this *in vitro* study has resulted in a subtle effect on the early stages of neuritogenesis. Even though early neuritogenesis may be mildly affected, the later stages of neuronal development and function are unknown. To further analyse the later stages of neuritogenesis, the synaptic function of neurons will be investigated in future experiments. However these results from *in vitro* studies may not necessarily reflect the situation *in vivo*. Therefore, the depletion of Tm5NM1/2 on the effect of neurite length and branching as well as synaptic function still needs to be investigated. Impaired cognitive function and memory may result from defects in dendritic branching and synaptic function. One possibility is that dendritic branching may be decreased but synaptic function is normal. This scenario may limit the signals which dendrites may receive as these post synaptic terminals may not be able to spread out to all the axons sending signals. Another alternative is that dendritic branching is normal but synaptic function is impaired. In this event, all the dendrites may be able to connect with axons but the impairment of synaptic function may cause problems in the propagation of signals between neurons. If defects in dendritic branching and synaptic function are observed in the *in vivo* model then behavioural studies on Tm5NM1/2 KO mice, especially tests that analyse motoric function and memory, will be performed in future experiments to determine the impact that these neurons have on cognitive function.

References

Ahnert-Hilger, G., Höltje, M., Große, G., Pickert, G., Mucke, C., Nixdorf-Bergweiler, B., Boquet, P., Hofmann, F., and Just, I. (2004). Differential effects of Rho GTPases on axonal and dendritic development in hippocampal neurones. *Journal of Neurochemistry* **90**(1)**,** 9-18.

Aizawa, H., Wakatsuki, S., Ishii, A., Moriyama, K., Sasaki, Y., Ohashi, K., Sekine-Aizawa, Y., Sehara-Fujisawa, A., Mizuno, K., Goshima, Y., and Yahara, I. (2001). Phosphorylation of cofilin by LIM-kinase is necessary for semaphorin 3A-induced growth cone collapse. *Nature Neuroscience* **4**(4)**,** 367-73.

Alberts, B., Johnson, A., Lewis, J., Raff, M., Roberts, K., and Walter, P. (2002). "Molecular Biology of the Cell." 4th ed. Garland Publishing Inc., New York, NY.

Amann, K. J., and Pollard, T. D. (2001). The Arp2/3 complex nucleates actin filament branches from the sides of pre-existing filaments. *Nature Cell Biology* **3**(3)**,** 306-310.

Araya, E., Berthier, C., Kim, E., Yeung, T., Wang, X., and Helfman, D. M. (2002). Regulation of Coiled-Coil Assembly in Tropomyosins. *Journal of Structural Biology* **137**(1-2)**,** 176-183.

Arimura, N., and Kaibuchi, K. (2007). Neuronal polarity: from extracellular signals to intracellular mechanisms. *Nature Reviews Neuroscience* **8**(3)**,** 194-205.

Bamburg, J. R., and Bray, D. (1987). Distribution and cellular localization of actin depolymerizing factor. *Journal of Cell Biology* **105**(6)**,** 2817-2825.

Bar-Sagi, D., and Hall, A. (2000). Ras and Rho GTPases: A Family Reunion *Cell* **103**(2)**,** 227-238

Bentley, D., and Toroian-Raymond, A. (1986). Disoriented pathfinding by pioneer neurone growth cones deprived of filopodia by cytochalasin treatment. *Nature* **323,** 712–715.

Bernstein, B. W., and Bamburg, J. R. (1982). Tropomyosin binding to F-actin protects the F-actin from disassembly by brain actin-depolymerizing factor (ADF). *Cell Motility and the Cytoskeleton* **2**(1)**,** 1-8.

Bito, H., Furuyashiki, T., Ishihara, H., Shibasaki, Y., Ohashi, K., Mizuno, K., Maekawa, M., Ishizaki, T., and Narumiya, S. (2000). A Critical Role for a Rho-Associated Kinase, p160ROCK, in Determining Axon Outgrowth in Mammalian CNS Neurons. *Neuron* **26**(2)**,** 431-441.

Blanchoin, L., Pollard, T. D., and Hitchcock-DeGregori, S. E. (2001). Inhibition of the Arp2/3 complex-nucleated actin polymerization and branch formation by tropomyosin **11**(16)**,** 1300-1304.

Bridgman, P. C., Dave, S., Asnes, C. F., Tullio, A. N., and Adelstein, R. S. (2001). Myosin IIB Is Required for Growth Cone Motility. *Journal of Neuroscience* **21**(16)**,** 6159-6169.

Brown, M. D., Cornejo, B. J., Kuhn, T. B., and Bamburg, J. R. (2000). Cdc42 stimulates neurite outgrowth and formation of growth cone filopodia and lamellipodia. *Journal of Neurobiology* **43**(4)**,** 352-364.

Brown, M. E., and Bridgman, P. C. (2003). Retrograde flow rate is increased in growth cones from myosin IIB knockout mice. *Journal of Cell Science* **116**(Pt 6)**,** 1087-94.

Bryce, N. S., Schevzov, G., Ferguson, V., Percival, J. M., Lin, J. J. C., Matsumura, F., Bamburg, J. R., Jeffrey, P. L., Hardeman, E. C., Gunning, P., and Weinberger, R. P. (2003). Specification of Actin Filament Function and Molecular Composition by Tropomyosin Isoforms. *Molecular Biology of the Cell* **14**(3)**,** 1002-1016.

Chen, H., and Firestein, B. L. (2007). RhoA Regulates Dendrite Branching in Hippocampal Neurons by Decreasing Cypin Protein Levels. *Journal of Neuroscience* **27**(31)**,** 8378-8386.

Cooper, J. A. (2002). Actin Dynamics: Tropomyosin Provides Stability. *Current Biology* **12**(15)**,** R523-R525.

Creed, S. J., Bryce, N., Naumanen, P., Weinberger, R., Lappalainen, P., Stehn, J., and Gunning, P. (2008). Tropomyosin isoforms define distinct microfilament populations with different drug susceptibility. *European Journal of Cell Biology* **87**(8-9)**,** 709-720.

Da Silva, J. S., and Dotti, C. G. (2002). Breaking the neuronal sphere: regulation of the actin cytoskeleton in neuritogenesis. *Nature Reviews Neuroscience* **3**(9)**,** 694-704.

Dehmelt, L., Smart, F. M., Ozer, R. S., and Halpain, S. (2003). The Role of Microtubule-Associated Protein 2c in the Reorganization of Microtubules and Lamellipodia during Neurite Initiation. *Journal of Neuroscience* **23**(29)**,** 9479-9490.

Dent, E. W., Barnes, A. M., Tang, F., and Kalil, K. (2004). Netrin-1 and Semaphorin 3A Promote or Inhibit Cortical Axon Branching, Respectively, by Reorganization of the Cytoskeleton. *Journal of Neuroscience* **24**(12)**,** 3002-3012.

Dent, E. W., and Gertler, F. B. (2003). Cytoskeletal Dynamics and Transport in Growth Cone Motility and Axon Guidance. *Neuron* **40**(2)**,** 209-227.

DesMarais, V., Ichetovkin, I., Condeelis, J., and Hitchcock-DeGregori, S. E. (2002). Spatial regulation of actin dynamics: a tropomyosin-free, actin-rich compartment at the leading edge. *Journal of Cell Science* **115**(23)**,** 4649-4660.

Dos Remedios, C. G., Chhabra, D., Kekic, M., Dedova, I. V., Tsubakihara, M., Berry, D. A., and Nosworthy, N. J. (2003). Actin Binding Proteins: Regulation of Cytoskeletal Microfilaments. *Physiological Reviews* **83**(2)**,** 433-473.

Eden, S., Rohatgi, R., Podtelejnikov, A. V., Mann, M., and Kirschner, M. W. (2002). Mechanism of regulation of WAVE1-induced actin nucleation by Rac1 and Nck. *Nature* **418**(6899)**,** 790-793.

Edwards, D. C., Sanders, L. C., Bokoch, G. M., and Gill, G. N. (1999). Activation of LIM-kinase by Pak1 couples Rac/Cdc42 GTPase signalling to actin cytoskeletal dynamics.[see comment]. *Nature Cell Biology* **1**(5)**,** 253-9.

Endo, M., Ohashi, K., and Mizuno, K. (2007). LIM kinase and slingshot are critical for neurite extension. *Journal of Biological Chemistry* **282**(18)**,** 13692-702.

Engel, J., and Neidl, C. (1979). Exchange of ADP, ATP and 1:N⁶-Ethenoadenosine 5'-Triphosphate at G-Actin. *European Journal of Biochemistry* **101**(1)**,** 163-169.

Even-Faitelson, L., Rosenberg, M., and Ravid, S. (2005). PAK1 regulates myosin II-B phosphorylation, filament assembly, localization and cell chemotaxis. *Cellular Signalling* **17**(9)**,** 1137-1148.

Fath, T., Ke, Y. D., Gunning, P., Gotz, J., and Ittner, L. M. (2009). Primary support cultures of hippocampal and substantia nigra neurons. *Nature Protocols* **4**(1)**,** 78-85.

Fujita, H., Katoh, H., Ishikawa, Y., Mori, K., and Negishi, M. (2002). Rapostlin Is a Novel Effector of Rnd2 GTPase Inducing Neurite Branching. *Journal of Biological Chemistry* **277**(47)**,** 45428-45434.

Gallo, G. (2006). RhoA-kinase coordinates F-actin organization and myosin II activity during semaphorin-3A-induced axon retraction. *Journal of Cell Science* **119**(16)**,** 3413-3423.

Garvalov, B. K., Flynn, K. C., Neukirchen, D., Meyn, L., Teusch, N., Wu, X., Brakebusch, C., Bamburg, J. R., and Bradke, F. (2007). Cdc42 Regulates Cofilin during the Establishment of Neuronal Polarity. *Journal of Neuroscience* **27**(48)**,** 13117-13129.

Gehler, S., Gallo, G., Veien, E., and Letourneau, P. C. (2004a). p75 Neurotrophin Receptor Signaling Regulates Growth Cone Filopodial Dynamics through Modulating RhoA Activity. *Journal of Neuroscience* **24**(18)**,** 4363-4372.

Gehler, S., Shaw, A. E., Sarmiere, P. D., Bamburg, J. R., and Letourneau, P. C. (2004b). Brain-Derived Neurotrophic Factor Regulation of Retinal Growth Cone Filopodial Dynamics Is Mediated through Actin Depolymerizing Factor/Cofilin. *Journal of Neuroscience* **24**(47)**,** 10741-10749.

Gimona, M., Watakabe, A., and Helfman, D. M. (1995). Specificity of dimer formation in tropomyosins: influence of alternatively spliced exons on homodimer and heterodimer assembly. *Proceedings of the National Academy of Sciences of the United States of America* **92**(21)**,** 9776-9780.

Goldberg, D. J., and Burmeister, D. W. (1986). Stages in axon formation: observations of growth of Aplysia axons in culture using video-enhanced contrast-differential interference contrast microscopy. *Journal of Cell Biology* **103**(5)**,** 1921-31.

Govek, E.-E., Newey, S. E., and Van Aelst, L. (2005). The role of the Rho GTPases in neuronal development. *Genes & Development* **19**(1)**,** 1-49.

Gualdoni, S., Albertinazzi, C., Corbetta, S., Valtorta, F., and de Curtis, I. (2007). Normal levels of Rac1 are important for dendritic but not axonal development in hippocampal neurons. *Biology of the Cell* **099**(8)**,** 455-464.

Gunning, P., O'Neill, G., and Hardeman, E. (2008). Tropomyosin-Based Regulation of the Actin Cytoskeleton in Time and Space. *Physiological Reviews* **88**(1)**,** 1-35.

Gunning, P. W., Schevzov, G., Kee, A. J., and Hardeman, E. C. (2005). Tropomyosin isoforms: divining rods for actin cytoskeleton function. *Trends in Cell Biology* **15**(6)**,** 333-341.

Had, L., Faivre-Sarrailh, C., Legrand, C., Mery, J., Brugidou, J., and Rabie, A. (1994). Tropomyosin isoforms in rat neurons: the different developmental profiles and distributions of TM-4 and TMBr-3 are consistent with different functions. *Journal of Cell Science* **107**(10)**,** 2961-2973.

Hannan, A. J., Gunning, P., Jeffrey, P. L., and Weinberger, R. P. (1998). Structural Compartments within Neurons: Developmentally Regulated Organization of Microfilament Isoform mRNA and Protein. *Molecular and Cellular Neuroscience* **11**(5-6)**,** 289-304.

Hannan, A. J., Schevzov, G., Gunning, P., Jeffrey, P. L., and Weinberger, R. P. (1995). Intracellular Localization of Tropomyosin mRNA and Protein Is Associated with Development of Neuronal Polarity. *Molecular and Cellular Neuroscience* **6**(5)**,** 397-412.

Heasman, S. J., and Ridley, A. J. (2008). Mammalian Rho GTPases: new insights into their functions from in vivo studies. *Nature Reviews Molecular Cell Biology* **9**(9)**,** 690-701.

Helfman, D. M., Cheley, S., Kuismanen, E., Finn, L. A., and Yamawaki-Kataoka, Y. (1986). Nonmuscle and muscle tropomyosin isoforms are expressed from a single gene by alternative RNA splicing and polyadenylation. *Molecular and Cellular Biology* **6**(11)**,** 3582-3595.

Hook, J., Lemckert, F., Qin, H., Schevzov, G., and Gunning, P. (2004). Gamma Tropomyosin Gene Products Are Required for Embryonic Development. *Molecular and Cellular Biology* **24**(6)**,** 2318-2323.

Ishikawa, R., and Kohama, K. (2007). Actin-Binding Proteins in Nerve Cell Growth Cones. *Journal of Pharmacological Sciences*.

Ishikawa, R., Yamashiro, S., and Matsumura, F. (1989a). Annealing of gelsolin-severed actin fragments by tropomyosin in the presence of Ca2+. Potentiation of the annealing process by caldesmon. *Journal of Biological Chemistry* **264**(28)**,** 16764-16770.

Ishikawa, R., Yamashiro, S., and Matsumura, F. (1989b). Differential modulation of actin-severing activity of gelsolin by multiple isoforms of cultured rat cell tropomyosin. Potentiation of protective ability of tropomyosins by 83-kDa nonmuscle caldesmon. *Journal of Biological Chemistry* **264**(13)**,** 7490-7497.

Jacobs, T., Causeret, F., Nishimura, Y. V., Terao, M., Norman, A., Hoshino, M., and Nikolic, M. (2007). Localized activation of p21-activated kinase controls neuronal polarity and morphology. *Journal of Neuroscience* **27**(32)**,** 8604-15.

Klooster, J. P. t., Evers, E. E., Janssen, L., Machesky, L. M., Michiels, F., Hordijk, P., and Collard, J. G. (2006). Interaction between Tiam1 and the Arp2/3 complex links activation of Rac to actin polymerization. *Biochemical Journal* **397**(39–45).

Korobova, F., and Svitkina, T. (2008). Arp2/3 Complex Is Important for Filopodia Formation, Growth Cone Motility, and Neuritogenesis in Neuronal Cells. *Molecular Biology of the Cell* **19**(4)**,** 1561-1574.

Kurita, S., Gunji, E., Ohashi, K., and Mizuno, K. (2007). Actin filaments-stabilizing and -bundling activities of cofilin-phosphatase Slingshot-1. *Genes to Cells* **12**(5)**,** 663-676.

Lebrand, C., Dent, E. W., Strasser, G. A., Lanier, L. M., Krause, M., Svitkina, T. M., Borisy, G. G., and Gertler, F. B. (2004). Critical Role of Ena/VASP Proteins for Filopodia Formation in Neurons and in Function Downstream of Netrin-1. *Neuron* **42**(1)**,** 37-49.

Lees-Miller, J. P., and Helfman, D. M. (1991). The molecular basis for tropomyosin isoform diversity. *BioEssays* **13**(9)**,** 429-437.

Lin, C. H., Espreafico, E. M., Mooseker, M. S., and Forscher, P. (1997). Myosin Drives Retrograde F-Actin Flow in Neuronal Growth Cones. *Biol Bull* **192**(1)**,** 183-185.

Loudon, R. P., Silver, L. D., Yee Jr, H. F., and Gallo, G. (2006). RhoA-kinase and myosin II are required for the maintenance of growth cone polarity and guidance by nerve growth factor. *Journal of Neurobiology* **66**(8)**,** 847-867.

Lu, M., Witke, W., Kwiatkowski, D. J., and Kosik, K. S. (1997). Delayed Retraction of Filopodia in Gelsolin Null Mice. *Journal of Cell Biology* **138**(6)**,** 1279-1287.

Luo, L. (2000). Rho GTPases in neuronal morphogenesis. *Nature Reviews Neuroscience* **1**(3)**,** 173-180.

Maciver, S. K., Ternent, D., and McLaughlin, P. J. (2000). Domain 2 of gelsolin binds directly to tropomyosin. *FEBS Letters* **473**(1)**,** 71-75.

Matsumura, F., and Yamashiro-Matsumura, S. (1985). Purification and characterization of multiple isoforms of tropomyosin from rat cultured cells. *Journal of Biological Chemistry* **260**(25)**,** 13851-13859.

McGough, A., Pope, B., Chiu, W., and Weeds, A. (1997). Cofilin Changes the Twist of F-Actin: Implications for Actin Filament Dynamics and Cellular Function. *Journal of Cell Biology* **138**(4)**,** 771-781.

Meberg, P. J., and Bamburg, J. R. (2000). Increase in Neurite Outgrowth Mediated by Overexpression of Actin Depolymerizing Factor. *Journal of Neuroscience* **20**(7)**,** 2459-2469.

Miyado, K., Kimura, M., and Taniguchi, S. (1996). Decreased Expression of a Single Tropomyosin Isoform, TM5/TM30nm, Results in Reduction in Motility of Highly Metastatic B16-F10 Mouse Melanoma Cells. *Biochemical and Biophysical Research Communications* **225**(2)**,** 427-435.

Moraczewska, J., Nicholson-Flynn, K., and Hitchcock-DeGregori, S. E. (1999). The Ends of Tropomyosin Are Major Determinants of Actin Affinity and Myosin Subfragment 1-Induced Binding to F-Actin in the Open State. *Biochemistry* **38**(48)**,** 15885-15892.

Nakagawa, H., Miki, H., Ito, M., Ohashi, K., Takenawa, T., and Miyamoto, S. (2001). N-WASP, WAVE and Mena play different roles in the organization of actin cytoskeleton in lamellipodia. *Journal of Cell Science* **114**(8)**,** 1555-1565.

Nakanishi, O., Suetsugu, S., Yamazaki, D., and Takenawa, T. (2007). Effect of WAVE2 Phosphorylation on Activation of the Arp2/3 Complex. *Journal of Biochemistry* **141**(3)**,** 319-325.

Ng, J., and Luo, L. (2004). Rho GTPases regulate axon growth through convergent and divergent signaling pathways. *Neuron* **44**(5)**,** 779-93.

Novy, R. E., Sellers, J. R., Liu, L.-F., and Lin, J. J.-C. (1993). In vitro functional characterization of bacterially expressed human fibroblast tropomyosin isoforms and their chimeric mutants. *Cell Motility and the Cytoskeleton* **26**(3)**,** 248-261.

Nyakern-Meazza, M., Narayan, K., Schutt, C. E., and Lindberg, U. (2002). Tropomyosin and Gelsolin Cooperate in Controlling the Microfilament System. *Journal of Biological Chemistry* **277**(32)**,** 28774-28779.

O'Neill, G. M., Stehn, J., and Gunning, P. W. (2008). Tropomyosins as interpreters of the signalling environment to regulate the local cytoskeleton. *Seminars in Cancer Biology* **18**(1)**,** 35-44.

O'Kane, E. M., Stone, T. W., and Morris, B. J. (2003). Distribution of Rho family GTPases in the adult rat hippocampus and cerebellum *Molecular Brain Research* **114**(1)**,** 1-8.

Ono, S., and Ono, K. (2002). Tropomyosin inhibits ADF/cofilin-dependent actin filament dynamics. *Journal of Cell Biology* **156**(6)**,** 1065-1076.

Parri, M., Buricchi, F., Giannoni, E., Grimaldi, G., Mello, T., Raugei, G., Ramponi, G., and Chiarugi, P. (2007). EphrinA1 Activates a Src/Focal Adhesion Kinase-mediated Motility Response Leading to Rho-dependent Actino/Myosin Contractility. *Journal of Biological Chemistry* **282**(27)**,** 19619-19628.

Percival, J. M., Hughes, J. A. I., Brown, D. L., Schevzov, G., Heimann, K., Vrhovski, B., Bryce, N., Stow, J. L., and Gunning, P. W. (2004). Targeting of a Tropomyosin Isoform to Short Microfilaments Associated with the Golgi Complex. *Molecular Biology of the Cell* **15**(1)**,** 268-280.

Percival, J. M., Thomas, G., Cock, T.-A., Gardiner, E. M., Jeffrey, P. L., Lin, J. J. C., Weinberger, R. P., and Gunning, P. (2000). Sorting of tropomyosin isoforms in synchronised NIH 3T3 fibroblasts: Evidence for distinct microfilament populations. *Cell Motility and the Cytoskeleton* **47**(3)**,** 189-208.

Perry, S. V. (2001). Vertebrate tropomyosin: distribution, properties and function *Journal of Muscle Research and Cell Motility* **22**(1)**,** 5-49.

Phillips, G. N., Lattman, E. E., Cummins, P., Lee, K. Y., and Cohen, C. (1979). Crystal structure and molecular interactions of tropomyosin. *Nature* **278**(5703)**,** 413-417.

Pinyol, R., Haeckel, A., Ritter, A., Qualmann, B., and Kessels, M. M. (2007). Regulation of N-WASP and the Arp2/3 complex by Abp1 controls neuronal morphology. *PLoS ONE* **2**(5)**,** e400.

Ridley, A. J., and Hall, A. (1992). The small GTP-binding protein rho regulates the assembly of focal adhesions and actin stress fibers in response to growth factors. *Cell* **70**(3)**,** 389-399.

Ridley, A. J., Paterson, H. F., Johnston, C. L., Diekmann, D., and Hall, A. (1992). The small GTP-binding protein rac regulates growth factor-induced membrane ruffling. *Cell* **70**(3)**,** 401-410.

Rochlin, M. W., Itoh, K., Adelstein, R. S., and Bridgman, P. C. (1995). Localization of myosin II A and B isoforms in cultured neurons. *Journal of Cell Science* **108**(12)**,** 3661-3670.

Rodriguez, O. C., Schaefer, A. W., Mandato, C. A., Forscher, P., Bement, W. M., and Waterman-Storer, C. M. (2003). Conserved microtubule-actin interactions in cell movement and morphogenesis. *Nature Cell Biology* **5**(7)**,** 599-609.

Rohatgi, R., Ma, L., Miki, H., Lopez, M., Kirchhausen, T., Takenawa, T., and Kirschner, M. W. (1999). The Interaction between N-WASP and the Arp2/3 Complex Links Cdc42-Dependent Signals to Actin Assembly *Cell* **97**(2)**,** 221-231.

Sanders, L. C., Matsumura, F., Bokoch, G. M., and de Lanerolle, P. (1999). Inhibition of Myosin Light Chain Kinase by p21-Activated Kinase. *Science* **283**(5410)**,** 2083(1).

Schevzov, G., Bryce, N. S., Almonte-Baldonado, R., Joya, J., Lin, J. J., Hardeman, E., Weinberger, R., and Gunning, P. (2005a). Specific features of neuronal size and shape are regulated by tropomyosin isoforms. *Molecular Biology of the Cell* **16**(7)**,** 3425-37.

Schevzov, G., Fath, T., Vrhovski, B., Vlahovich, N., Rajan, S., Hook, J., Joya, J. E., Lemckert, F., Puttur, F., Lin, J. J. C., Hardeman, E. C., Wieczorek, D. F., O'Neill, G. M., and Gunning, P. W. (2008). Divergent Regulation of the Sarcomere and the Cytoskeleton. *Journal of Biological Chemistry* **283**(1)**,** 275-283.

Schevzov, G., Gunning, P., Jeffrey, P. L., Temm-Grove, C., Helfman, D. M., Lin, J. J. C., and Weinberger, R. P. (1997). Tropomyosin Localization Reveals Distinct Populations of Microfilaments in Neurites and Growth Cones. *Molecular and Cellular Neuroscience* **8**(6)**,** 439-454.

Schevzov, G., Vrhovski, B., Bryce, N. S., Elmir, S., Qiu, M. R., O'Neill G, M., Yang, N., Verrills, N. M., Kavallaris, M., and Gunning, P. W. (2005b). Tissue-specific tropomyosin isoform composition. *Journal of Histochemistry and Cytochemistry* **53**(5)**,** 557-70.

Schwamborn, J. C., and Puschel, A. W. (2004). The sequential activity of the GTPases Rap1B and Cdc42 determines neuronal polarity. *Nature Neuroscience* **7**(9)**,** 923-929.

Scott, E. K., Reuter, J. E., and Luo, L. (2003). Small GTPase Cdc42 Is Required for Multiple Aspects of Dendritic Morphogenesis. *Journal of Neuroscience* **23**(8)**,** 3118-3123.

Sells, M. A., Pfaff, A., and Chernoffa, J. (2000). Temporal and Spatial Distribution of Activated Pak1 in Fibroblasts. *Journal of Cell Biology* **151**(7)**,** 1449-1458.

Stehn, J. R., Schevzov, G., Neill, G. M., and Gunning, P. W. (2006). Specialisation of the Tropomyosin Composition of Actin Filaments Provides New Potential Targets for Chemotherapy. *Current Cancer Drug Targets* **6,** 245-256.

Steketee, M. B., and Tosney, K. W. (2002). Three Functionally Distinct Adhesions in Filopodia: Shaft Adhesions Control Lamellar Extension. *Journal of Neuroscience* **22**(18)**,** 8071-8083.

Strasser, G. A., Rahim, N. A., VanderWaal, K. E., Gertler, F. B., and Lanier, L. M. (2004). Arp2/3 Is a Negative Regulator of Growth Cone Translocation. *Neuron* **43**(1)**,** 81-94.

Sun, H. Q., Yamamoto, M., Mejillano, M., and Yin, H. L. (1999). Gelsolin, a Multifunctional Actin Regulatory Protein. *Journal of Biological Chemistry* **274**(47)**,** 33179-33182.

Szendrei, G. I., Lee, V. M. Y., and L. Otvos, J. (1993). Recognition of the minimal epitope of monoclonal antibody Tau-1 depends upon the presence of a phosphate group but not its location. *Journal of Neuroscience Research* **34**(2)**,** 243-249.

Takenawa, T., and Miki, H. (2001). WASP and WAVE family proteins: key molecules for rapid rearrangement of cortical actin filaments and cell movement. *Journal of Cell Science* **114**(10)**,** 1801-1809.

Temm-Grove, C. J., Guo, W., and Helfman, D. M. (1996). Low molecular weight rat fibroblast tropomyosin 5 (TM-5): cDNA cloning, actin-binding, localization, and coiled-coil interactions. *Cell Motility and the Cytoskeleton* **33**(3)**,** 223-40.

Ueda, K., Murata-Hori, M., Tatsuka, M., and Hosoya, H. (2002). Rho-kinase contributes to diphosphorylation of myosin II regulatory light chain in nonmuscle cells. *Oncogene* **21**(38)**,** 5852-60.

Uehata, M., Ishizaki, T., Satoh, H., Ono, T., Kawahara, T., Morishita, T., Tamakawa, H., Yamagami, K., Inui, J., Maekawa, M., and Narumiya, S. (1997). Calcium sensitization of smooth muscle mediated by a Rho-associated protein kinase in hypertension. *Nature* **389**(6654)**,** 990-994.

van Leeuwen, F. N., van Delft, S., Kain, H. E., van der Kammen, R. A., and Collard, J. G. (1999). Rac regulates phosphorylation of the myosin-II heavy chain, actinomyosin disassembly and cell spreading. *Nature Cell Biology* **1**(4)**,** 242-248.

Vrhovski, B., Lemckert, F., and Gunning, P. (2004). Modification of the tropomyosin isoform composition of actin filaments in the brain by deletion of an alternatively spliced exon. *Neuropharmacology* **47**(5)**,** 684-93.

Vrhovski, B., Schevzov, G., Dingle, S., Lessard, J. L., Gunning, P., and Weinberger, R. P. (2003). Tropomyosin isoforms from the γ gene differing at the C-terminus are spatially and developmentally regulated in the brain. *Journal of Neuroscience Research* **72**(3)**,** 373-383.

Wang, F.-S., Wolenski, J. S., Cheney, R. E., Mooseker, M. S., and Jay, D. G. (1996). Function of myosin-V in filopodial extension of neuronal growth cones. *Science* **273**(5275)**,** 660-663.

Watanabe, N., Madaule, P., Reid, T., Ishizaki, T., Watanabe, G., Kakizuka, A., Saito, Y., Nakao, K., Jockusch, B. M., and Narumiya, S. (1997). p140mDia, a mammalian homolog of Drosophila diaphanous, is a target protein for Rho small GTPase and is a ligand for profilin. *EMBO Journal* **16**(11)**,** 3044–3056.

Wawro, B., Greenfield, N. J., Wear, M. A., Cooper, J. A., Higgs, H. N., and Hitchcock-DeGregori, S. E. (2007). Tropomyosin Regulates Elongation by Formin at the Fast-Growing End of the Actin Filament. *Biochemistry* **46**(27)**,** 8146-8155.

Weinberger, R., Schevzov, G., Jeffrey, P., Gordon, K., Hill, M., and Gunning, P. (1996). The molecular composition of neuronal microfilaments is spatially and temporally regulated. *Journal of Neuroscience* **16**(1)**,** 238-252.

Zhang, X.-F., Schaefer, A. W., Burnette, D. T., Schoonderwoert, V. T., and Forscher, P. (2003). Rho-Dependent Contractile Responses in the Neuronal Growth Cone Are Independent of Classical Peripheral Retrograde Actin Flow. *Neuron* **40**(5)**,** 931-944.